

AD-A205 976

IC FILE COPY

1

AFGL-TR-88-0034
ENVIRONMENTAL RESEARCH PAPERS, NO. 396

VLF/LF Reflection Properties of the Low
Latitude Ionosphere

WAYNE I. KLEMETTI
PAUL A. KOSSEY
JOHN E. RASMUSSEN
MARIA SUELI da SILVEIRA MACEDO MOURA

DTIC
ELECTE
MAR 24 1989
S D
D Cg



4 February 1988



Approved for public release; distribution unlimited.



IONOSPHERIC PHYSICS DIVISION

PROJECT 2310

AIR FORCE GEOPHYSICS LABORATORY

HANSCOM AFB, MA 01731

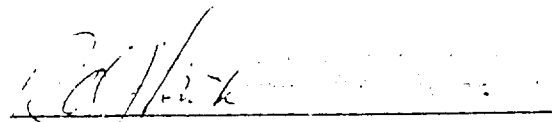
89 3 22 158

This technical report has been reviewed and is approved for publication.

FOR THE COMMANDER



JOHN E. RASMUSSEN, Chief
Ionospheric Interactions Branch



ROBERT A. SKRIVANEK, Director
Ionospheric Physics Division

This document has been reviewed by the ESD Public Affairs Office (PA) and is releasable to the National Technical Information Service (NTIS).

Qualified requestors may obtain additional copies from the Defense Technical Information Center. All others should apply to the National Technical Information Service.

If your address has changed, or if you wish to be removed from the mailing list, or if the addressee is no longer employed by your organization, please notify AFGL/DAA, Hanscom AFB, MA 01731. This will assist us in maintaining a current mailing list.

REPORT DOCUMENTATION PAGE

1a. REPORT SECURITY CLASSIFICATION Unclassified			1b. RESTRICTIVE MARKINGS N/A		
2a. SECURITY CLASSIFICATION AUTHORITY			3. DISTRIBUTION / AVAILABILITY OF REPORT Approved for public release; distribution unlimited.		
2b. DECLASSIFICATION / DOWNGRADING SCHEDULE					
4. PERFORMING ORGANIZATION REPORT NUMBER(S) AFGL-TR-88-0034 ERP. No. 996			5. MONITORING ORGANIZATION REPORT NUMBER(S)		
6a. NAME OF PERFORMING ORGANIZATION Air Force Geophysics Laboratory		6b. OFFICE SYMBOL (If applicable) LID	7a. NAME OF MONITORING ORGANIZATION		
6c. ADDRESS (City, State, and ZIP Code) Hanscom AFB Massachusetts 01731-5000			7b. ADDRESS (City, State, and ZIP Code)		
8a. NAME OF FUNDING / SPONSORING ORGANIZATION AFOSR		8b. OFFICE SYMBOL (If applicable)	9. PROCUREMENT INSTRUMENT IDENTIFICATION NUMBER		
8c. ADDRESS (City, State, and ZIP Code) Bolling AFB Washington, DC 20332-6448			10. SOURCE OF FUNDING NUMBERS		
			PROGRAM ELEMENT NO 61102F	PROJECT NO 2310	TASK NO G3
11. TITLE (Include Security Classification) VLF/LF Reflection Properties of the Low Latitude Ionosphere					
12. PERSONAL AUTHOR(S) Klemetti, W.I., Kossey, P.A., Rasmussen, J.E. and Maria Sueli da Silveira Macedo Moura*					
13a. TYPE OF REPORT Scientific Interim		13b. TIME COVERED FROM _____ TO _____		14. DATE OF REPORT (Year, Month, Day) 1988 February 4	
15. PAGE COUNT					
16. SUPPLEMENTARY NOTATION *IAE: Instituto de Atividades Espaciais, CTA, 12.200 SaoJose dos Campos, SP, Brazil					
17. COSATI CODES			18. SUBJECT TERMS (Continue on reverse if necessary and identify by block number)		
FIELD	GROUP	SUB-GROUP	-> VLF Propagation LF Propagation Ionospheric Reflectivity D+Region, 312		
04	01				
17	02				
19. ABSTRACT (Continue on reverse if necessary and identify by block number) Low latitude observations of VLF/LF pulse reflections from the lower ionosphere obtained at nine locations to the east and west of a transmitter in southeastern Brazil are described. The data, acquired during a two-month experimental campaign conducted by the Air Forces of the United States and Brazil, provide a variety of information on the reflection properties of the ionosphere below about 90 km altitude. Aspects of the data are presented in quasi three-dimensional formats useful for identifying ionospheric structure and variability, and detailed analyses of portions of the data are provided, which characterize the effective heights of the reflection and the reflection coefficients of the ionosphere at noon and midnight, over a frequency range from 15 to 65 kHz. Electron density models of the ionosphere, derived from the VLF/LF reflection data are also discussed. Page 30.					
20. DISTRIBUTION / AVAILABILITY OF ABSTRACT <input checked="" type="checkbox"/> UNCLASSIFIED/UNLIMITED <input type="checkbox"/> SAME AS RPT <input type="checkbox"/> DTIC USERS			21. ABSTRACT SECURITY CLASSIFICATION Unclassified		
22a. NAME OF RESPONSIBLE INDIVIDUAL Wayne I. Klemetti			22b. TELEPHONE (Include Area Code) (617) 377-8767		22c. OFFICE SYMBOL AFGL/LID

Preface

The authors are indebted to the many people who made this cooperative effort between the Air Forces of the United States and Brazil possible. The research program was a highly successful joint endeavor, with responsibilities and efforts equally shared by the United States and Brazil. The U.S. team expresses their deep appreciation for the warm hospitality and the outstanding cooperation shown by all the Brazilian organizations and individuals involved. Their skill and generosity not only guaranteed the success of the program, but also made the effort a distinct pleasure for the U.S. personnel. Although it is virtually impossible to mention all the individuals who contributed, we wish to especially acknowledge the following: Dr. Jose Luiz Rodolpho Muzzio and Captain Basilio Baranoff, both of Centro Tecnico Aeroespacial (CTA), San Jose Dos Campos, Brazil, who were the focal points in the Brazilian Air Force for organizing and carrying out the program; and Prof. Phenix M. Ramirez Pardo, of Fundacao Educacional da Regiao de Blumenau (FURB), who planned the day-to-day experimental efforts and who provided valuable technical insight and guidance to all aspects of the program. In addition, the authors wish to warmly acknowledge Dr. Edward A. Lewis who, as a U.S. Air Force scientist, conceived the novel pulse ionosounding technique used for obtaining the VLF/LF reflection data described in this report.

Accession For	
NTIS	CRA&I <input checked="checked" type="checkbox"/>
DTIC	TAB <input type="checkbox"/>
Unannounced <input type="checkbox"/>	
Justification _____	
By _____	
Distribution /	
Availability Codes	
Dist	Avail and/or Special
A-1	



Contents

1. INTRODUCTION	1
2. VLF/LF IONOSOUNDING TECHNIQUE	1
3. DATA DISPLAY AND REDUCTION FORMATS	4
3.1 Three-dimensional Data Displays	8
3.2 Reflection Heights and Coefficients as a Function of Time	8
3.3 Reflection Heights and Coefficients as a Function of Frequency	8
4. DATA FROM EACH OF THE RECEIVING LOCATIONS	12
5. SELECTED FEATURES OF THE REFLECTION DATA	73
5.1 Day/Night Reflection Heights	73
5.2 Day/Night Variations in the Reflection Coefficients	73
5.3 Azimuthal Variations in the Reflection Coefficients	73
5.4 Variations in the Reflection Coefficients with Range	76
5.5 Comparison of Normal and Converted Reflection Coefficients	76
5.6 Evidence of Weak Reflections from Below the Normal D-Region	80
5.7 Unusual Moving High Altitude Nighttime Reflections	83
6. ELECTRON DENSITY MODELS OF THE LOWER IONOSPHERE	84
7. SUMMARY	87
REFERENCES	88

Illustrations

1.	Brazilian Air Force High Resolution VLF/LF Ionosounding Transmitter Site in Paula Freitas, Brazil.	2
2.	Transmitting and Receiving Field Sites for the May-June 1980 Measurements.	3
3.	Basic VLF/LF Ionosounding Technique.	5
4.	Orthogonal Loop Antennas used During Experiment (Small Loop used to Induce Calibration Signals). Site Pictured was at Blumenau, Brazil.	6
5.	Example of Observed Waveforms.	7
6.	Fourier Spectrum for Groundwave Pulse Shown in Figure 5.	7
7.	Example of 3-Dimensional Display of Groundwave and Normal Skywave Pulses Received at Canasvieiras Stacked Front to Back with Advancing Time.	9
8.	Example of Group Heights of Reflection and Normal Reflection Coefficients Derived from Data Presented in Figure 7. Group Heights Calculated from Data at 30.5 kHz and Normal Reflection Coefficients Calculated at 15, 30, 45 and 60 kHz.	10
9.	Example of Group Heights of Reflection and Normal Reflection Coefficients vs Frequency at Local Midnight (a) and Local Noon (b) Derived from Data of 16 May (Day of Year 137) 1980.	11
10.	Solar Zenith Angle Variations for the Transmitter at Paula Freitas During the Measurements Between 8 May and 27 June, 1980.	13
11.	Path Parameters for Paula Freitas to Dr. Pedrinho	15
11.1.	Three-Dimensional Display of Data Received at Dr. Pedrinho.	
	a. Normal Skywave.	16
	b. Converted Skywave.	17

Illustrations

11.2. Group Heights of Reflection and Reflection Coefficients vs Frequency Derived from Data Received at Dr. Pedrinho.	
a. Local Midnight (0315 UT).	18
b. Local Noon (1515 UT).	18
11.3. Group Heights of Reflection and Reflection Coefficients vs Frequency Derived from Data Received at Dr. Pedrinho.	
a. Local Midnight (0315 UT).	19
b. Local Noon (1515 UT).	20
11.4. Averaged Values of Group Heights of Reflection and Reflection Coefficients vs. Frequency Derived from Data Received at Dr. Pedrinho.	
a. Group Heights of Reflection.	21
b. Reflection Coefficients.	21
12. Path Parameters for Paula Freitas to Timbo.	23
12.1. Three-Dimensional Display of Data Received at Timbo.	
a. Normal Skywave.	24
b. Converted Skywave.	25
12.2. Group Heights of Reflection for 30.5 kHz and Reflection Coefficients at 15, 30, 45 and 60 kHz from Data Received at Timbo.	
a. Normal Skywave.	26
b. Converted Skywave.	26
12.3. Group Heights of Reflection and Reflection Coefficients vs Frequency Derived from Data Received at Timbo.	
a. Local Midnight (0315 UT).	27
b. Local Noon (1515 UT).	28
12.4. Averaged Values of Group Heights of Reflection and Reflection Coefficients vs Frequency Derived from Data Received at Timbo.	
a. Group Heights of Reflection.	29
b. Reflection Coefficients.	29
13. Path Parameters for Paula Freitas to Blumenau.	31
13.1. Three-Dimensional Display of Data Received at Blumenau.	
a. Normal Skywave.	32
b. Converted Skywave.	34
13.2. Group Heights of Reflection for 30.5 kHz and Reflection Coefficients at 15, 30, 45 and 60 kHz from Data Received at Blumenau.	
a. Normal Skywave.	35
b. Converted Skywave.	35

Illustrations

13.3. Group Heights of Reflection and Reflection Coefficients vs Frequency Derived from Data Received at Blumenau.	
a. Local Midnight (0315 UT).	36
b. Local Noon (1515 UT).	37
13.4. Averaged Values of Group Heights of Reflection and Reflection Coefficients vs Frequency Derived from Data Received at Blumenau.	
a. Group Heights of Reflection.	38
b. Reflection Coefficients.	38
14. Path Parameters for Paula Freitas to Gaspar.	39
14.1. Three-Dimensional Display of Normal Skywave Data Received at Gaspar.	40
14.2. Group Heights of Reflection for 30.5 kHz and Reflection Coefficients at 15, 30, 45 and 60 kHz Derived from Normal Skywave Data Received at Gaspar.	44
14.3. Group Heights of Reflection and Reflection Coefficients vs Frequency Derived from Data Received at Gaspar.	
a. Local Midnight (0315 UT).	45
b. Local Noon (1515 UT).	45
14.4. Averaged Values of Group Heights of Reflection and Reflection Coefficients vs Frequency Derived from Data Received at Gaspar.	
a. Group Heights of Reflection.	46
b. Reflection Coefficients.	46
15. Path Parameters for Paula Freitas to Camboriu.	47
15.1. Three-Dimensional Display of Normal Skywave Data Received at Camboriu.	48
15.2. Group Heights of Reflection for 30.5 kHz and Reflection Coefficients at 15, 30, 45 and 60 kHz Derived from Normal Skywave Data Received at Camboriu.	52
15.3. Group Heights of Reflection and Reflection Coefficients vs Frequency Derived from Data Received at Camboriu.	
a. Local Midnight (0315 UT).	53
b. Local Noon (1515 UT).	53
15.4. Averaged Values of Group Heights of Reflection and Reflection Coefficients vs Frequency Derived from Data Received at Camboriu.	
a. Group Heights of Reflection.	54
b. Reflection Coefficients.	54
16. Path Parameters for Paula Freitas to Canasvieiras.	55
16.1. Three-Dimensional Display of Normal Skywave Data Received at Canasvieiras.	56
16.2. Group Heights of Reflection for 30.5 kHz and Reflection Coefficients at 15, 30, 45 and 60 kHz Derived from Normal Skywave Data Received at Canasvieiras.	56

Illustrations

16.3. Group Heights of Reflection and Reflection Coefficients vs Frequency Derived from Data Received at Canasvieiras.	
a. Local Midnight (0315 UT).	57
b. Local Noon (1515 UT).	57
16.4. Averaged Values of Group Heights of Reflection and Reflection Coefficients vs Frequency Derived from Data Received at Canasvieiras.	
a. Group Heights of Reflection.	58
b. Reflection Coefficients.	58
17. Path Parameters for Paula Freitas to Figueira.	59
17.1. Three-Dimensional Display of Normal Skywave Data Received at Figueira.	60
17.2. Group Heights of Reflection for 30.5 kHz and Reflection Coefficients at 15, 30, 45 and 60 kHz Derived from Normal Skywave Data Received at Figueira.	61
17.3. Group Heights of Reflection and Reflection Coefficients vs Frequency Derived from Data Received at Figueira.	
a. Local Midnight (0315 UT).	62
b. Local Noon (1515 UT).	62
17.4. Averaged Values of Group Heights of Reflection and Reflection Coefficients vs Frequency Derived from Data Received at Figueira.	
a. Group Heights of Reflection.	63
b. Reflection Coefficients.	63
18. Path Parameters for Paula Freitas to Pinhalzinho.	65
18.1. Three-Dimensional Display of Normal Skywave Data Received at Pinhalzinho.	66
18.2. Group Heights of Reflection for 30.5 kHz and Reflection Coefficients at 15, 30, 45 and 60 kHz Derived from Normal Skywave Data Received at Pinhalzinho.	66
18.3. Group Heights of Reflection and Reflection Coefficients vs Frequency Derived from Data Received at Pinhalzinho.	
a. Local Midnight (0315 UT).	67
b. Local Noon (1515 UT).	67
18.4. Averaged Values of Group Heights of Reflection and Reflection Coefficients vs Frequency Derived from Data Received at Pinhalzinho.	
a. Group Heights of Reflection.	68
b. Reflection Coefficients.	68
19. Path Parameters for Paula Freitas to Irai.	69
19.1. Three-Dimensional Display of Normal Skywave Data Received at Irai.	70

Illustrations

19.2. Group Heights of Reflection for 30.5 kHz and Reflection Coefficients at 15, 30, 45 and 60 kHz Derived from Normal Skywave Data Received at Irai.	70
19.3. Group Heights of Reflection and Reflection Coefficients vs Frequency Derived from Data Received at Irai.	
a. Local Midnight (0315 UT).	71
b. Local Noon (1515 UT).	71
19.4. Averaged Values of Group Heights of Reflection and Reflection Coefficients vs Frequency Derived from Data Received at Irai.	
a. Group Heights of Reflection.	72
b. Reflection Coefficients.	72
20. Summary of Noon and Midnight Group Heights of Reflection Derived from Data Obtained at all the Receiving Locations.	74
21. Normal Reflection Coefficients for Midnight and Noon Derived from Data at Selected Locations to the East and West of the Transmitter.	
a. Approximately 200 km Propagation Paths (Paula Freitas to Blumenau/Figueira).	75
b. Approximately 215 km Propagation Paths (Paula Freitas to Gaspar/Pinhalzinho).	75
c. Approximately 250 km Propagation Paths (Paula Freitas to Camboriu/Irai).	75
22. Variation in Normal Reflection Coefficients with Range and Angle of Incidence for Locations East of the Transmitter.	77
23. Normal Reflection Coefficients for 20 kHz Derived from Midnight and Noon Data Obtained at Receiving Locations to the East and West of the Transmitter.	78
24. Normal and Converted Reflection Coefficients Derived from Midnight and Noon Data from Three Locations East of the Transmitter.	79
25. Data Obtained at Camboriu Showing Weak Reflections (Circled Areas) from Altitudes Below the Normal D-Region.	81
26. Data Recorded on 17 May (Day 138) 1980 at Timbo, Camboriu and Canasvieiras.	
a. Normal Skywave Data Showing Weak Reflections Below the Normal D-Region (C).	82
b. Normal Reflection Coefficients Derived from the "C" Portions of the Received Skywaves.	82
27. Data Obtained at Camboriu Showing Moving Reflections (Circled Areas) During the Nighttime Coming from Relatively High Altitudes Above the D-Region.	85
28. Electron Density Profiles of Low Latitude Ionosphere Derived from the VLF/LF Reflection Data Gathered During this Series of Measurements.	86

Table

1. Locations and Propagation Path Parameters of the Transmitting and Receiving Locations for the Experiment.

12

VFL/LF Reflection Properties of the Low Latitude Ionosphere

1. INTRODUCTION

This report summarizes data describing the longwave reflection properties of the low-latitude ionosphere in Brazil, obtained during an experimental program conducted jointly by the Air Forces of the United States and Brazil. The data were obtained during May and June of 1980 in southern Brazil using a unique VLF/LF pulse-ionosounding system operated by the Brazilian Air Force. The transmitter of the ionosounder was located near Paula Freitas (see Figures 1 and 2), and three portable receiving systems were used to obtain measurements at nine locations to the east and west of it, at distances ranging from 156 km to 280 km, as indicated in Figure 2.

2. VLF/LF IONOSOUNDING TECHNIQUE

Details of the VLF/LF pulse-ionosounding technique are given in a number of reports describing its use in other experiments conducted at low-, mid-, and high-latitudes (Rasmussen et al¹, Lewis et

(Received for publication on 25 January 1988)

1. Rasmussen, J.E., Lewis, E.A., Kossey, P.A., Reginaldo Dos Santos, Edsel De Freitas Coutinho, Kahler, R.C., and Klemetti, W.I. (1975) *Low Frequency Wave-Reflection Properties of the Equatorial Ionosphere*, AFCRL-TR-75-0615, AD A025111.



Figure 1. Brazilian Air Force High Resolution VLF/LF Ionosounding Transmitter Site At Paula Freitas, Brazil.

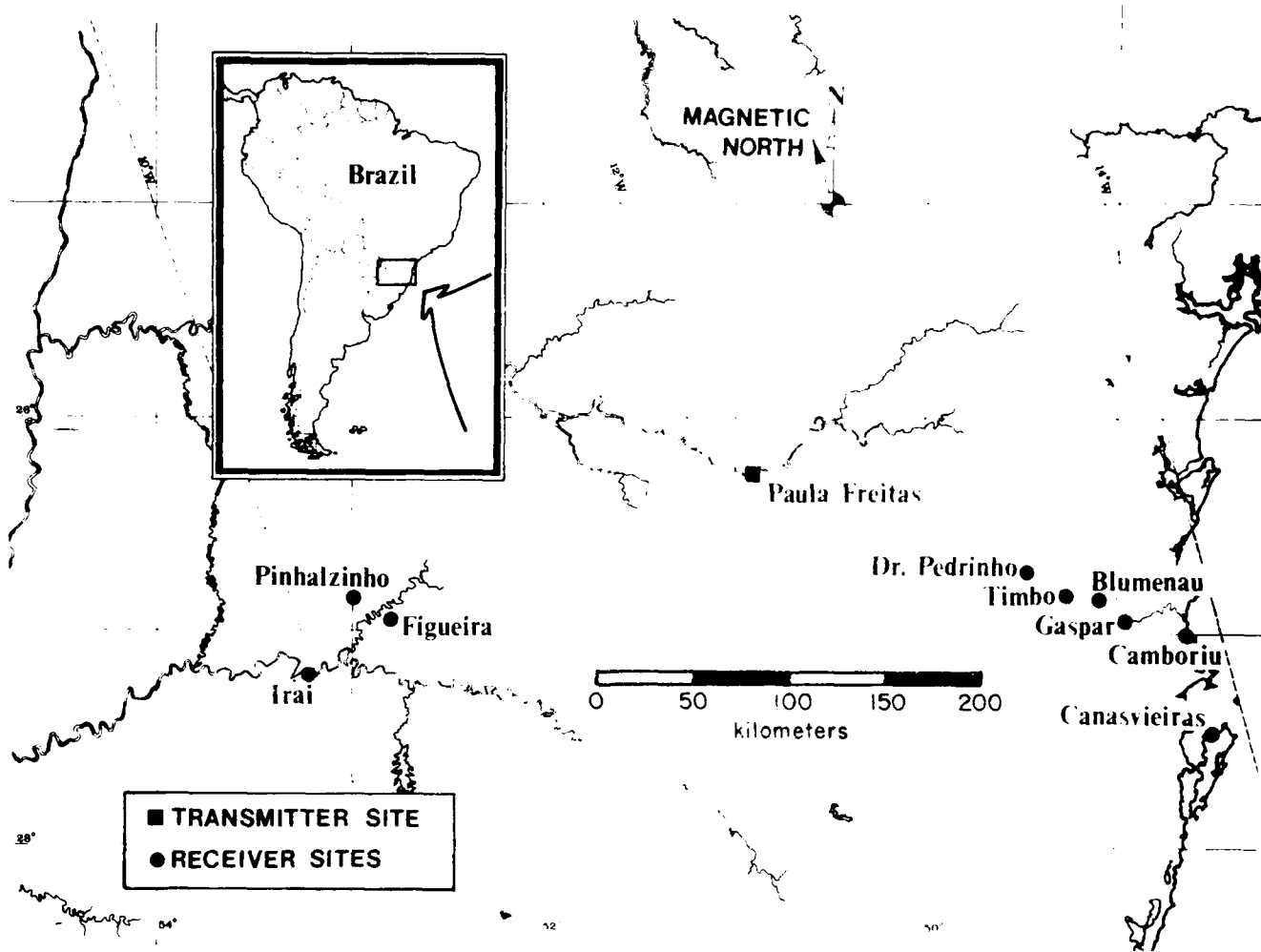


Figure 2. Transmitting and Receiving Field Sites for the May-June 1980 Measurements.

al², and Kossey et al³, respectively). Figure 3 illustrates the technique. The transmissions consist of a series of extremely short pulses (55 μ sec for the experiment in Brazil), precisely controlled by a cesium beam time standard, and radiated from a vertical antenna (130 m in Brazil). The transmitted pulses are so short that, for distances out to several hundred kilometers, the groundwaves arrive and are recorded before the arrival of the ionospherically reflected skywaves. Thus, data are received free of ambiguities arising from groundwave and skywave interference. The transmitted pulses are vertically polarized, but because of the effects of the geomagnetic field the reflected skywaves are elliptically polarized. Separate loop antennas are used to sense the so-called "normal" (\parallel -) and "converted" (\perp -) components of the downcoming skywaves. One antenna, with its axis oriented in the plane of propagation, senses the groundwaves and the normal components of the skywaves, while the other antenna, orthogonal to it, is nulled on the groundwaves and senses the converted components of the skywaves. Examples of the loop antennas used in Brazil are shown in Figure 4.

Figure 5 gives typical examples of groundwave and skywave pulses received in Brazil. The separation in time between the normal skywave pulse and the groundwave pulse, which is a feature of the ionosounding technique, is illustrated clearly in the figure. Figure 6 shows the Fourier spectrum of a transmitted pulse to illustrate the wide range of VLF/LF frequencies which were available to probe the ionosphere. In practice, the pulses were transmitted at a precisely controlled repetition rate of 399 pulses/sec, so that the spectrum of the received pulses consisted of discrete frequency components, 399 Hz apart.

As described by Lewis et al² (op. cit.), after Fourier analyses of the received pulses, the group delays between the skywaves and groundwaves can be used to determine effective heights of the ionosphere; and, the relative amplitudes of the skywave and groundwave frequency components can be used to determine magnitudes of the normal ($\parallel R_{\parallel}$) and converted ($\parallel R_{\perp}$) reflection coefficients of the ionosphere⁴. The experiments in Brazil yielded ionospheric reflection heights and effective plane-wave reflection coefficients over a range of about 15-65 kHz. Such data provide a means for developing phenomenological models of the lower ionosphere, useful for VLF/LF propagation prediction purposes.

3. DATA DISPLAY AND REDUCTION FORMATS

Three formats have been chosen for representing the data obtained during the experiments, and for describing the VLF/LF reflection properties of the lower ionosphere that were derived from it. A

-
2. Lewis, E.A., Rasmussen, J.E., and Kossey, P.A. (1973) Measurements of ionospheric reflectivity from 6 to 35 kHz, *J. Geophys. Res.* **78**: 3903-3912.
 3. Kossey, P.A., Turtle, J.P., Pagliarulo, R.P., Klemetti, W.I., and Rasmussen, J.E. (1983) VLF reflection properties of the normal and disturbed polar ionosphere in northern Greenland, *Radio Sci.* **18**: 907-916.
 4. Bracewell, R.N., Budden, K.G., Ratcliffe, J.A., Straker, T.W., and Weekes, K. (1951) The ionospheric propagation of low- and very-low-frequency radio waves over distances less than 1000 km, *Proc. Inst. Electr. Eng.* **98**(III), 221-236.

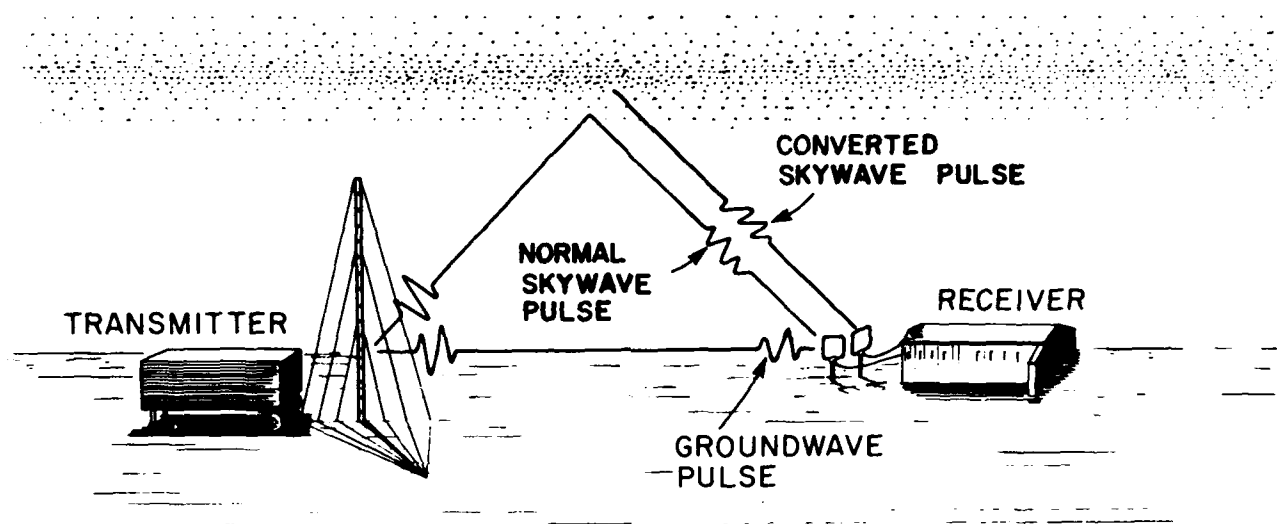


Figure 3. Basic VLF/LF Ionosounding Technique.

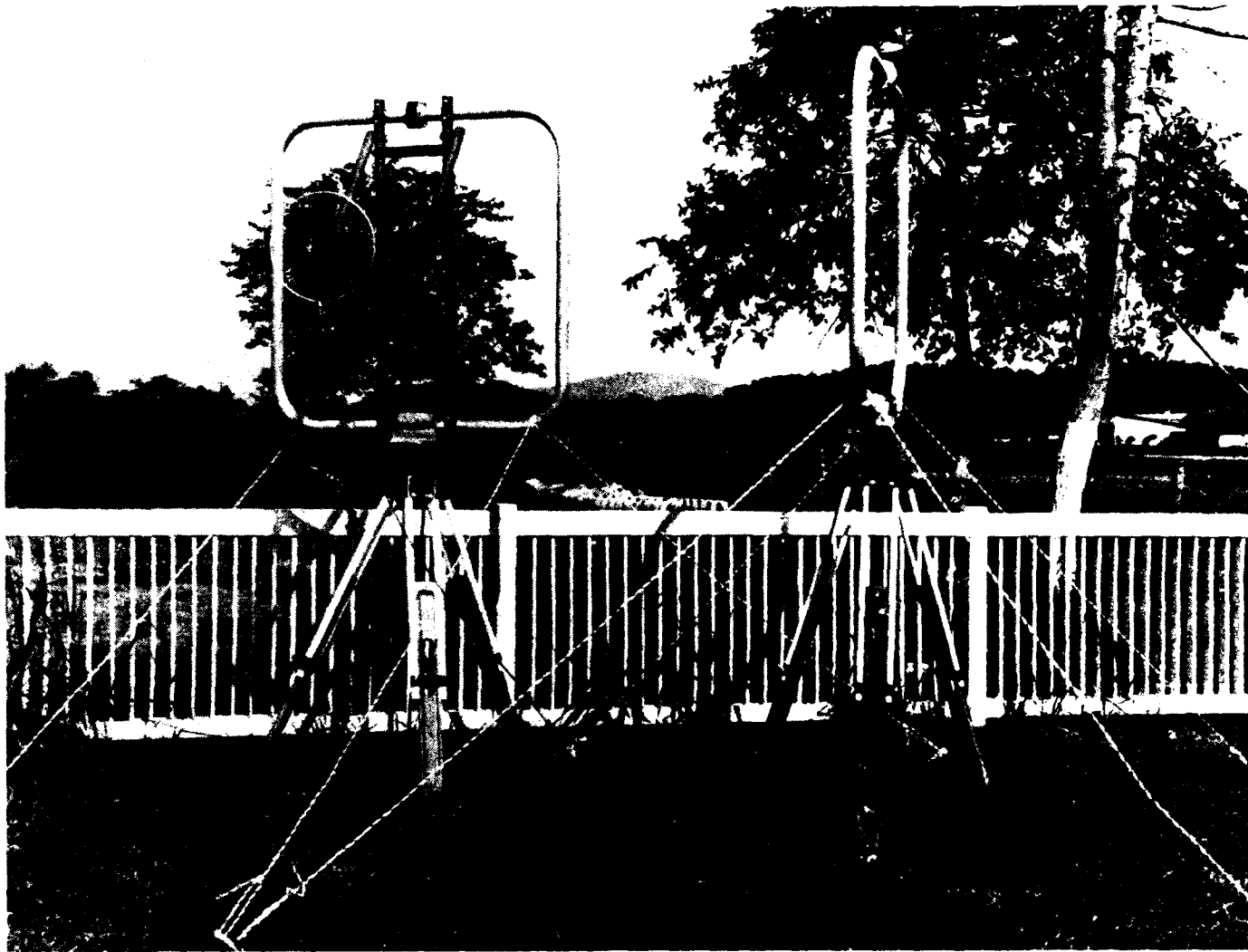


Figure 4. Orthogonal Loop Antennas Used During Experiment (Small Loop Used to Induce Calibration Signals). Site Pictured was at Blumenau, Brazil.

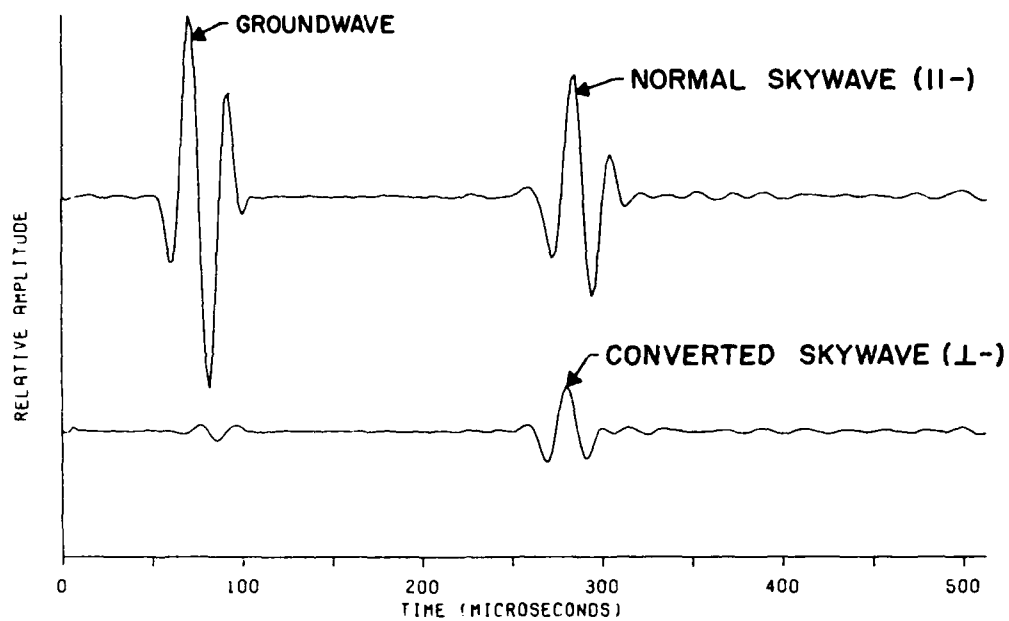


Figure 5. Example of Observed Waveforms.

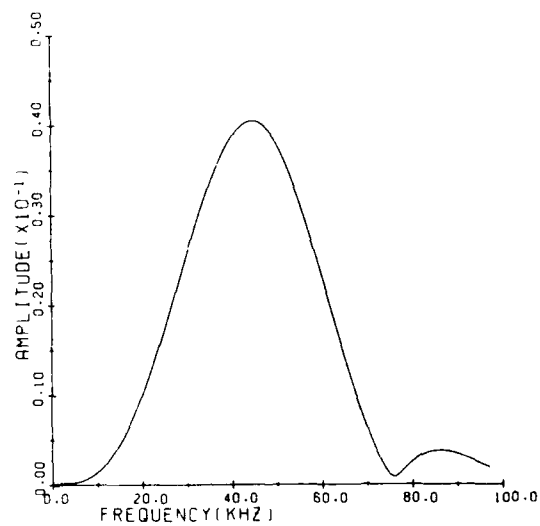


Figure 6. Fourier Spectrum for Groundwave Pulse Shown in Figure 5.

brief description and a few samples of the data formats are given below; following that, data obtained at each of the nine receiving locations are presented.

3.1. Three-Dimensional Data Displays

Figure 7 shows a three-dimensional presentation of a sample of data to illustrate the manner in which data from each receiving location were acquired and initially displayed. The presentation consists of waveforms stacked one-behind-the-other, with time progressing linearly from bottom-to-top, for (in this example) a three-day period. Although the raw data were recorded every 2.8 minutes, for display purposes each waveform in the figure represents a 15 minute-average of approximately 325,000 pulses. The horizontal scale is linear in time, measured from the start of the groundwaves. The groundwaves remain fixed in time, while the skywaves move back and forth in accordance with the solar zenith angle (and hence, in accordance with the varying effective height of the lower ionosphere). The waveforms represent the averaged wave amplitudes as a function of time, as sensed by the receiving-loop antennas. The data in Figure 7 correspond to the normal component of the ionospherically reflected waves. Similar displays are given later showing converted components of the reflected waves received at a number of locations during the experimental campaign.

3.2 Reflection Heights And Coefficients As A Function Of Time

Data, such as that illustrated in Figure 7, provide the bases for deriving effective heights of reflection and plane-wave reflection coefficients of the ionosphere, as outlined in Section 2 of this report. Figure 8 gives examples of reflection coefficients, plotted as a function of time for 15, 30, 45, and 60 kHz, as derived from the sample of data given in Figure 7. In doing this, the received skywave data were averaged over 2-hr intervals. Such data presentations are given to show longer-term trends in the data (days or weeks), rather than short-term characteristics (minutes or hours). Also shown in Figure 8 is a plot of the effective height of the lower ionosphere at 30.5 kHz, as derived from the same data.

3.3 Reflection Heights And Coefficients As A Function Of Frequency

By fixing a time (for example, local noon), the pulse reflection data can be used to derive effective heights of reflection and plane-wave reflection coefficients as a function of frequency. For example, Figure 9 illustrates the results of such an analysis, derived from the first day's data at local midnight and local noon, as shown in Figure 7. The data provide reflection properties of the lower ionosphere over a wide frequency range, from about 15-65 kHz. The resolution of the system is such that a change in the effective height of the ionosphere by as little as 0.5 km can be discerned. In addition, reflection coefficients as small as about 0.02 in amplitude can be determined. Data such as that shown in Figure 9 were derived from 15-min averages of the raw data.

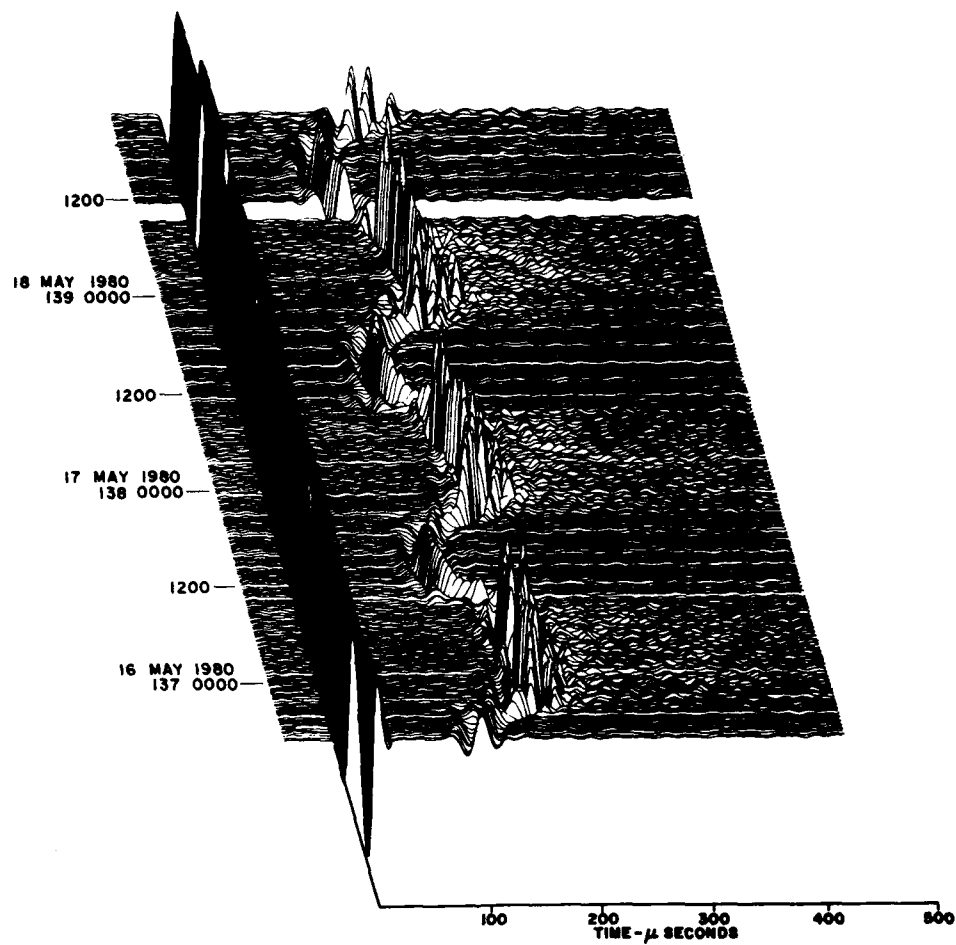


Figure 7. Example of 3-Dimensional Display of Groundwave and Normal Skywave Pulses Received at Canasvieiras Stacked Front to Back with Advancing Time.

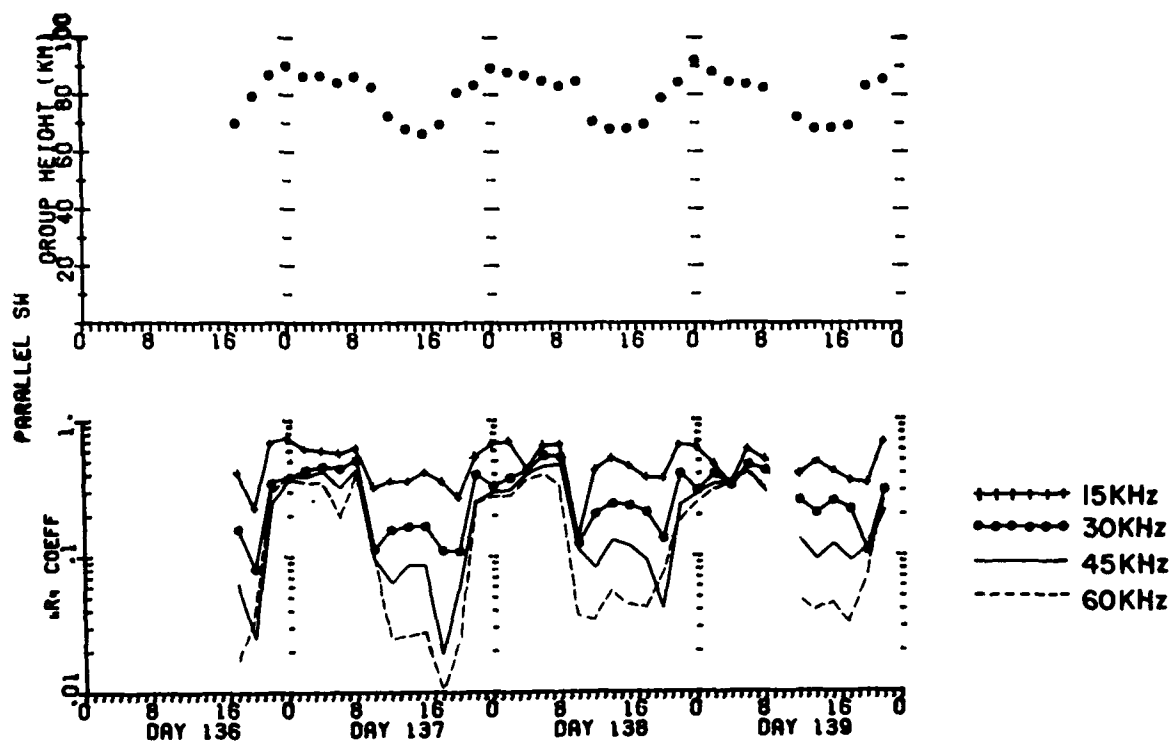
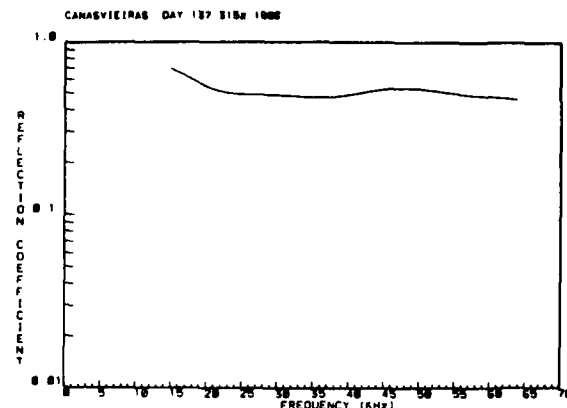
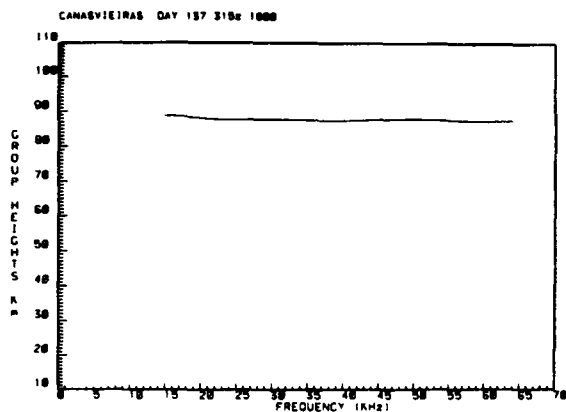
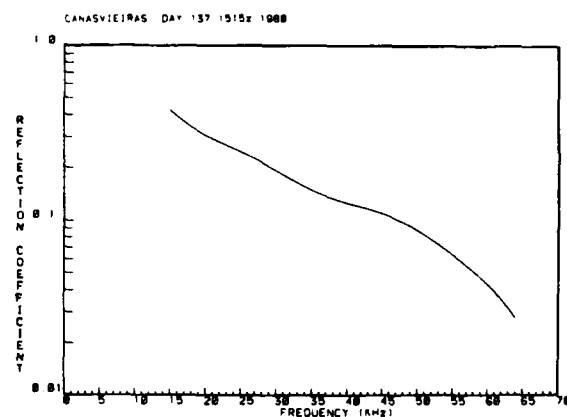
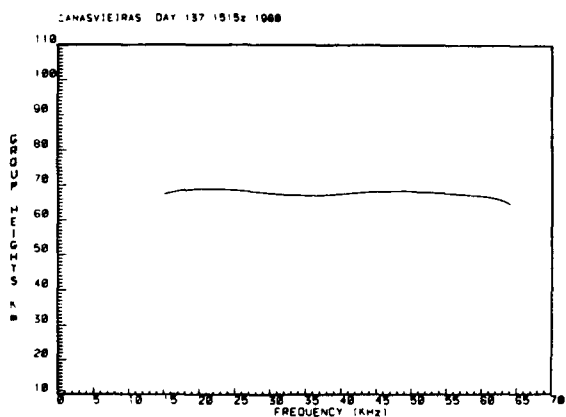


Figure 8. Example of Group Heights of Reflection and Normal Reflection Coefficients Derived from Data Presented in Figure 7. Group Heights Calculated from Data at 30.5 kHz and Normal Reflection Coefficients Calculated at 15, 30, 45 and 60 kHz.



a. LOCAL MIDNIGHT



b. LOCAL NOON

Figure 9. Example of Group Heights of Reflection and Normal Reflection Coefficients vs Frequency at Local Midnight (a) and Local Noon (b) Derived from Data of 16 May (Day of Year 137) 1980.

4. DATA FROM EACH OF THE RECEIVING LOCATIONS

In this section the data obtained during the experiment in Brazil are displayed. The data were taken during the late fall and early winter, when the day-to-day variations in the solar zenith angles, as a function of time of day, were not large and the periods of sunlight and darkness were about equal, as shown in Figure 10. In the presentations that follow, the displays parallel those described in Section 3; specifically: three-dimensional displays of the data are first shown; these are followed by plots of effective heights of reflection (at 30.5 kHz) and plane-wave reflection coefficients (at 15, 30, 45, and 60 kHz), as a function of time; finally, reflection heights and reflection coefficients are given, as a function of frequency, for local midnight and local noon for the days data were obtained at each receiving site. Table 1 gives the geomagnetic coordinates, the great-circle propagation distances, and the magnetic azimuths from the transmitter to each receiving location. The specific periods for which data were acquired at each of the receiving locations are shown on charts immediately preceding the data displays for that location. Those charts also indicate if only the normal components of the reflected skywaves were received, or whether the converted components were received as well.

Table 1. Locations and Propagation Path Parameters
of the Transmitting and Receiving Locations for the Experiment.

SITE	COORDINATES		DISTANCE KM.	MAGNETIC AZIMUTH
TRANSMITTER				
PAULA FREITAS	26°15'S	50°57'W		
RECEIVER				
DR. PEDRINHO	26°43'S	49°29'W	156	123°
TIMBO	26°49'S	49°16'W	180	124°
BLUMENAU	26°50'S	49°05'W	197	122°
GASPAR	26°55'S	48°55'W	215	123°
CAMBORIU	27°00'S	48°37'W	246	123°
CANASVIEIRAS	27°26'S	48°28'W	280	132°
FIGUEIRA	26°53'S	52°50'W	200	260°
PINHALZINHO	26°51'S	52°59'W	213	262°
IRAI	27°11'S	53°15'W	250	256°

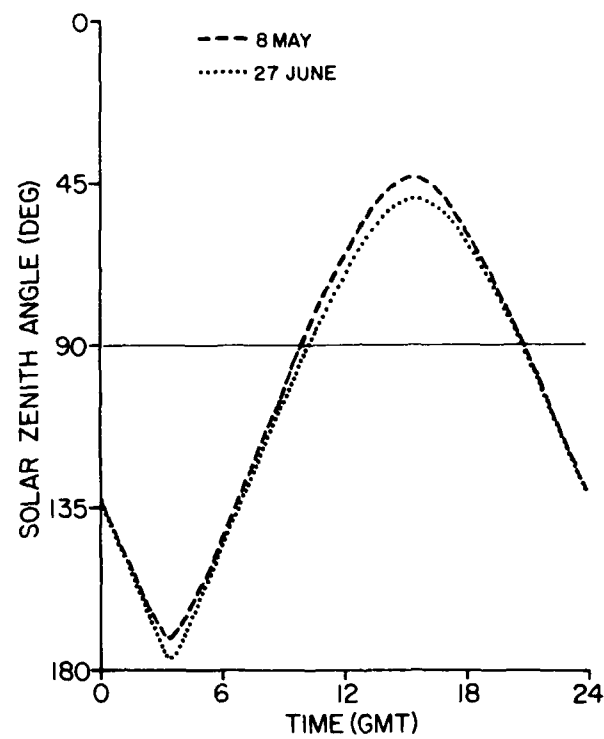


Figure 10. Solar Zenith Angle Variations for the Transmitter at Paula Freitas During the Measurements Between 8 May and 27 June, 1980.

DATA

PROPAGATION PATH: PAULA FREITAS TO DR. PEDRINHO (PF-PED)
DISTANCE; 156 KM
AZIMUTH: 123°
DATA: NORMAL AND CONVERTED POLARIZATIONS
MEASUREMENT PERIOD: 17 MAY - 21 MAY 1980

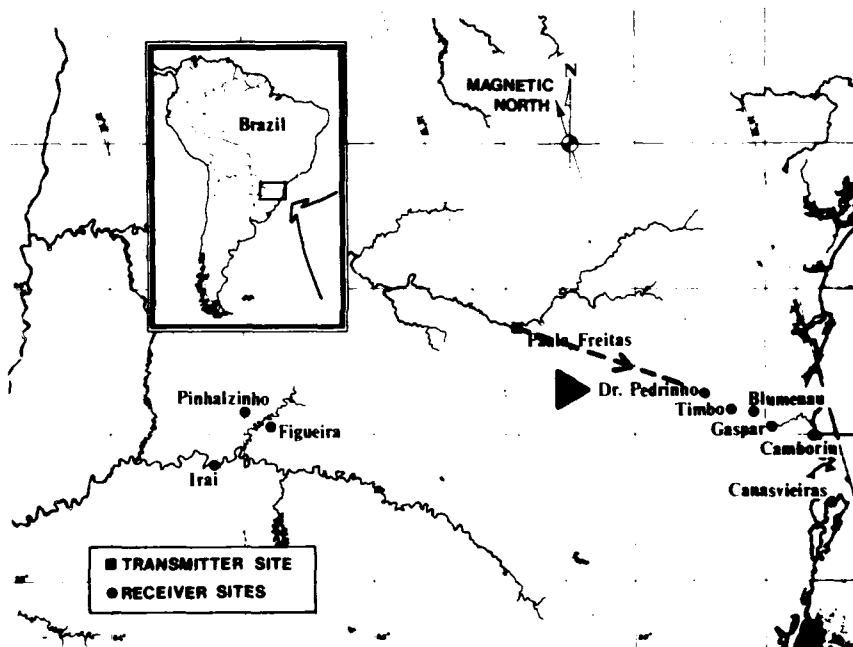


Figure 11. Path Parameters for Paula Freitas to Dr. Pedrinho.

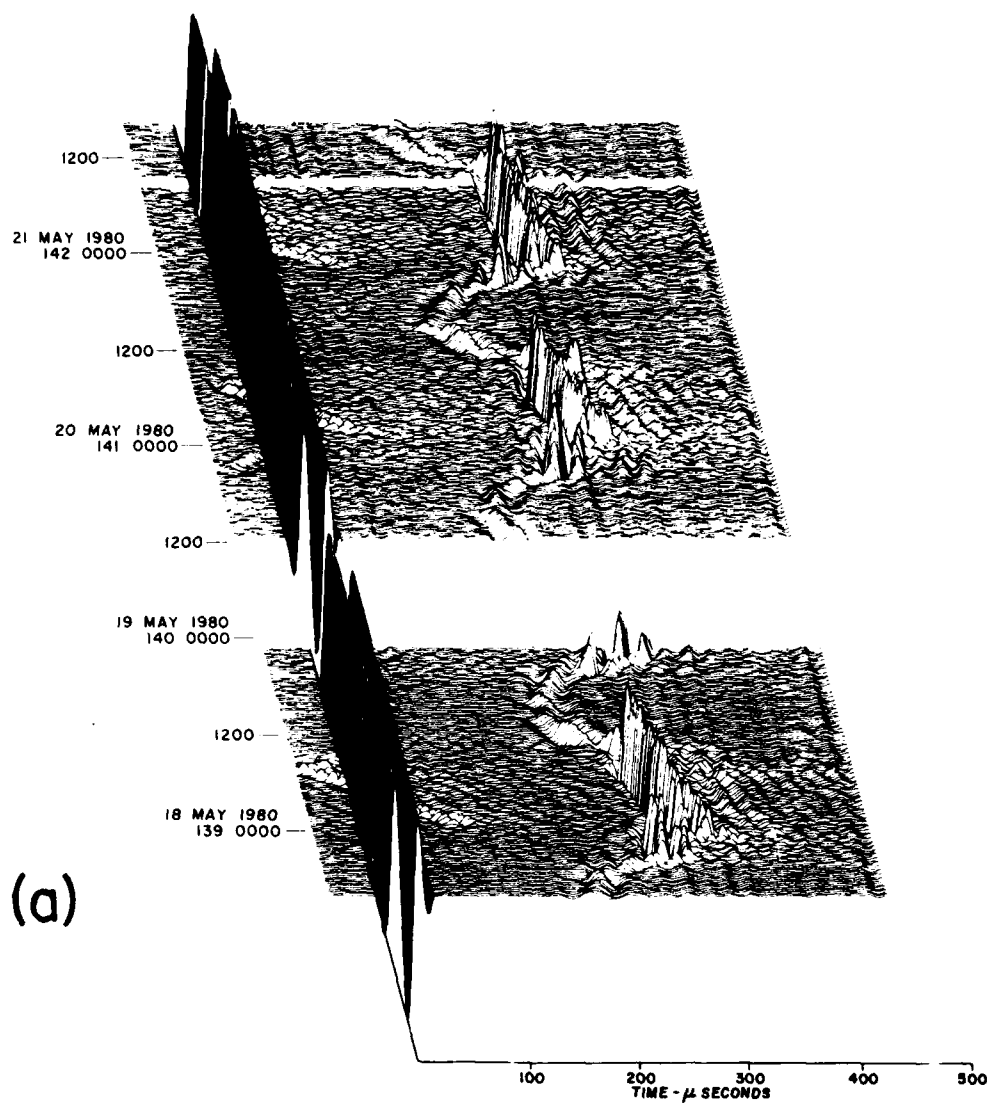


Figure 11.1. Three-Dimensional Display of Data Received at Dr. Pedrinho.

a. Normal Skywave.

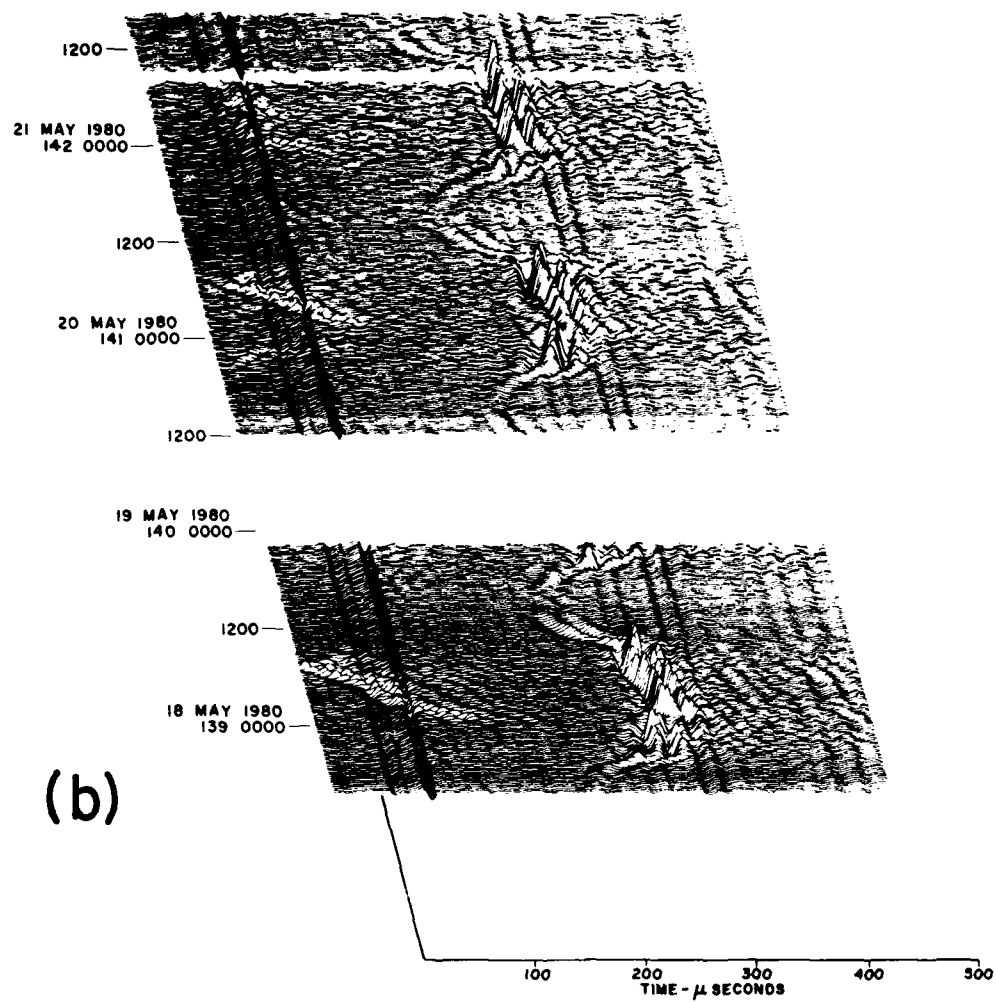
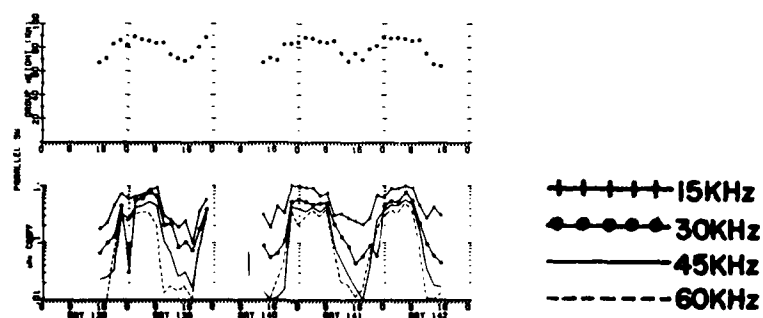
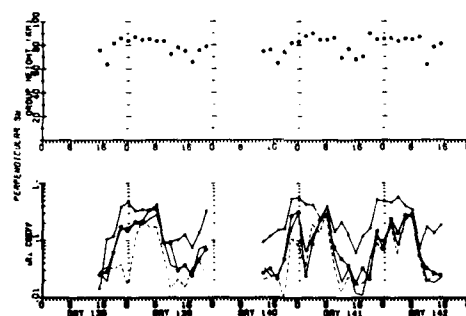


Figure 11.1. Three-Dimensional Display of Data Received at Dr. Pedrinho.

b. Converted Skywave.



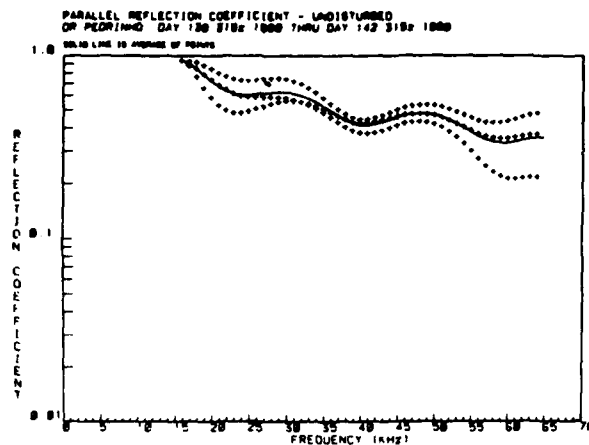
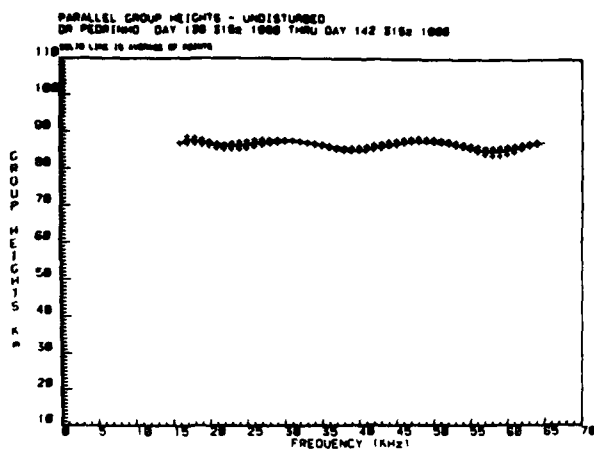
(a) NORMAL SKYWAVE



(b) CONVERTED SKYWAVE

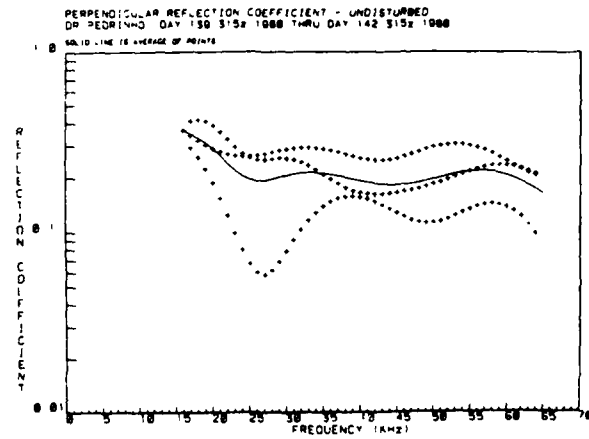
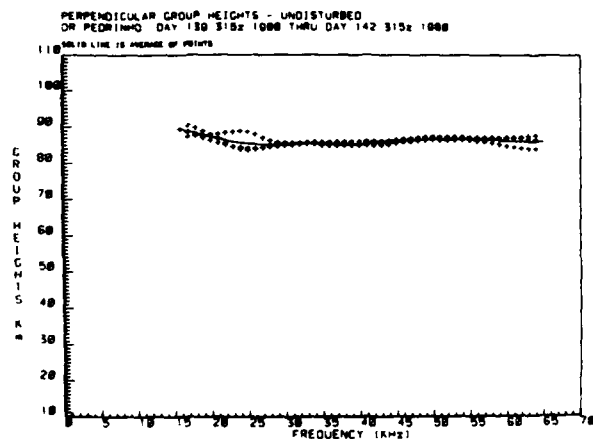
Figure 11.2. Group Heights of Reflection for 30.5 kHz and Reflection Coefficients at 15, 30, 45 and 60 kHz from Data Received at Dr. Pedrinho.

- a. Normal Skywave.
- b. Converted Skywave.



NORMAL SKYWAVE

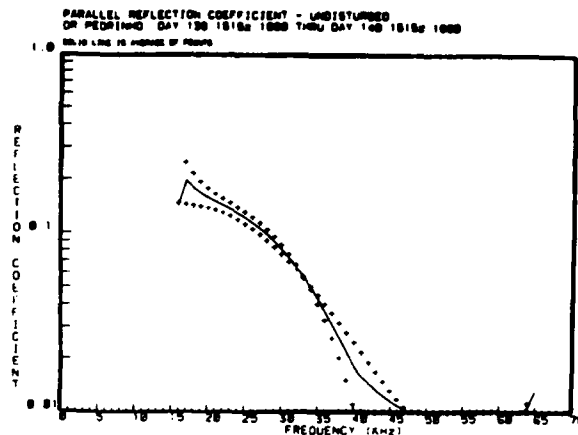
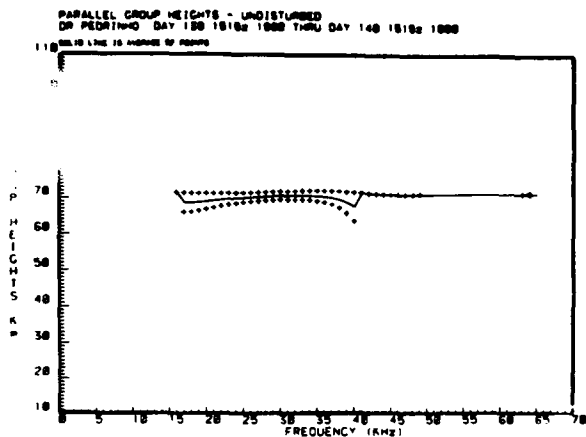
(a)



CONVERTED SKYWAVE

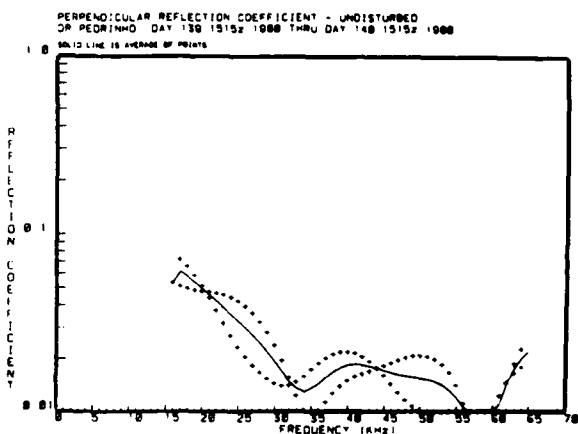
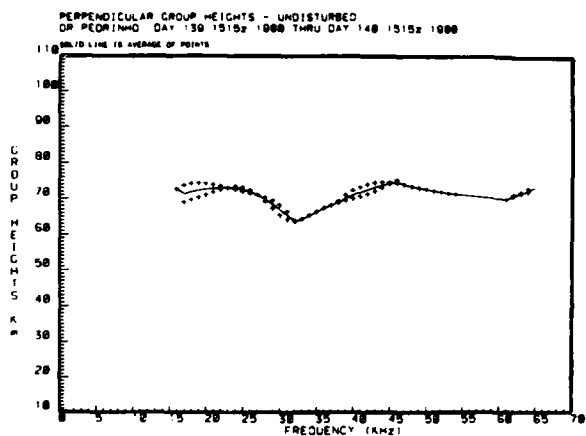
Figure 11.3. Group Heights of Reflection and Reflection Coefficients vs Frequency Derived from Data Received at Dr. Pedrinho.

a. Local Midnight (0315 UT)



NORMAL SKYWAVE

(b)



CONVERTED SKYWAVE

Figure 11.3. Group Heights of Reflection and Reflection Coefficients vs Frequency Derived from Data Received at Dr. Pedrinho.

b. Local Noon (1515 UT)

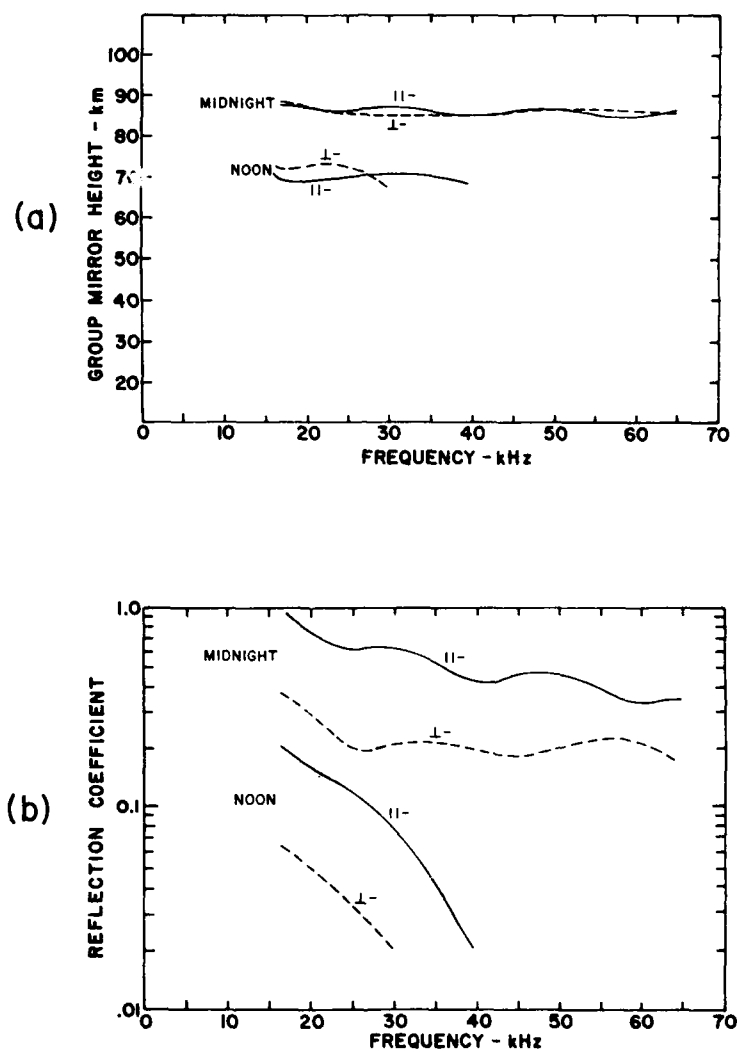


Figure 11.4. Averaged Values of Group Heights of Reflection and Reflection Coefficients vs Frequency Derived from Data Received at Dr. Pedrinho.

- a. Group Heights of Reflection.
- b. Reflection Coefficients.

DATA

PROPAGATION PATH: PAULA FREITAS TO TIMBO (PF-TIM)
DISTANCE: 180 KM
AZIMUTH: 124°
DATA: NORMAL AND CONVERTED POLARIZATIONS
MEASUREMENT PERIOD: 13 MAY - 17 MAY 1980

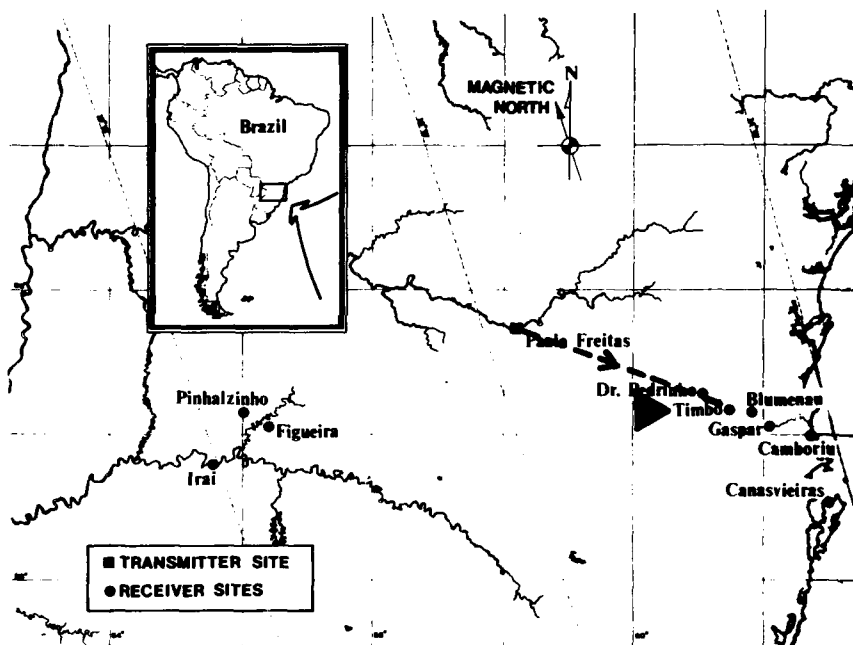


Figure 12. Path Parameters for Paula Freitas to Timbo.

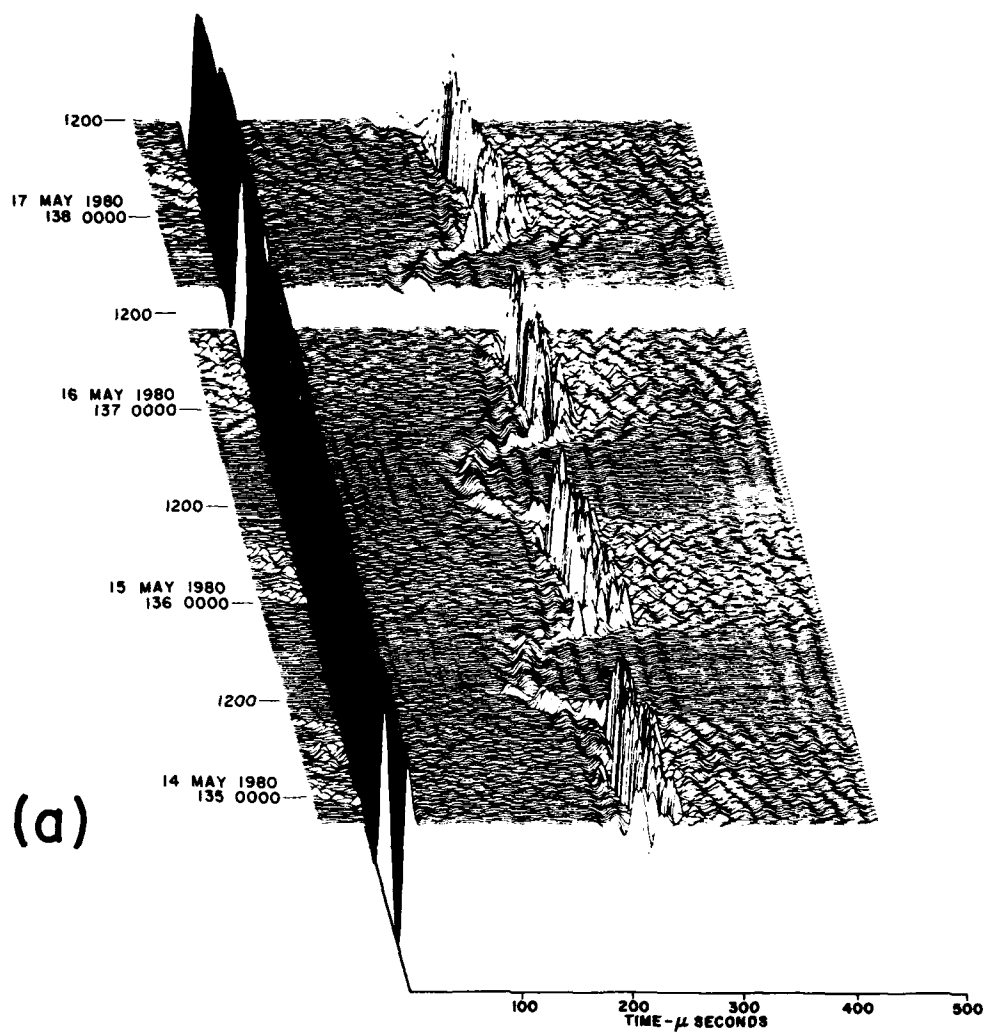


Figure 12.1. Three-Dimensional Display of Data Received at Timbo.

a. Normal Skywave.

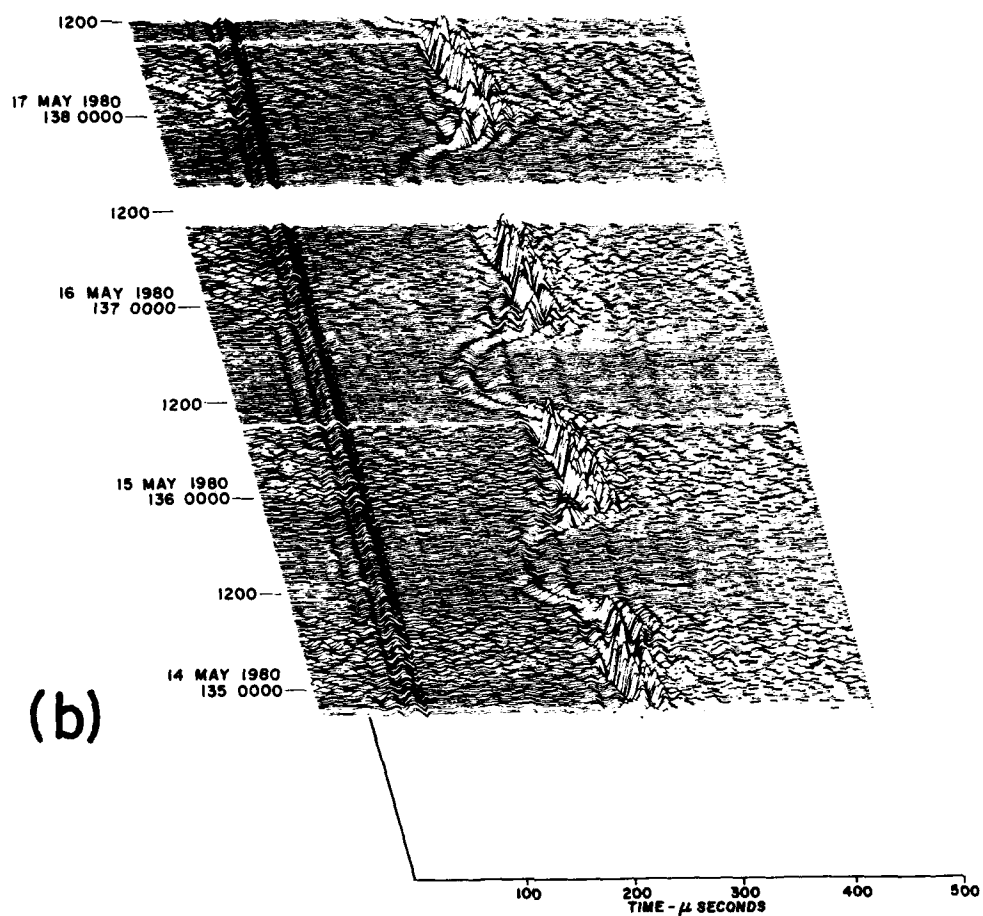
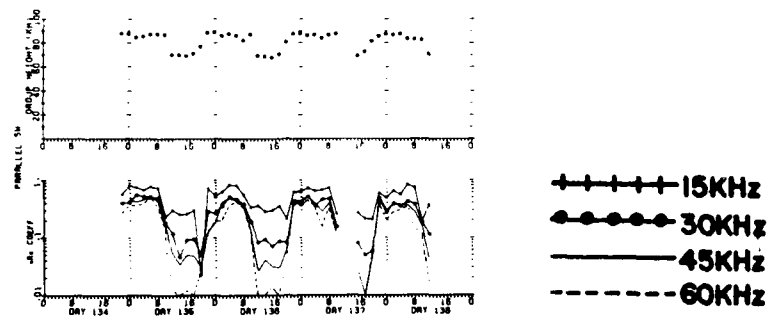
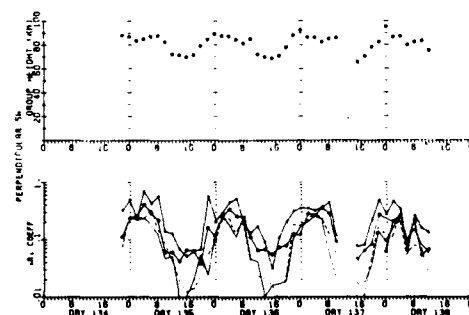


Figure 12.1. Three-Dimensional Display of Data Received at Timbo.

b. Converted Skywave.



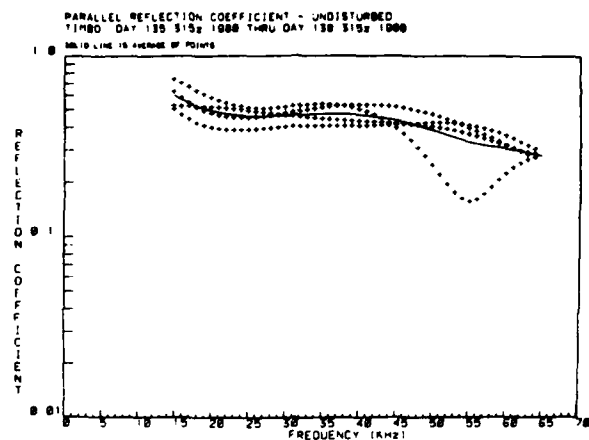
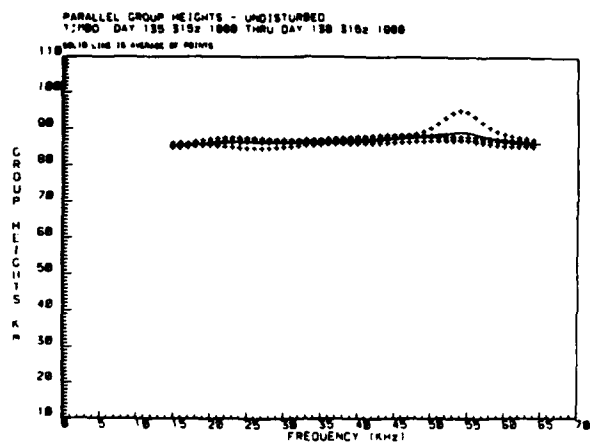
(a) NORMAL SKYWAVE



(b) CONVERTED SKYWAVE

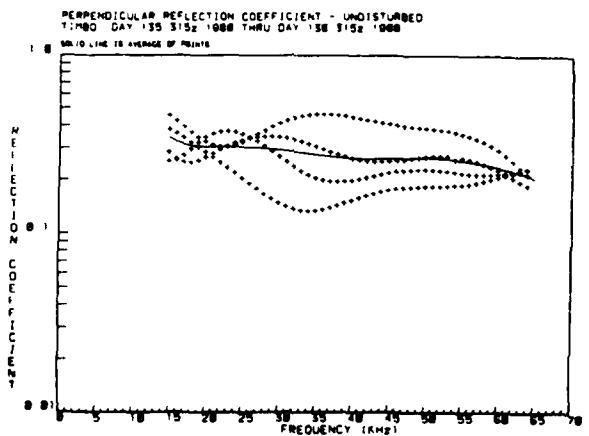
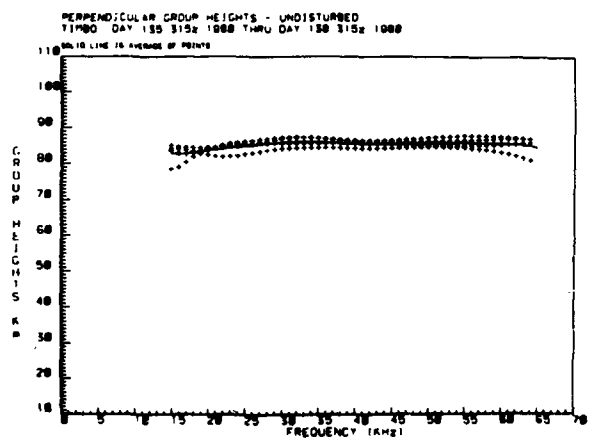
Figure 12.2. Group Heights of Reflection for 30.5 kHz and Reflection Coefficients at 15, 30, 45 and 60 kHz from Data Received at Timbo.

- a. Normal Skywave.
- b. Converted Skywave.



NORMAL SKYWAVE

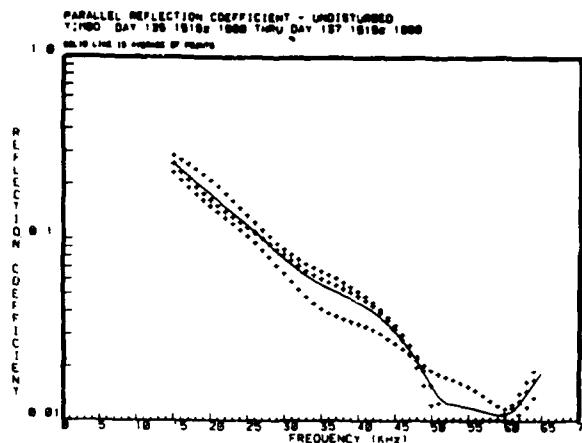
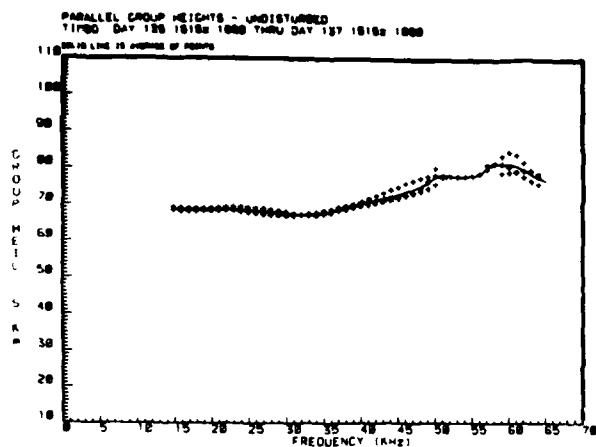
(a)



CONVERTED SKYWAVE

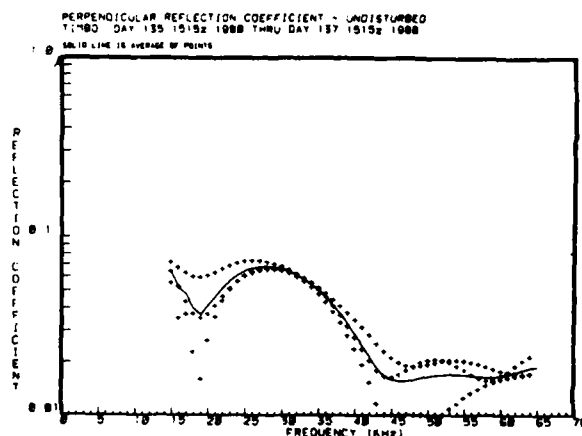
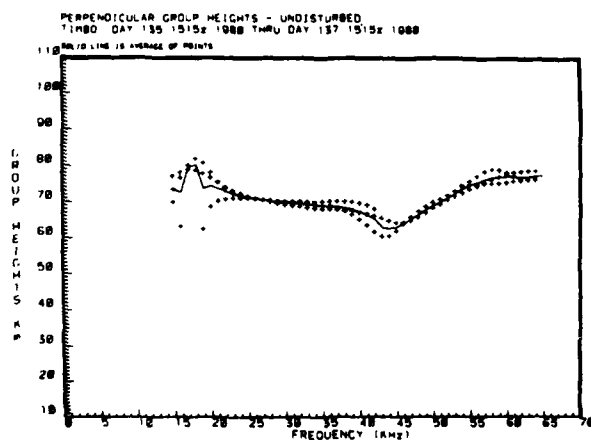
Figure 12.3. Group Heights of Reflection and Reflection Coefficients vs Frequency Derived from Data Received at Timbo.

a. Local Midnight (0315 UT).



NORMAL SKYWAVE

(b)



CONVERTED SKYWAVE

Figure 12.3. Group Heights of Reflection and Reflection Coefficients vs Frequency Derived from Data Received at Timbo.

b. Local Noon (1515 UT).

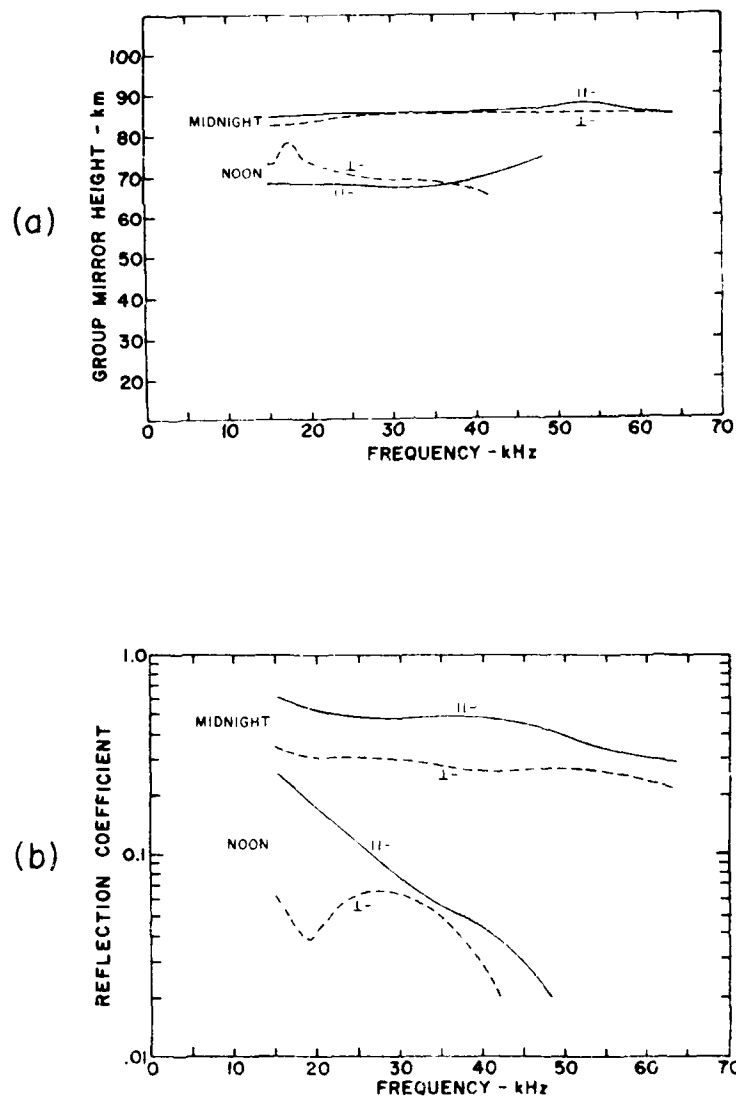


Figure 12.4. Averaged Values of Group Heights of Reflection and Reflection Coefficients vs Frequency Derived from Data Received at Timbo.

DATA

PROPAGATION PATH: PAULA FREITAS TO BLUMENAU (PF-BLU)
DISTANCE: 197 KM
AZIMUTH: 122°
DATA: NORMAL AND CONVERTED POLARIZATIONS
MEASUREMENT PERIOD: 21 MAY - 4 JUNE 1980

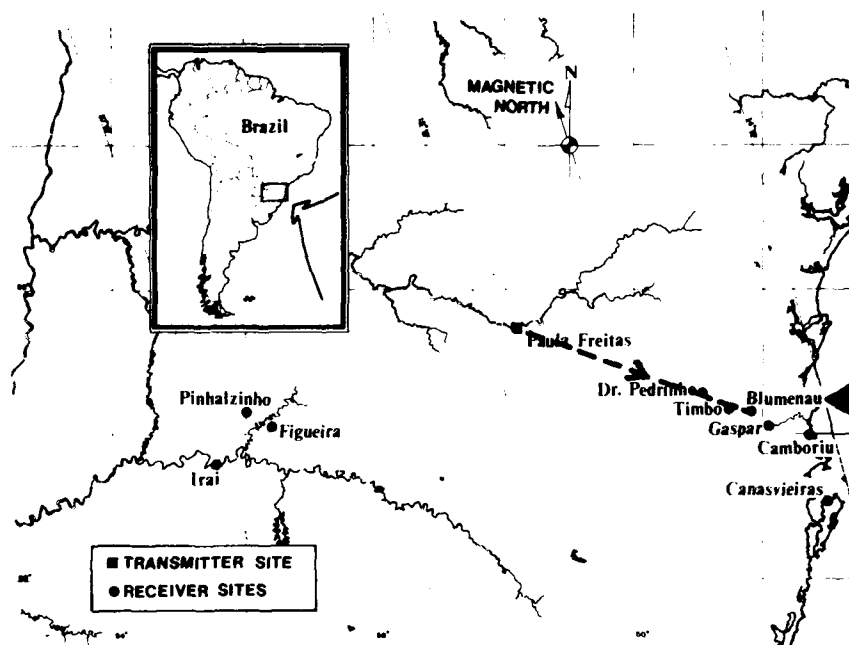


Figure 13. Path Parameters for Paula Freitas to Blumenau.

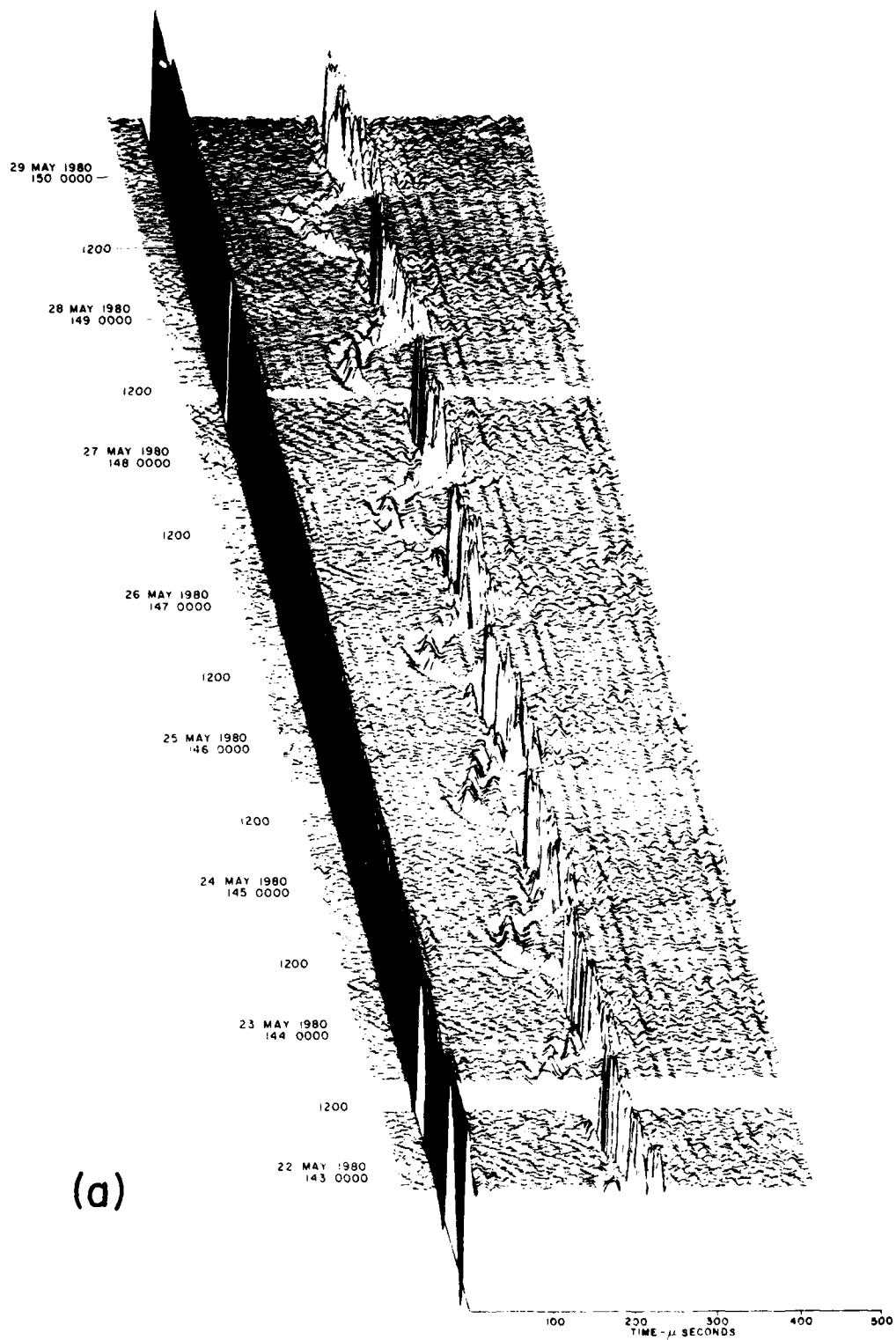


Figure 13.1. Three-Dimensional Display of Data Received at Blumenau.

a. Normal Skywave.

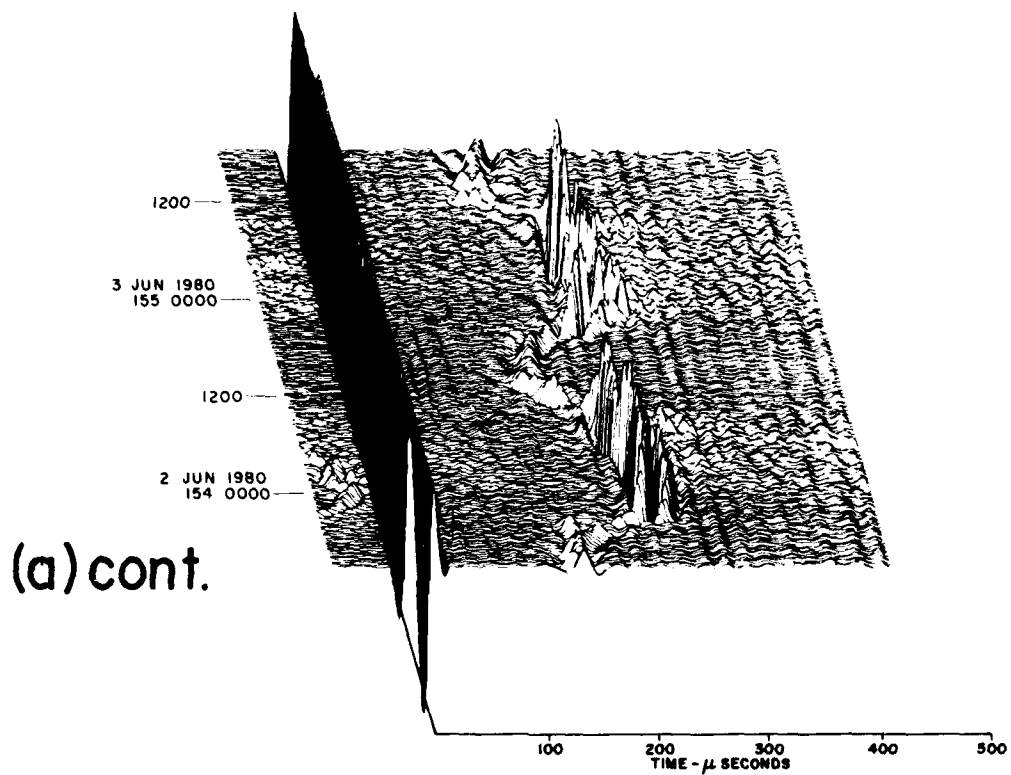


Figure 13.1. Three-Dimensional Display of Data Received at Blumenau.

a. Normal Skywave. (Cont.)

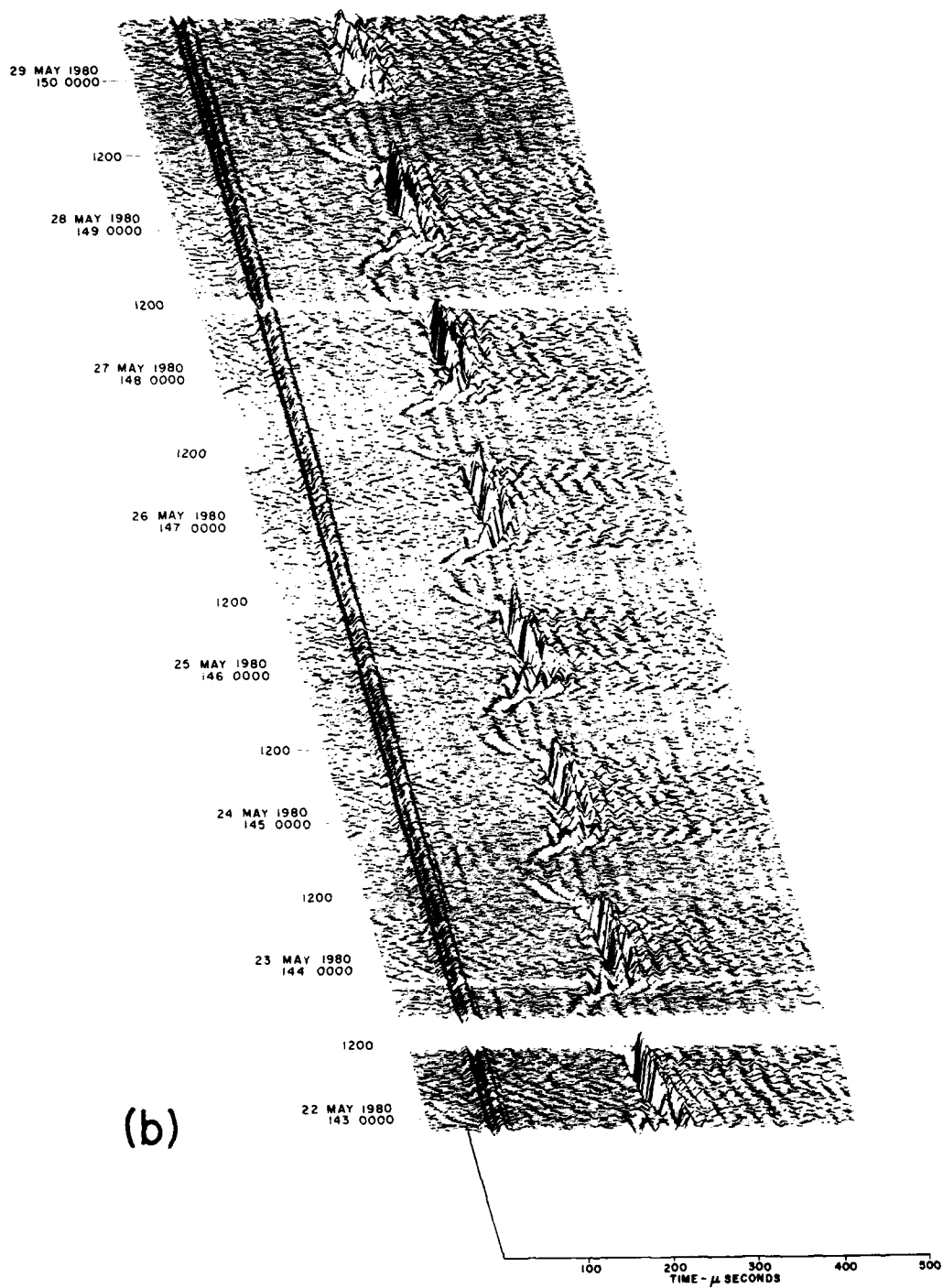
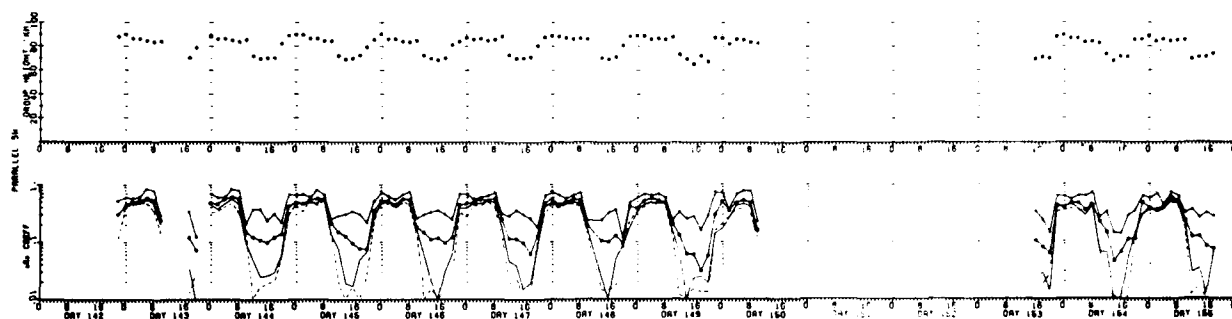
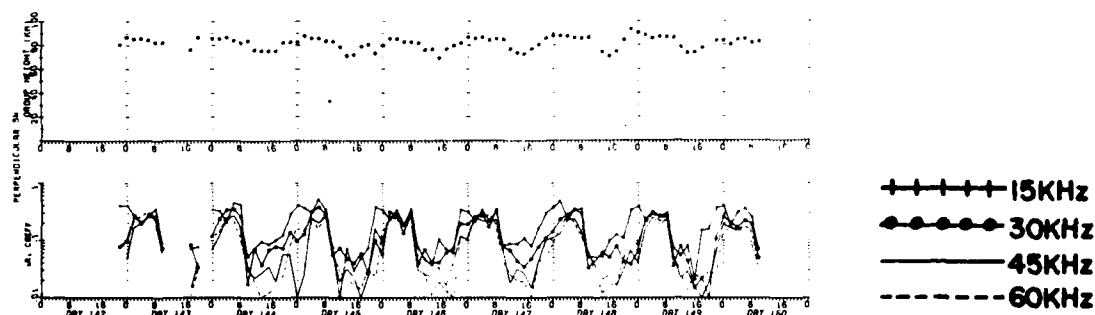


Figure 13.1. Three-Dimensional Display of Data Received at Blumenau.

b. Converted Skywave.



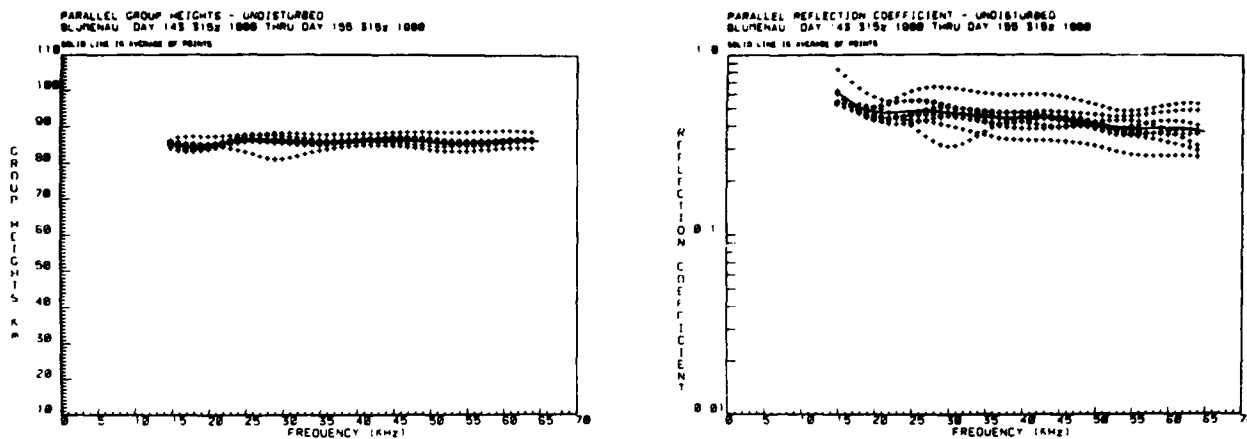
(a) NORMAL SKYWAVE



(b) CONVERTED SKYWAVE

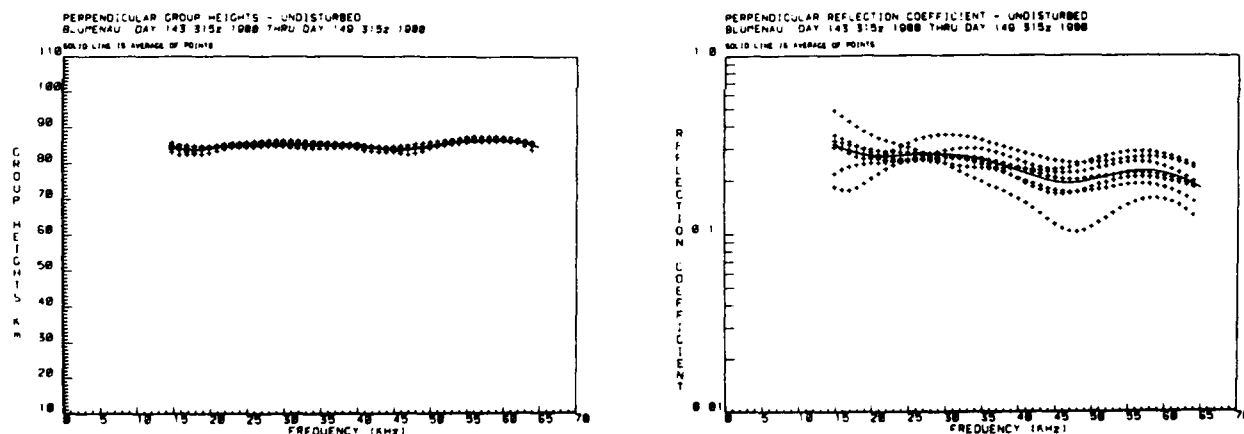
Figure 13.2. Group Heights of Reflection for 30.5 kHz and Reflection Coefficients at 15, 30, 45 and 60 kHz from Data Received at Blumenau.

- a. Normal Skywave.
- b. Converted Skywave.



NORMAL SKYWAVE

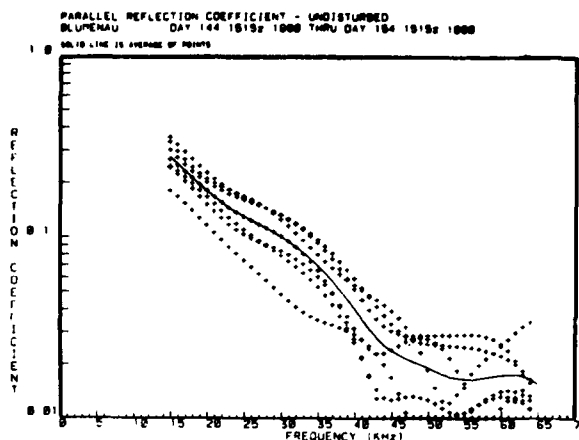
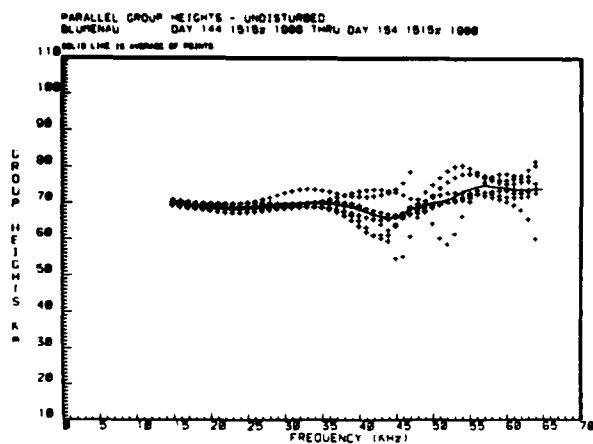
(a)



CONVERTED SKYWAVE

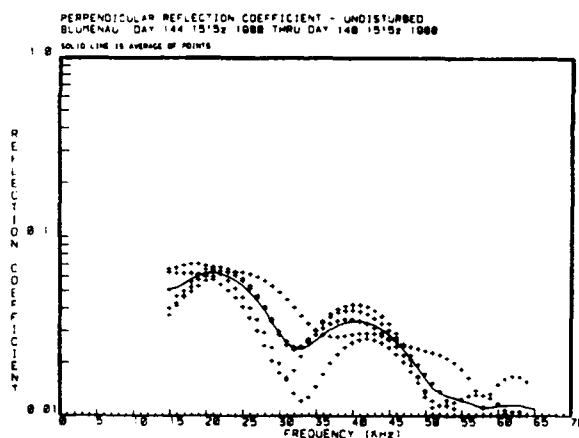
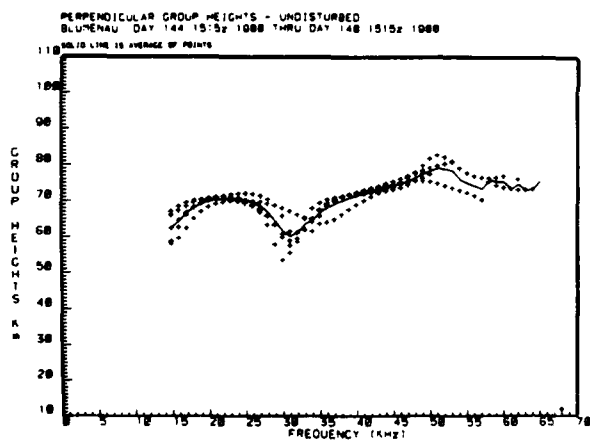
Figure 13.3. Group Heights of Reflection and Reflection Coefficients vs Frequency Derived from Data Received at Blumenau.

a. Local Midnight (0315 UT).



NORMAL SKYWAVE

(b)



CONVERTED SKYWAVE

Figure 13.3. Group Heights of Reflection and Reflection Coefficients vs Frequency Derived from Data Received at Blumenau.

b. Local Noon (1515 UT).

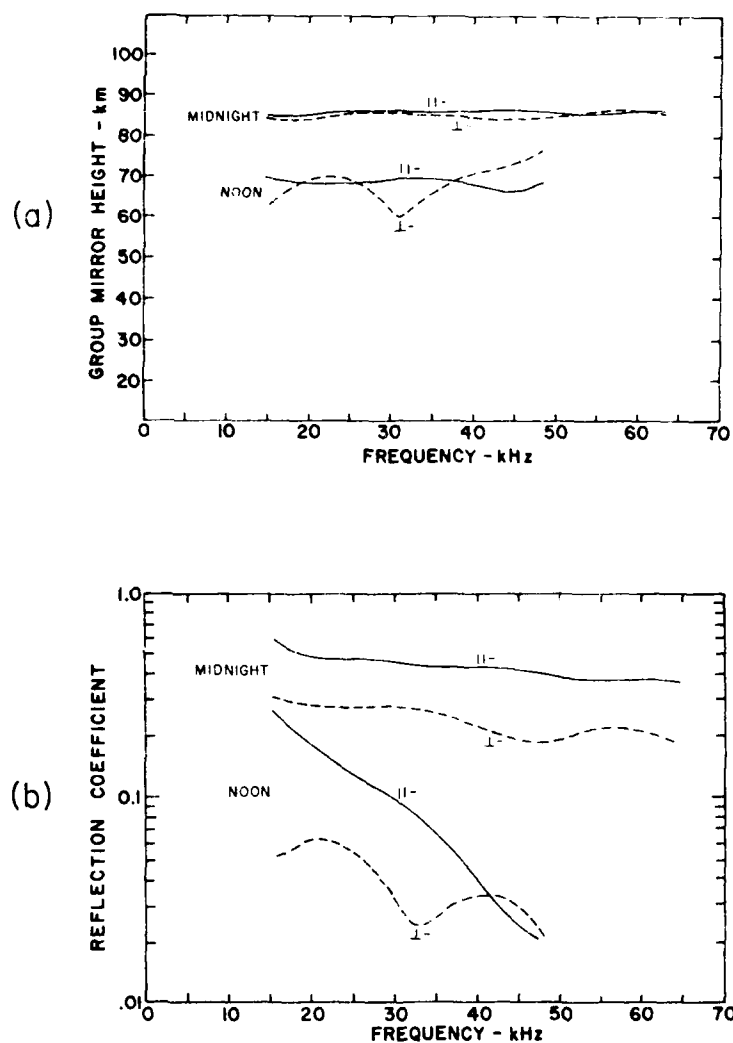


Figure 13.4. Averaged Values of Group Heights of Reflection and Reflection Coefficients vs Frequency Derived from Data Received at Blumenau.

DATA

DISTANCE: 215 KM

AZIMUTH: 123°

DATA: NORMAL POLARIZATION ONLY

MEASUREMENT PERIOD: 8 MAY - 15 MAY 1980

1 JUN - 27 JUN 1980

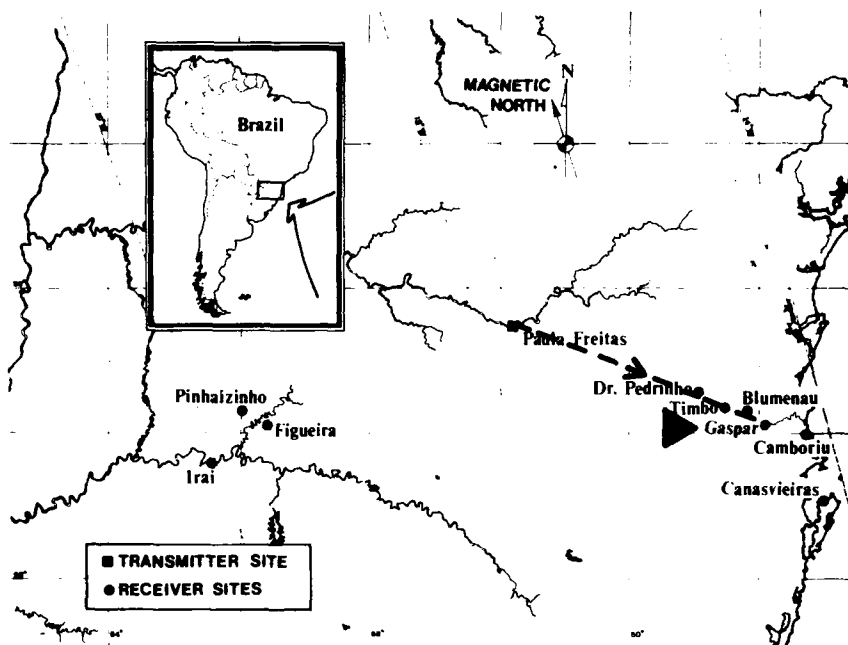


Figure 14. Path Parameters for Paula Freitas to Gaspar.

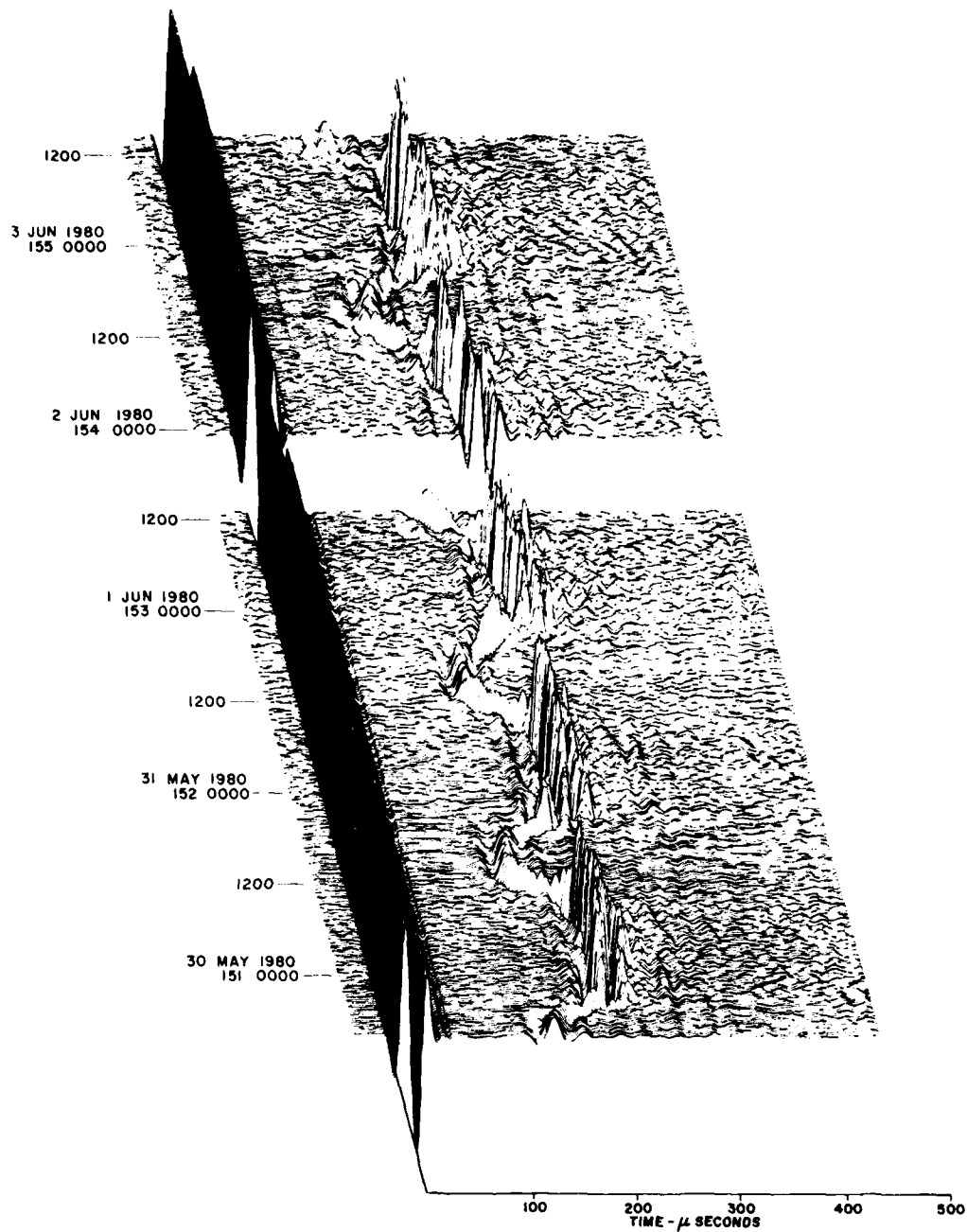


Figure 14.1. Three-Dimensional Display of Normal Skywave Data Received at Gaspar.

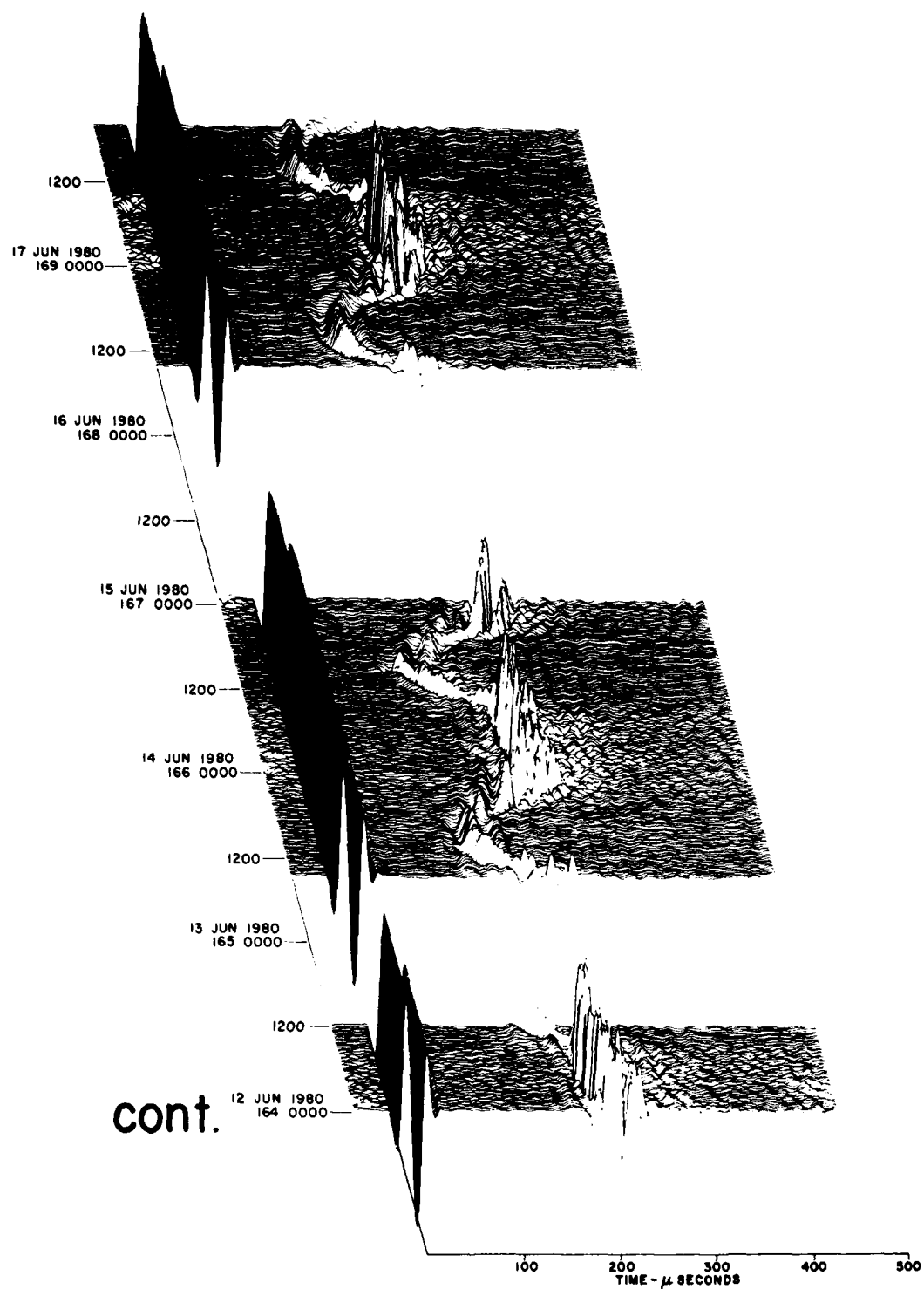


Figure 14.1. Three-Dimensional Display of Normal Skywave Data Received at Gaspar. (Cont.).

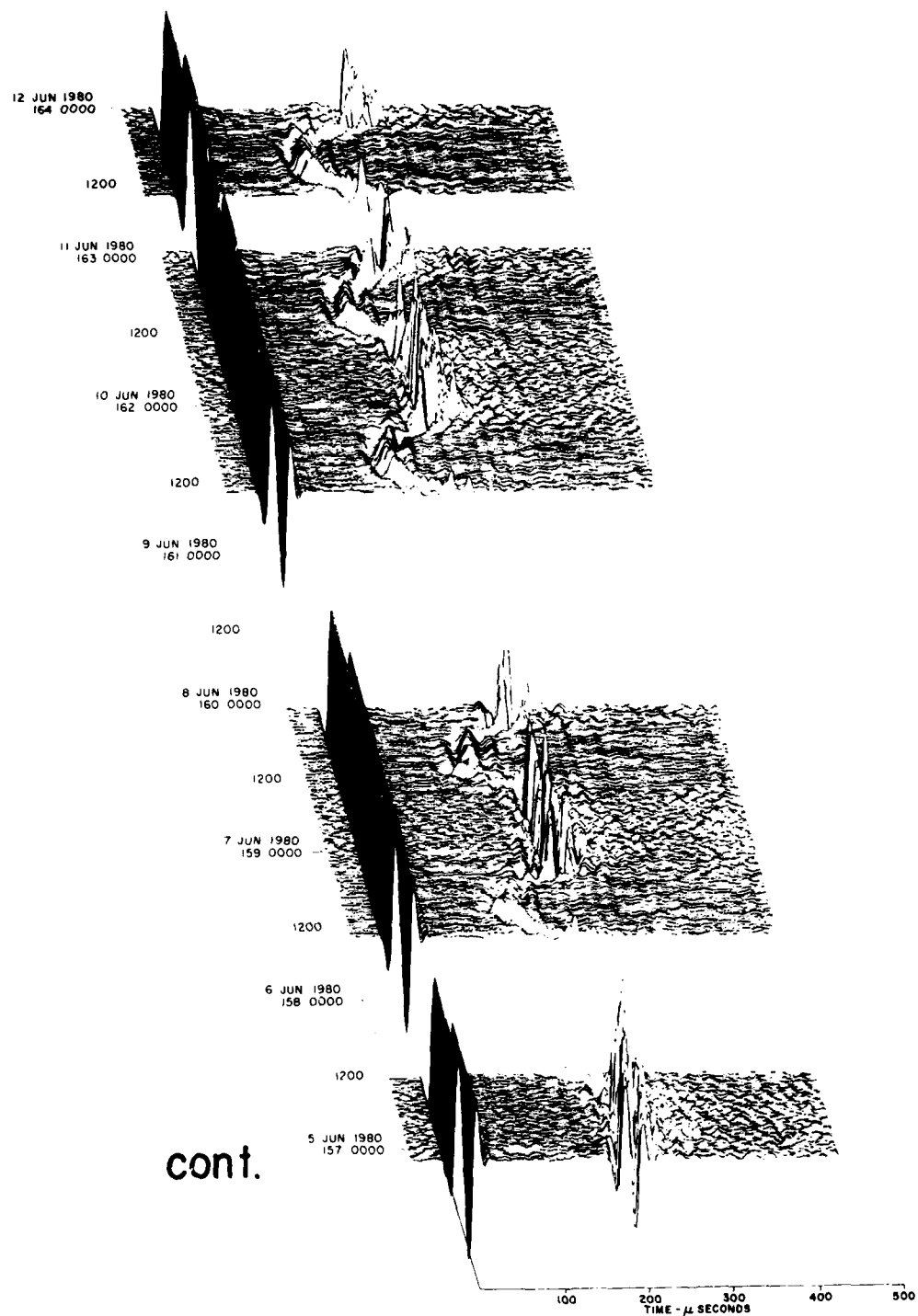


Figure 14.1. Three-Dimensional Display of Normal Skywave Data Received at Gaspar. (Cont.).

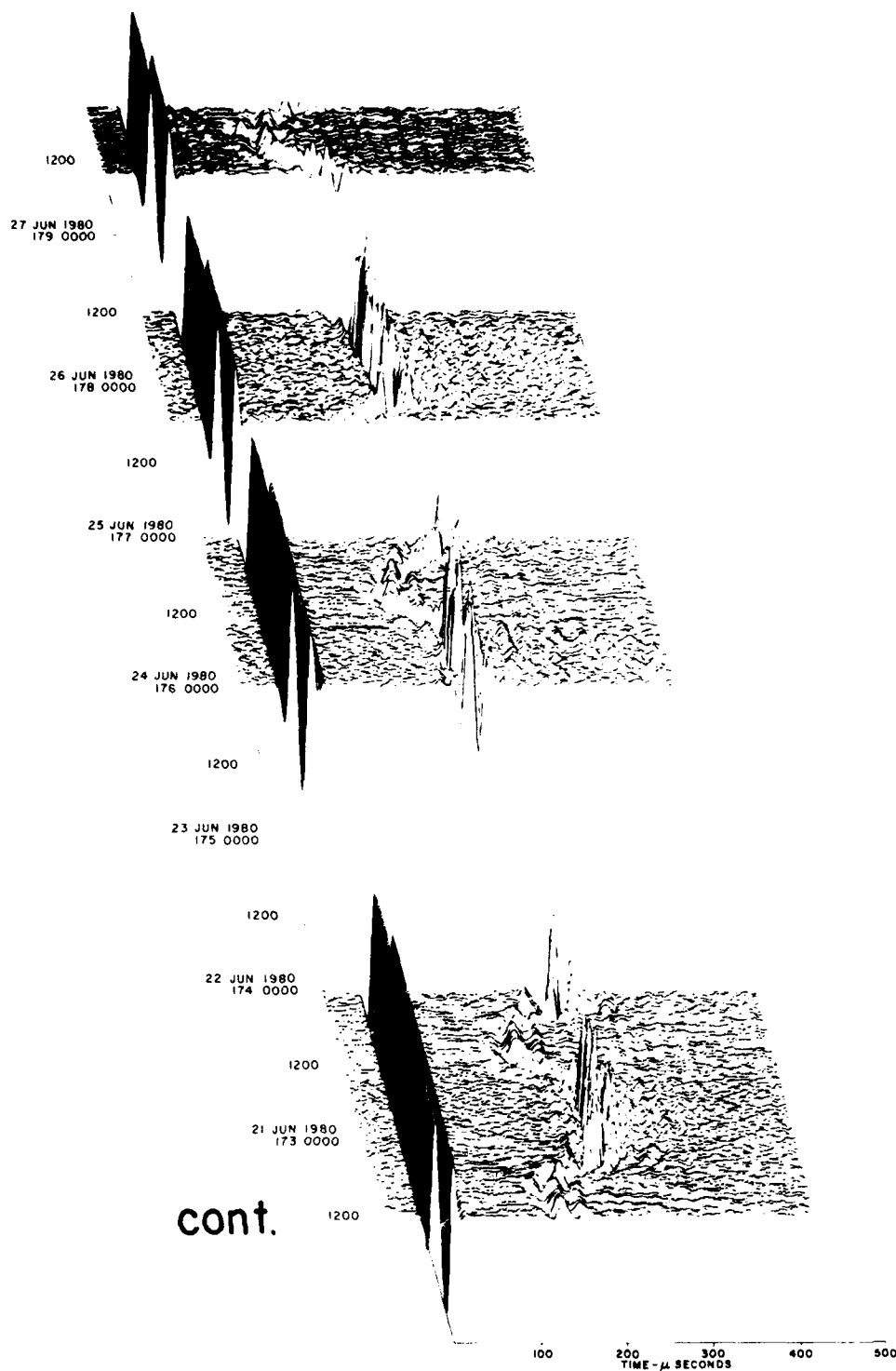


Figure 14.1. Three-Dimensional Display of Normal Skywave Data Received at Gaspar. (Cont.).

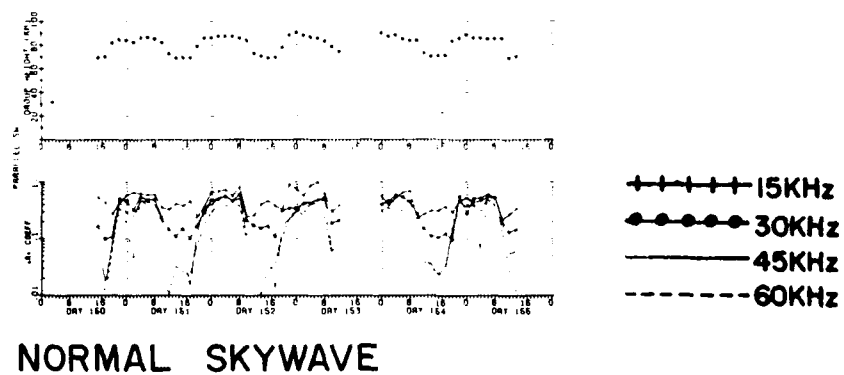
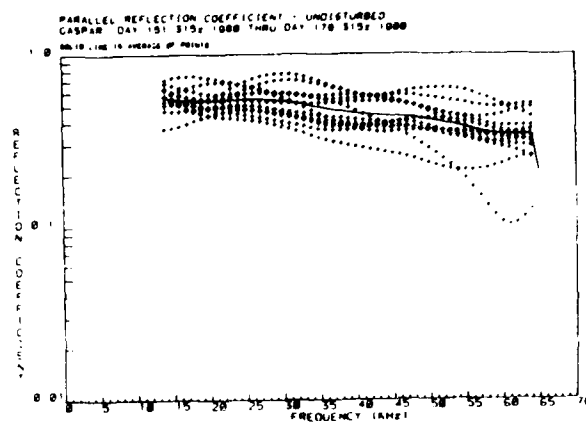
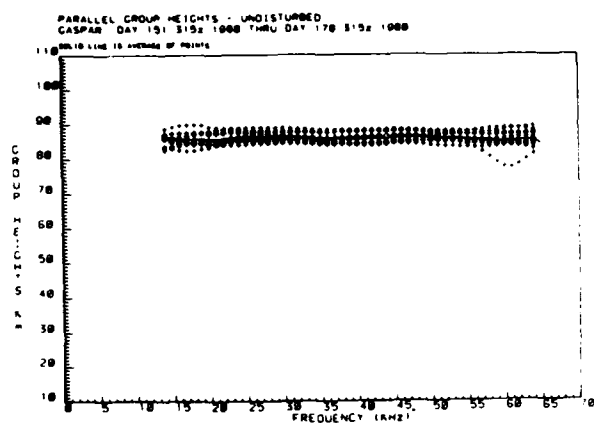


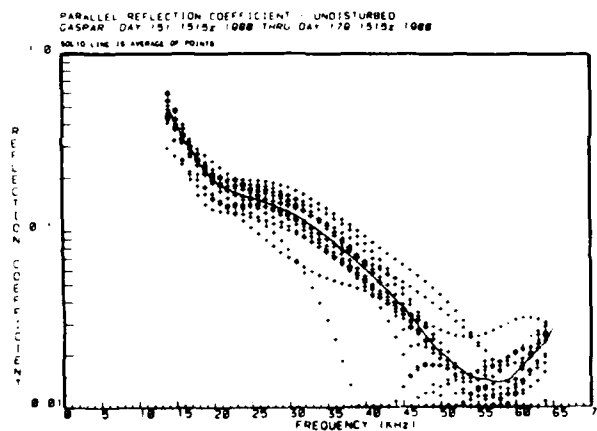
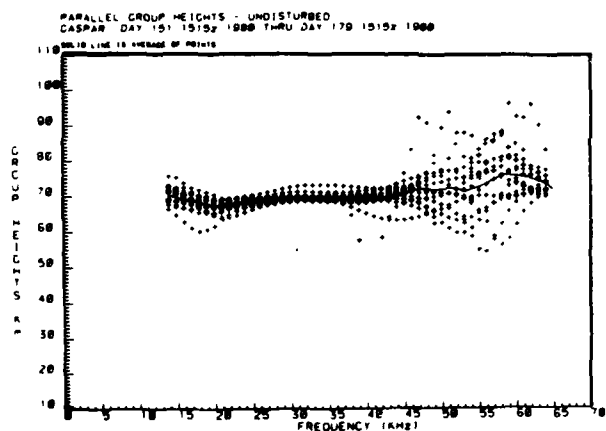
Figure 14.2. Group Heights of Reflection for 30.5 kHz and Reflection Coefficients at 15, 30, 45 and 60 kHz Derived from Normal Skywave Data Received at Gaspar.

(a)



NORMAL SKYWAVE

(b)



NORMAL SKYWAVE

Figure 14.3. Group Heights of Reflection and Reflection Coefficients vs Frequency Derived from Data Received at Gaspar.

- a. Local Midnight (0315 UT).
- b. Local Noon (1515 UT).

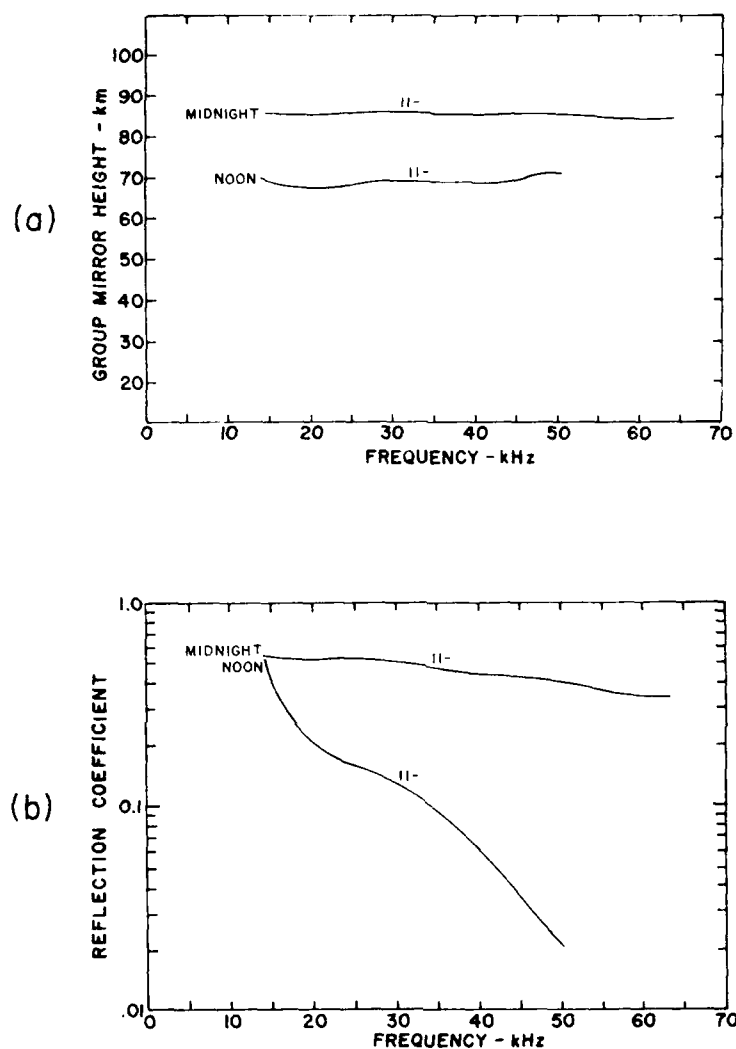


Figure 14.4. Averaged Values of Group Heights of Reflection and Reflection Coefficients vs Frequency Derived from Data Received at Gaspar.

- a. Group Heights of Reflection.
- b. Reflection Coefficients.

DATA

PROPAGATION PATH: PAULA FREITAS TO CAMBORIU (PF-CAM)
DISTANCE: 246 KM
AZIMUTH: 123°
DATA: NORMAL POLARIZATION ONLY
MEASUREMENT PERIOD: 12 MAY - 3 JUN 1980

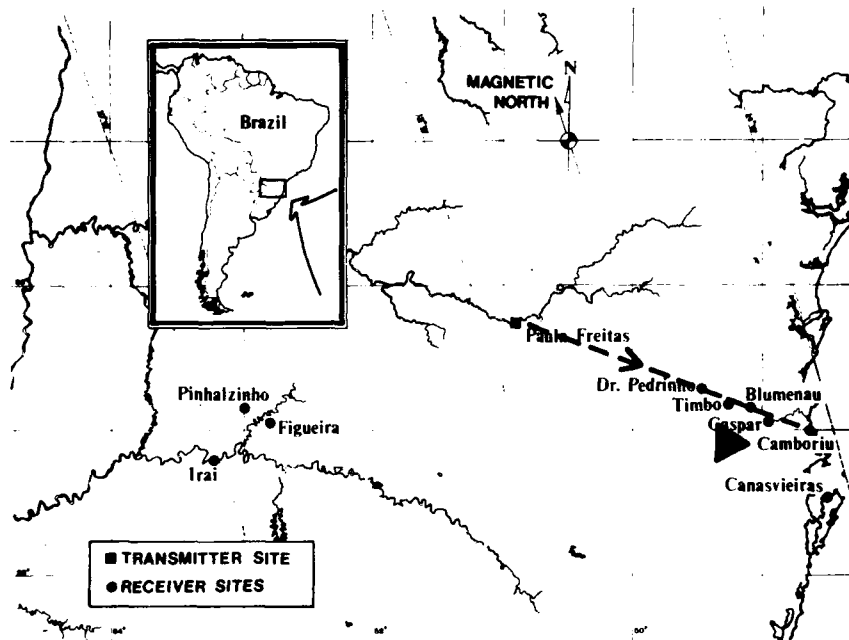


Figure 15. Path Parameters for Paula Freitas to Camboriu.

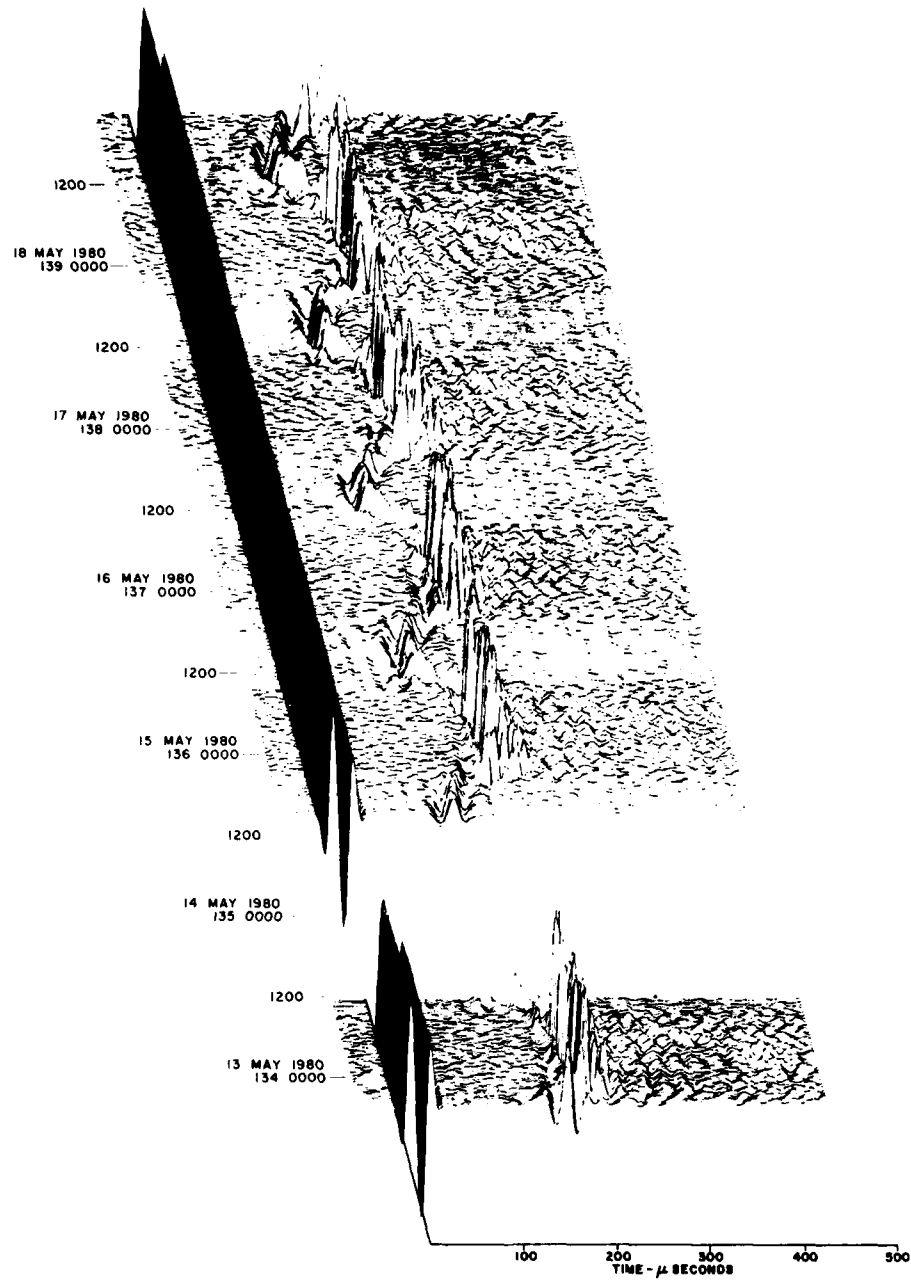


Figure 15.1. Three-Dimensional Display of Normal Skywave Data Received at Camboriu.

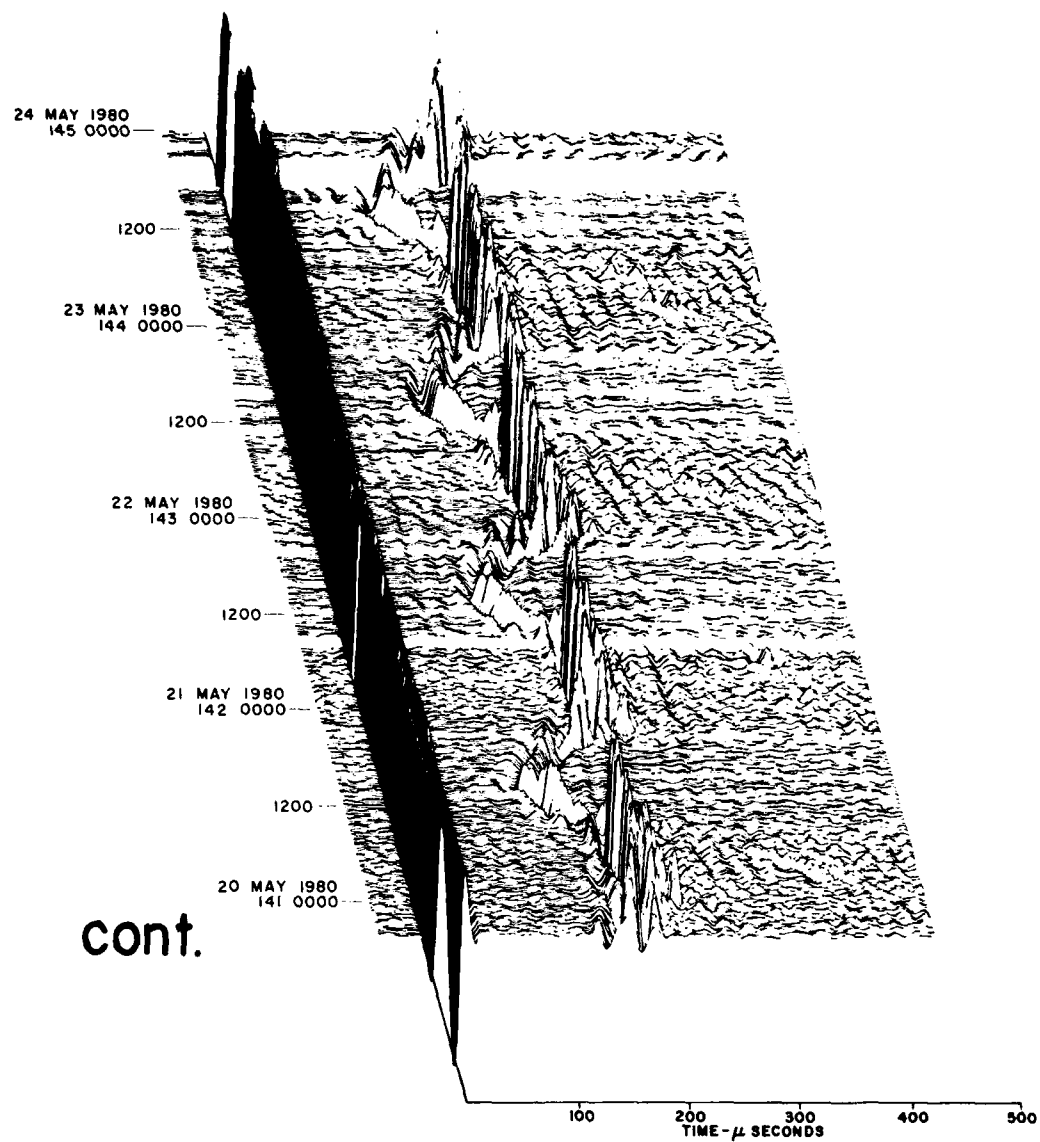


Figure 15.1. Three-Dimensional Display of Normal Skywave Data Received at Camboriu. (Cont.).

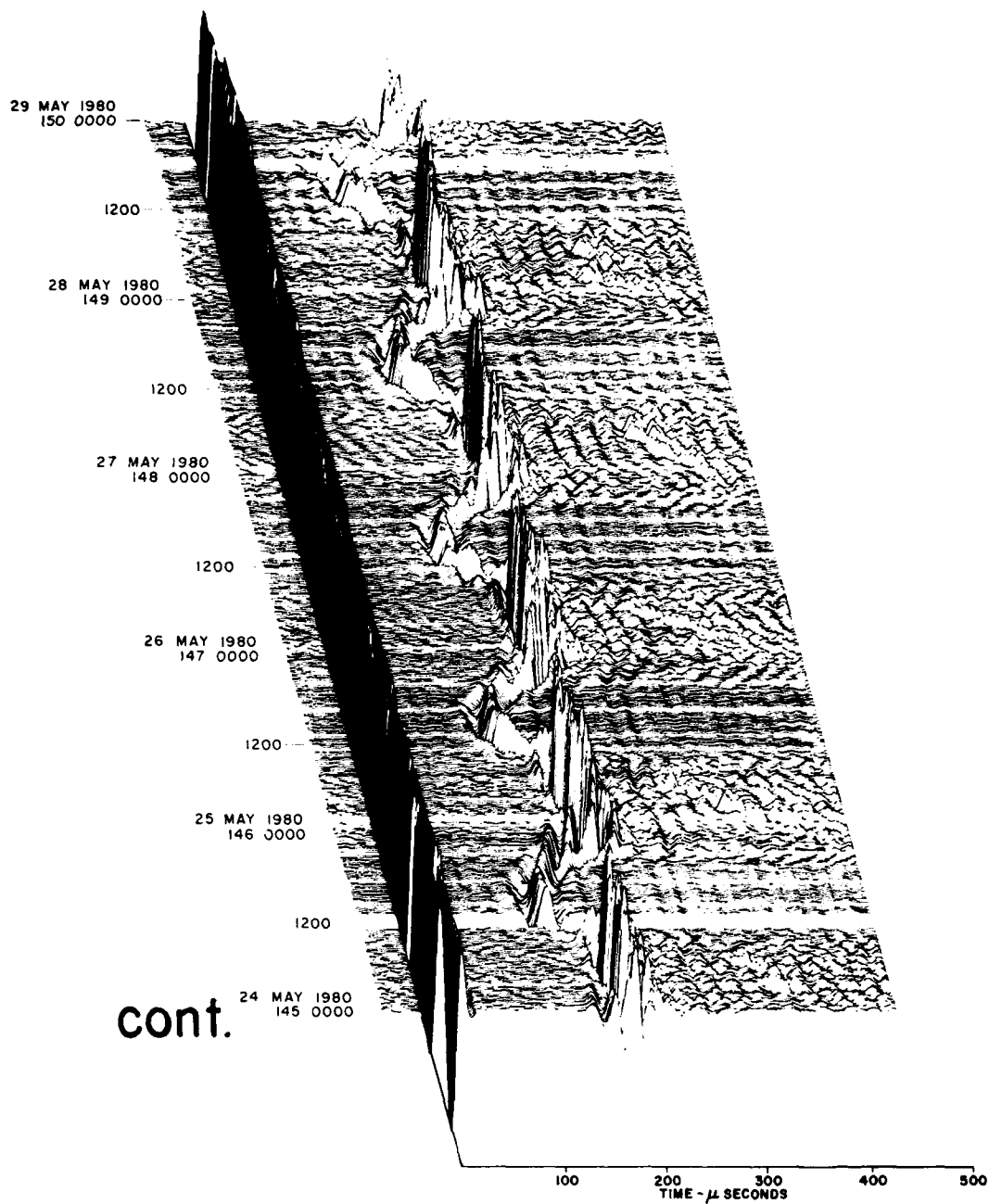


Figure 15.1. Three-Dimensional Display of Normal Skywave Data Received at Camboriu. (Cont.).

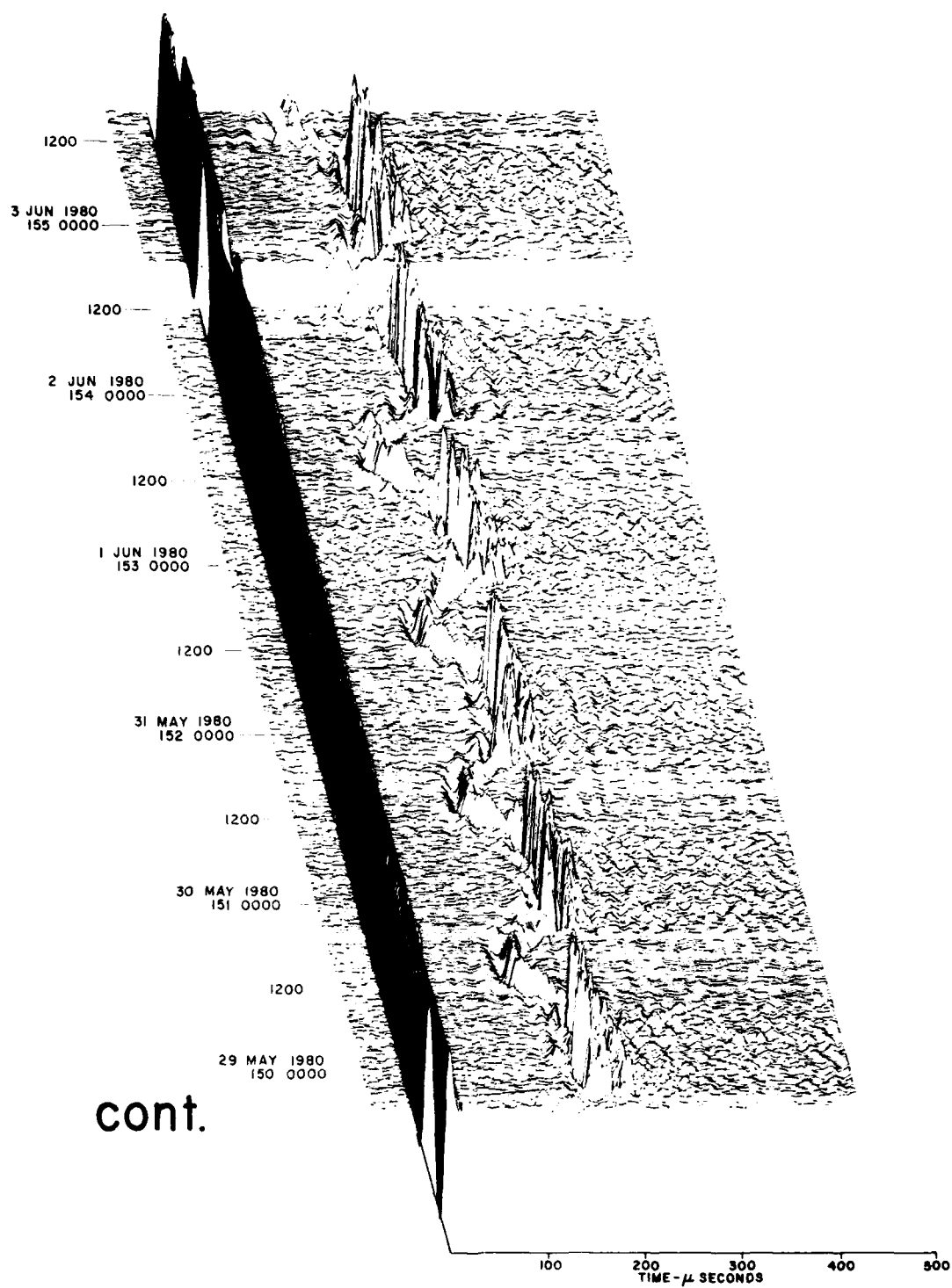
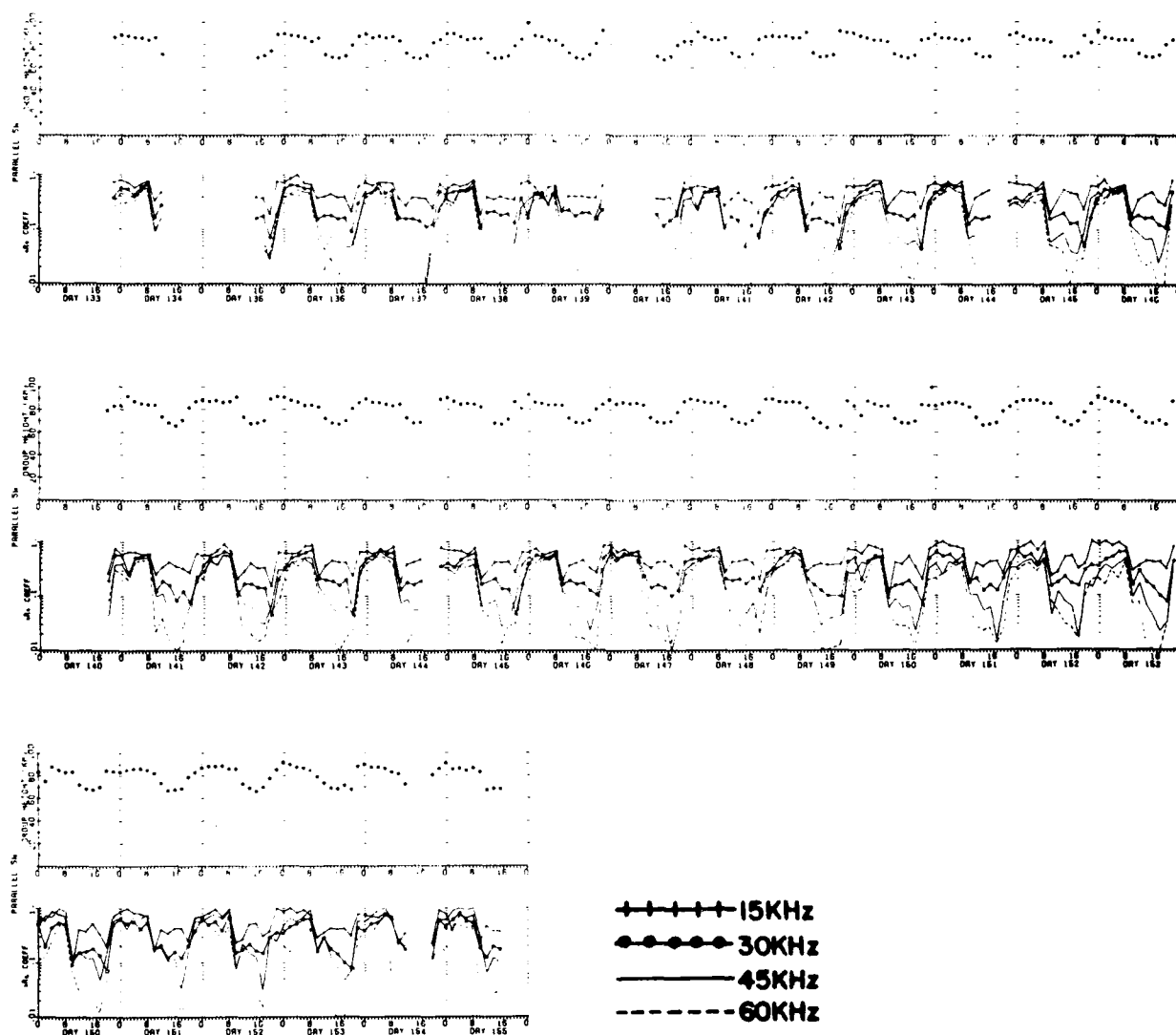


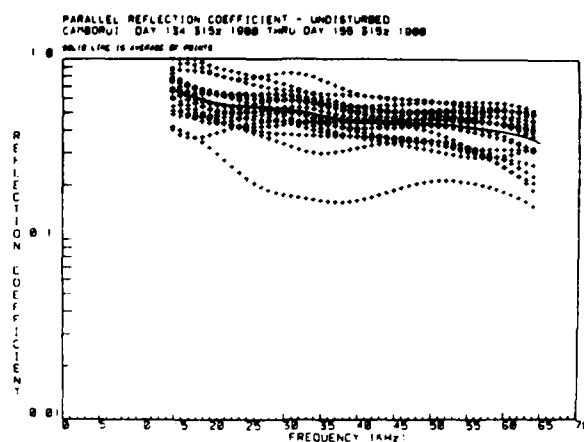
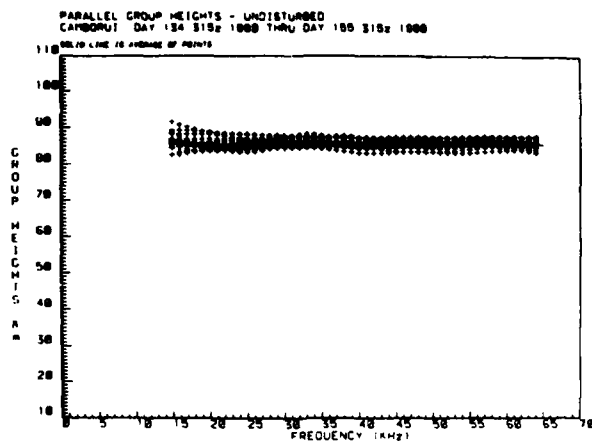
Figure 15.1. Three-Dimensional Display of Normal Skywave Data Received at Camboriu. (Cont.).



NORMAL SKYWAVE

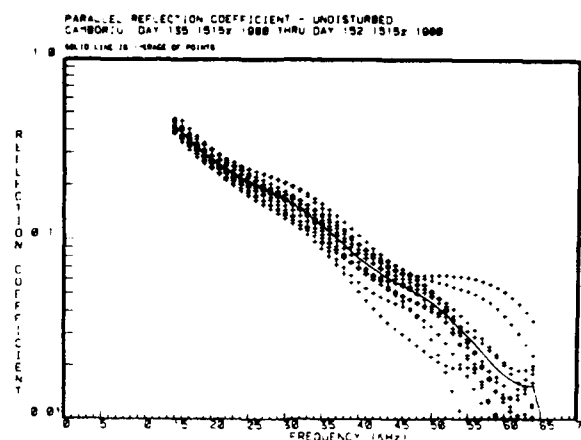
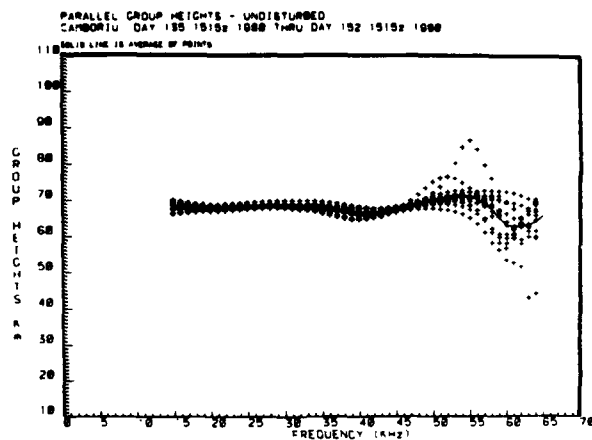
Figure 15.2. Group Heights of Reflection for 30.5 kHz and Reflection Coefficients at 15, 30, 45 and 60 kHz Derived from Normal Skywave Data Received at Camboriu.

(a)



NORMAL SKYWAVE

(b)



NORMAL SKYWAVE

Figure 15.3. Group Heights of Reflection and Reflection Coefficients vs Frequency Derived from Data Received at Camboriu.

- a. Local Midnight (0315 UT).
- b. Local Noon (1515 UT).

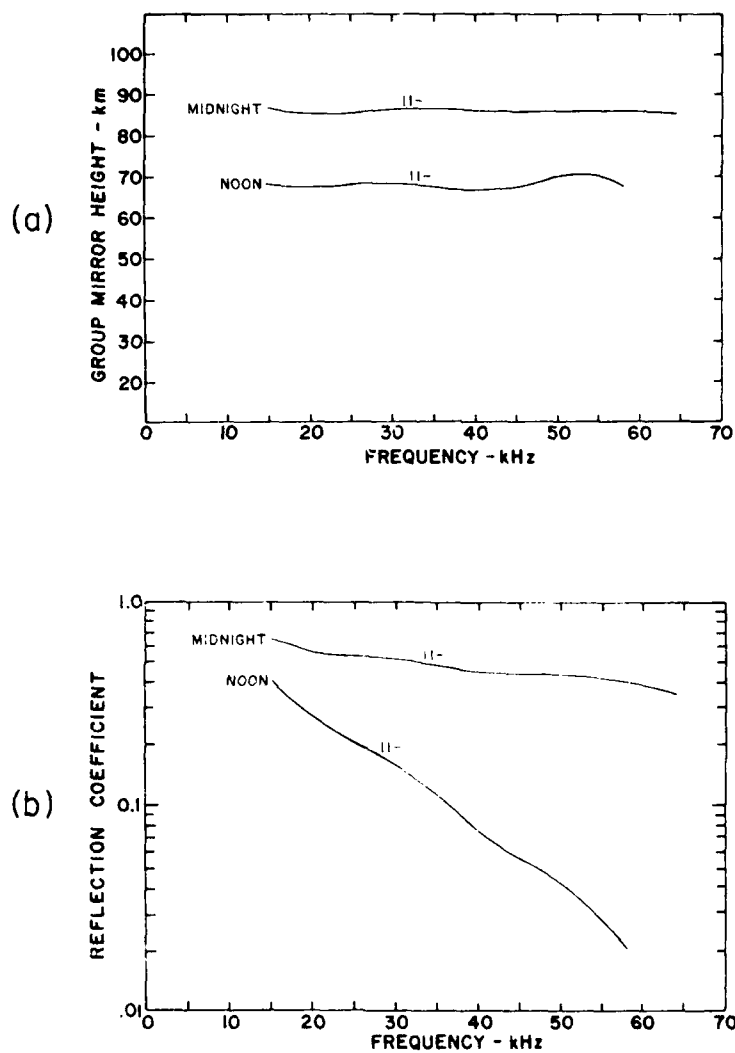


Figure 15.4. Averaged Values of Group Heights of Reflection and Reflection Coefficients vs Frequency Derived from Data Received at Camboriu.

- a. Group Heights of Reflection.
- b. Reflection Coefficients.

DATA

PROPAGATION PATH: PAULA FREITAS TO CANASVIEIRAS (PF-CAN)
DISTANCE: 280 KM
AZIMUTH: 132°
DATA: NORMAL POLARIZATION ONLY
MEASUREMENT PERIOD: 15 MAY - 19 MAY 1980

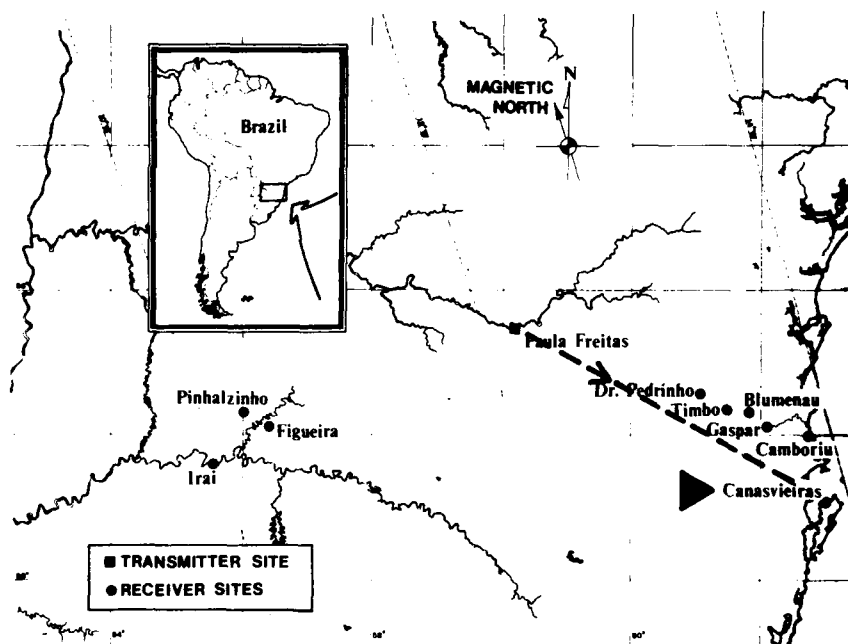


Figure 16. Path Parameters for Paula Freitas to Canasvieiras.

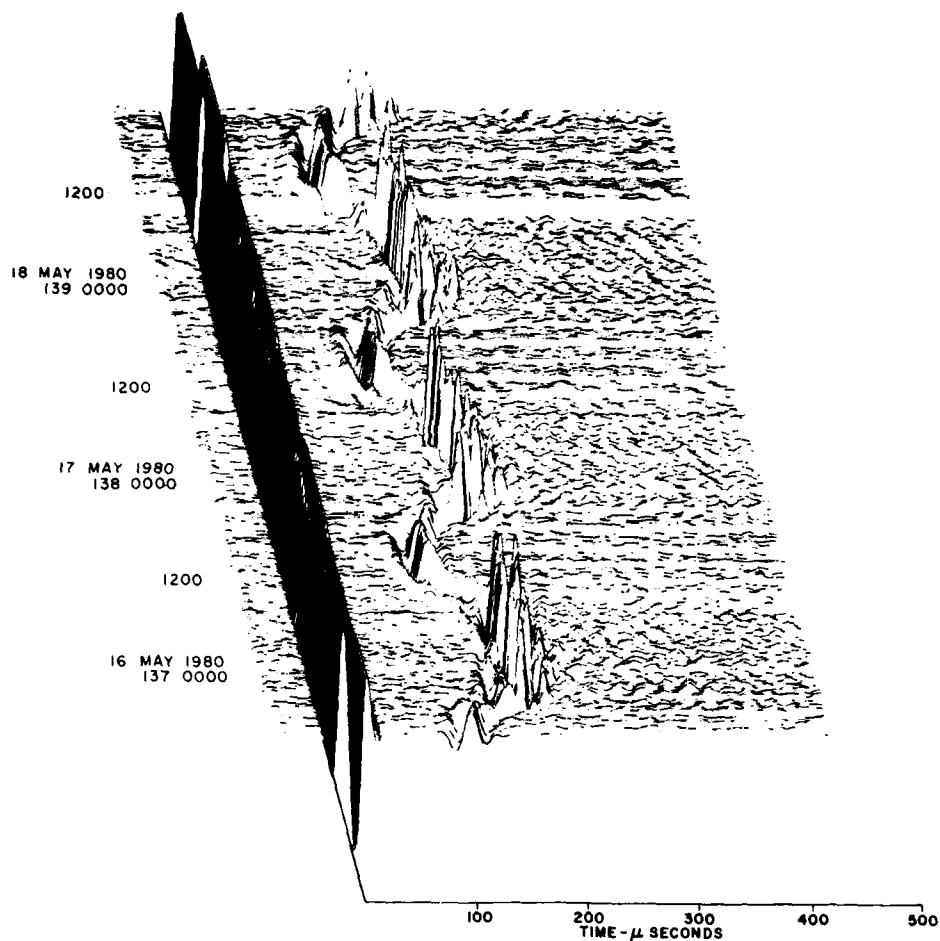


Figure 16.1. Three-Dimensional Display of Normal Skywave Data Received at Canasvieiras.

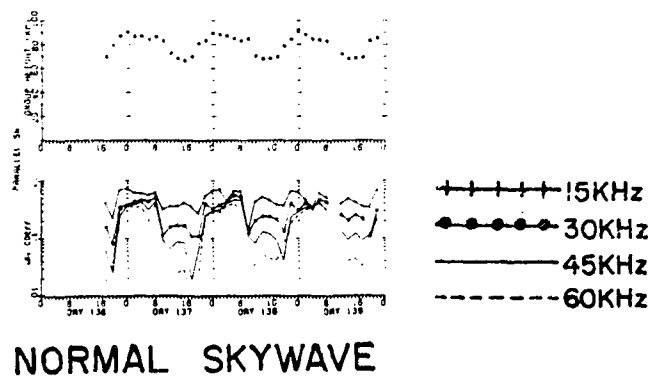
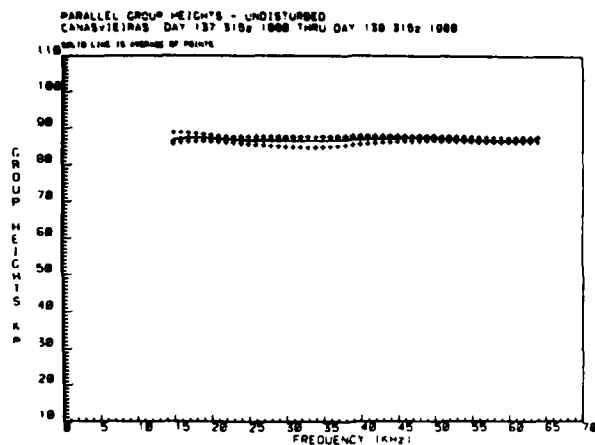


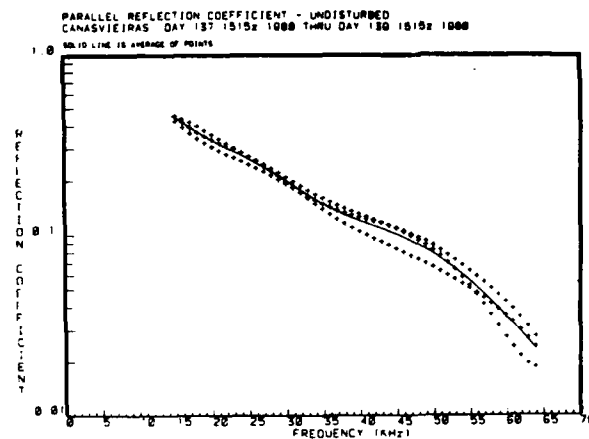
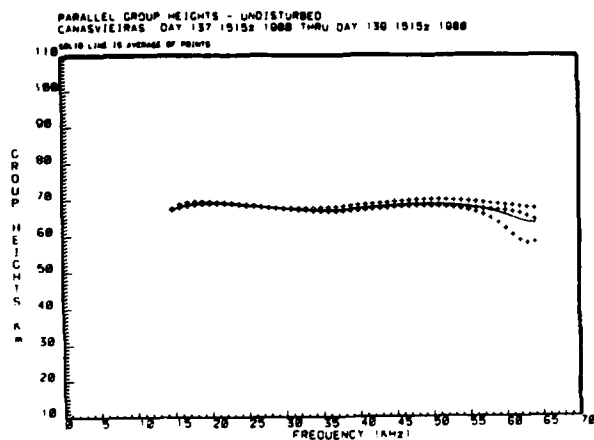
Figure 16.2. Group Heights of Reflection for 30.5 kHz and Reflection Coefficients at 15, 30, 45 and 60 kHz Derived from Normal Skywave Data Received at Canasvieiras.

(a)



NORMAL SKYWAVE

(b)



NORMAL SKYWAVE

Figure 16.3. Group Heights of Reflection and Reflection Coefficients vs Frequency Derived from Data Received at Canasvieiras.

- a. Local Midnight (0315 UT).
- b. Local Noon (1515 UT).

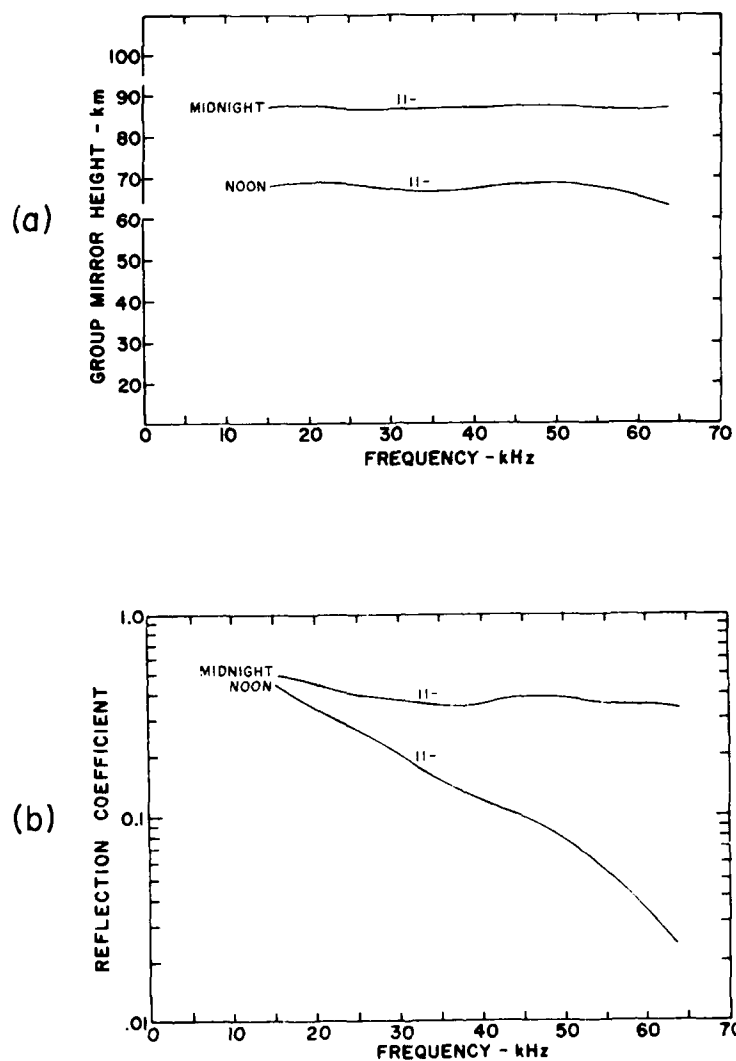


Figure 16.4. Averaged Values of Group Heights of Reflection and Reflection Coefficients vs Frequency Derived from Data Received at Canasvieiras.

- a. Group Heights of Reflection.
- b. Reflection Coefficients.

DATA

PROPAGATION PATH: PAULA FREITAS TO FIGUEIRA (PF-FIG)
DISTANCE: 200 KM
AZIMUTH: 260°
DATA: NORMAL POLARIZATION ONLY
MEASUREMENT PERIOD: 20 MAY - 26 MAY 1980

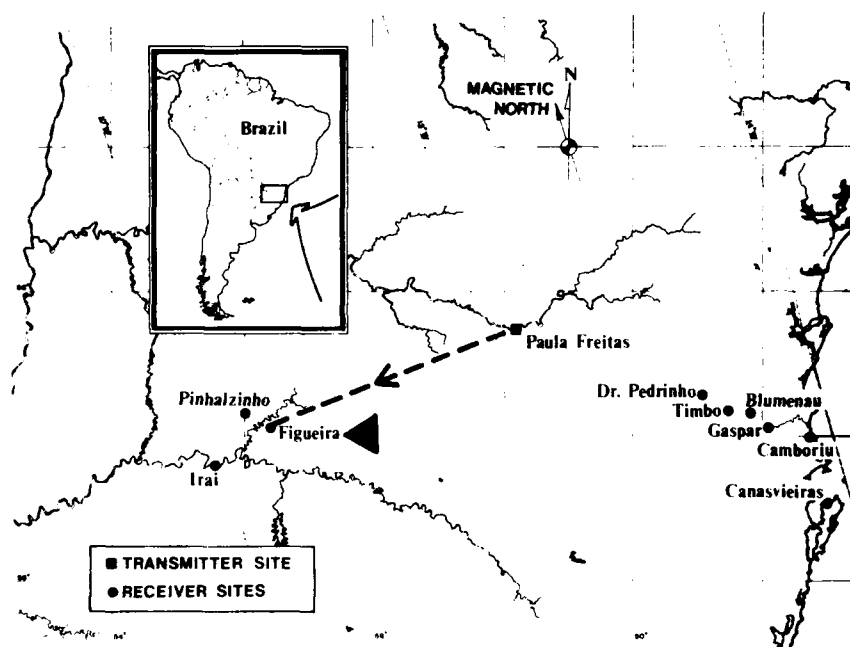


Figure 17. Path Parameters for Paula Freitas to Figueira.

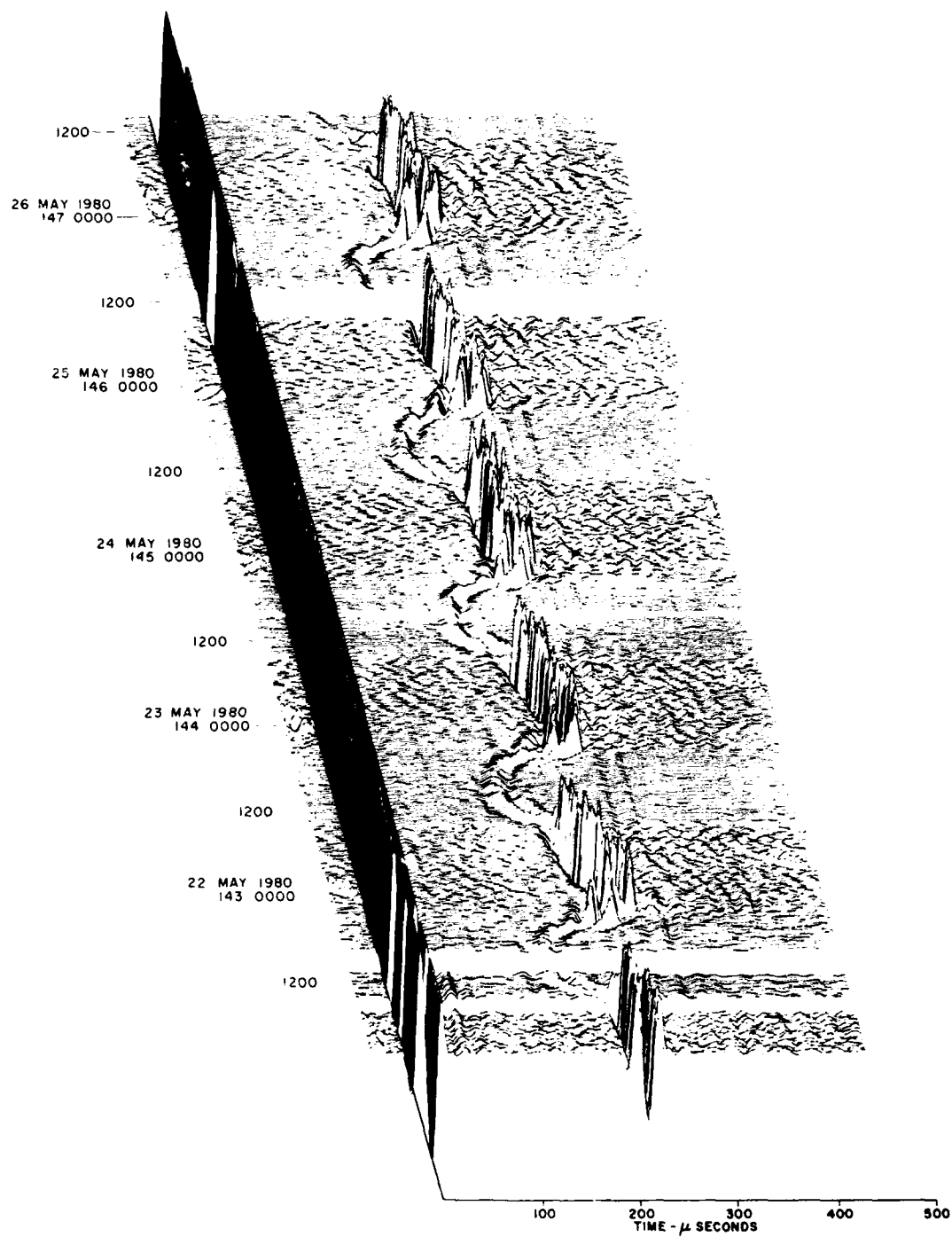


Figure 17.1. Three-Dimensional Display of Normal Skywave Data Received at Figueira.

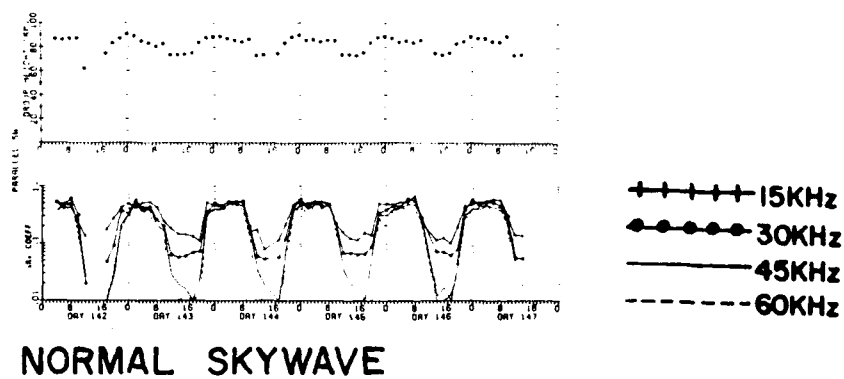
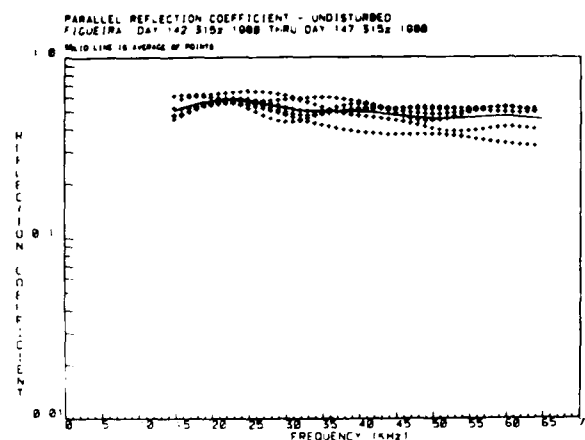
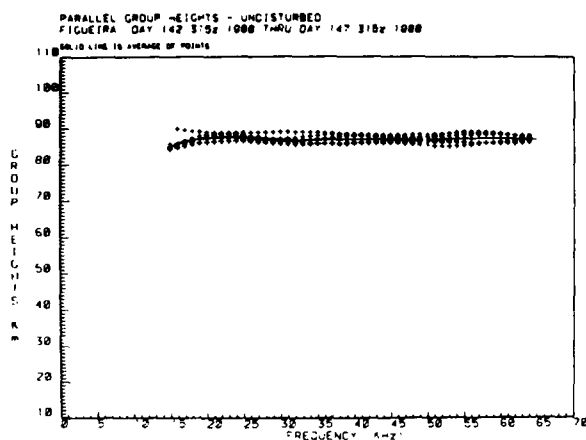


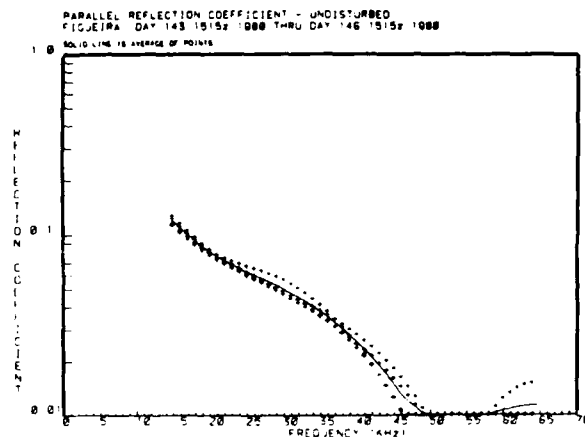
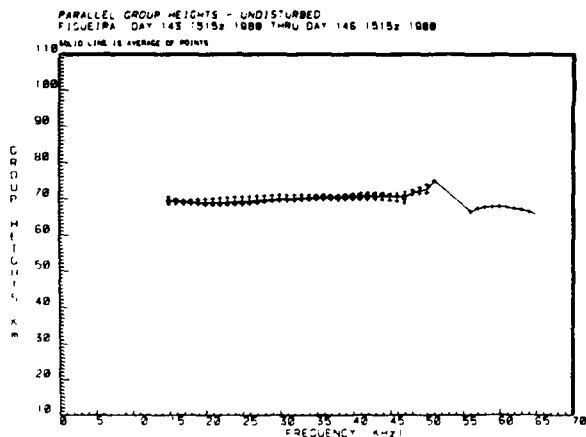
Figure 17.2. Group Heights of Reflection for 30.5 kHz and Reflection Coefficients at 15, 30, 45 and 60 kHz Derived from Normal Skywave Data Received at Figueira.

(a)



NORMAL SKYWAVE

(b)



NORMAL SKYWAVE

Figure 17.3. Group Heights of Reflection and Reflection Coefficients vs Frequency Derived from Data Received at Figueira.

- a. Local Midnight (0315 UT).
- b. Local Noon (1515 UT).

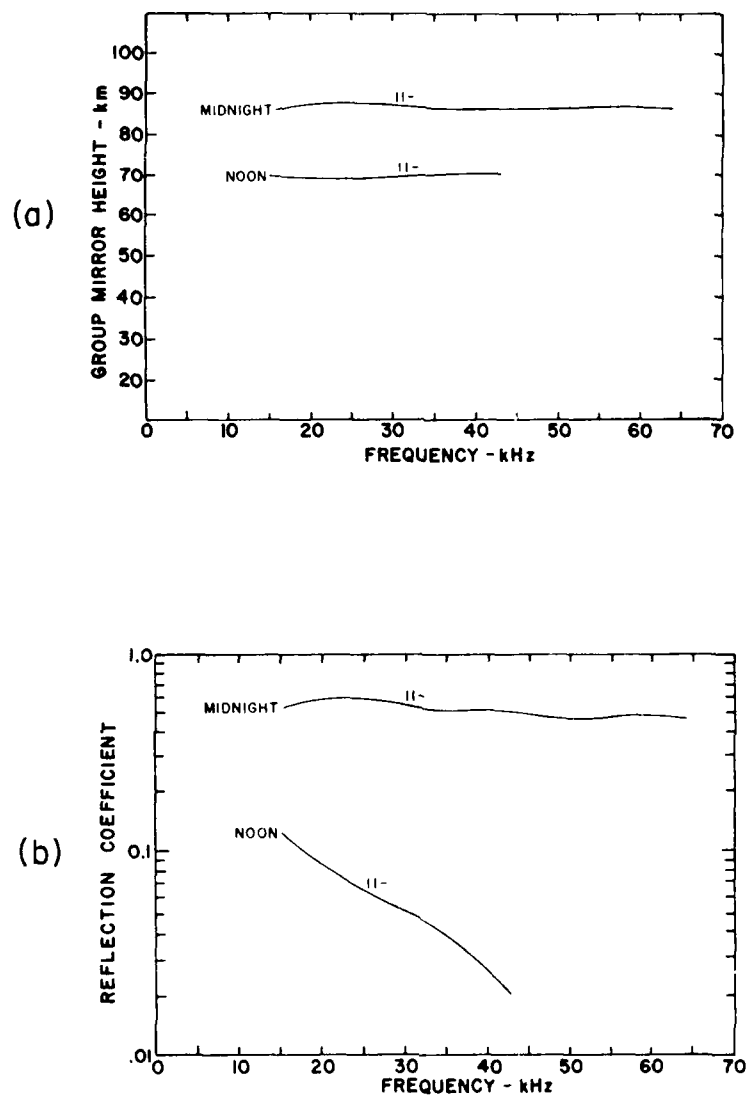


Figure 17.4. Averaged Values of Group Heights of Reflection and Reflection Coefficients vs Frequency Derived from Data Received at Figueira.

- a. Group Heights of Reflection.
- b. Reflection Coefficients.

DATA

PROPAGATION PATH: PAULA FREITAS TO PINHALZINHO (PF-PIN)
DISTANCE: 213 KM
AZIMUTH: 262°
DATA: NORMAL POLARIZATION ONLY
MEASUREMENT PERIOD: 29 MAY - 1 JUN 1980

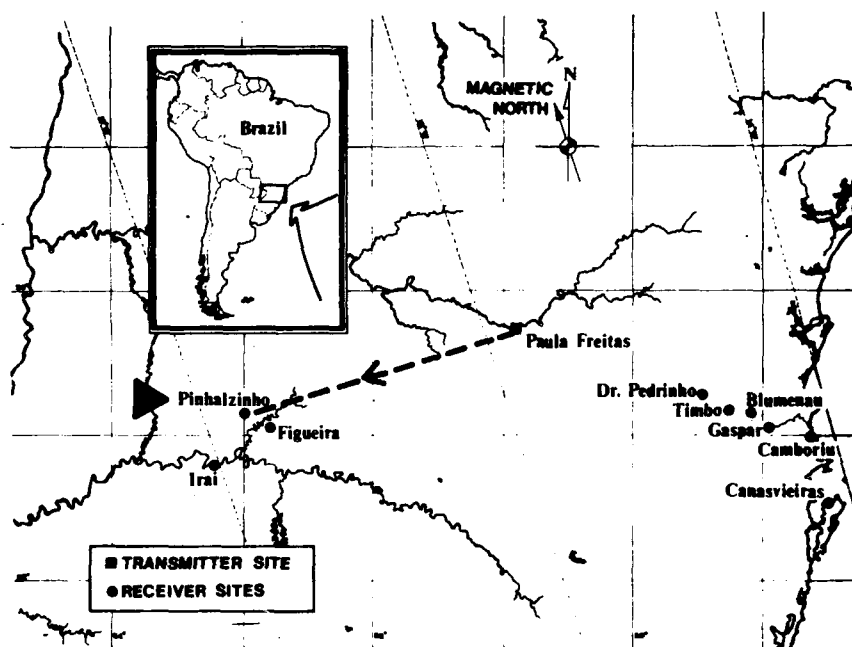


Figure 18. Path Parameters for Paula Freitas to Pinhalzinho.

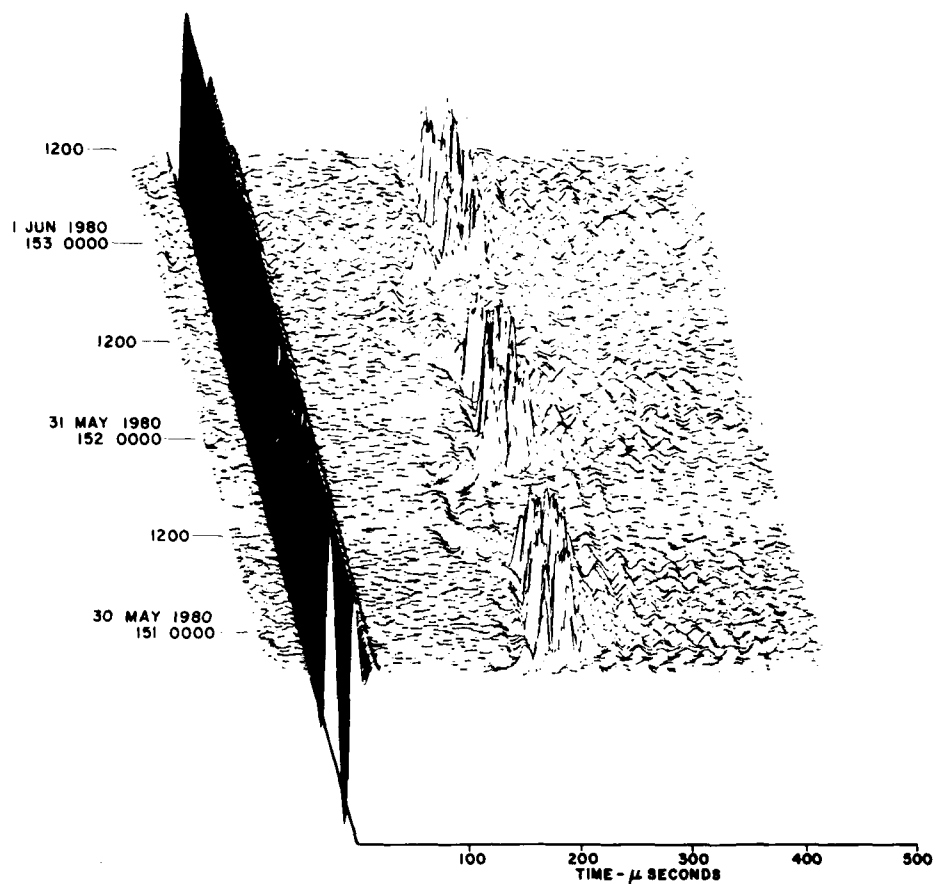


Figure 18.1. Three-Dimensional Display of Normal Skywave Data Received at Pinhalzinho.

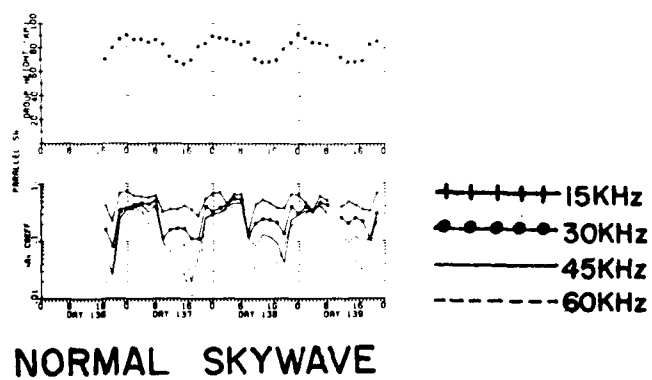
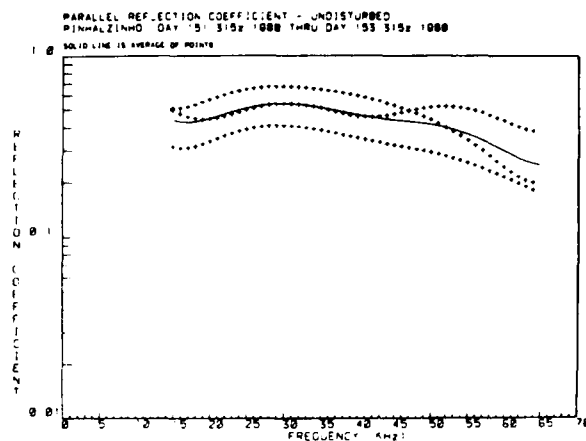
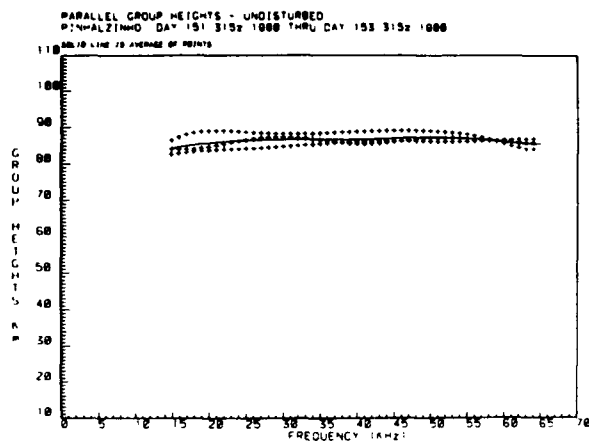


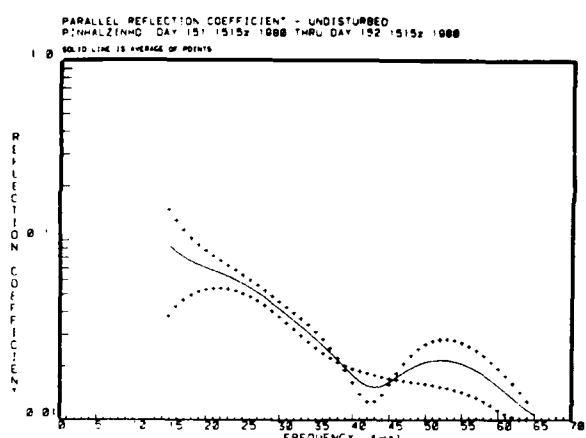
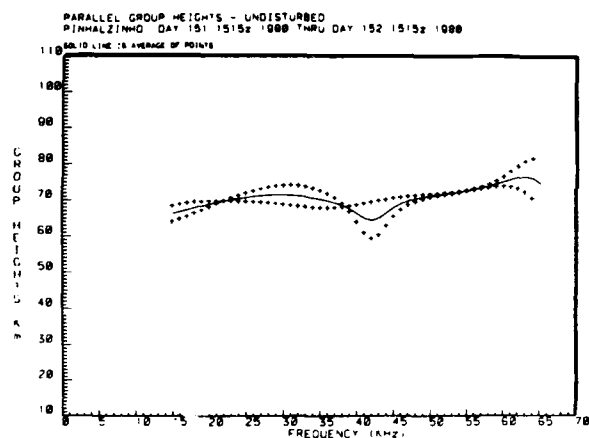
Figure 18.2. Group Heights of Reflection for 30.5 kHz and Reflection Coefficients at 15, 30, 45 and 60 kHz Derived from Normal Skywave Data Received at Pinhalzinho.

(a)



NORMAL SKYWAVE

(b)



NORMAL SKYWAVE

Figure 18.3. Group Heights of Reflection and Reflection Coefficients vs Frequency Derived from Data Received at Pinhalzinho.

- a. Local Midnight (0315 UT).
- b. Local Noon (1515 UT).

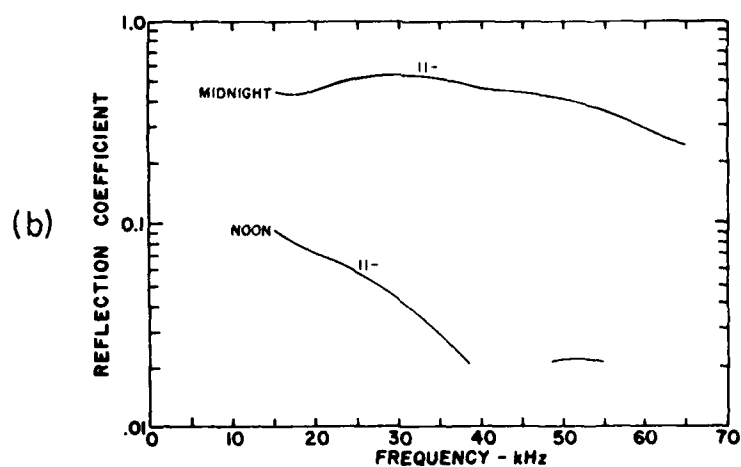
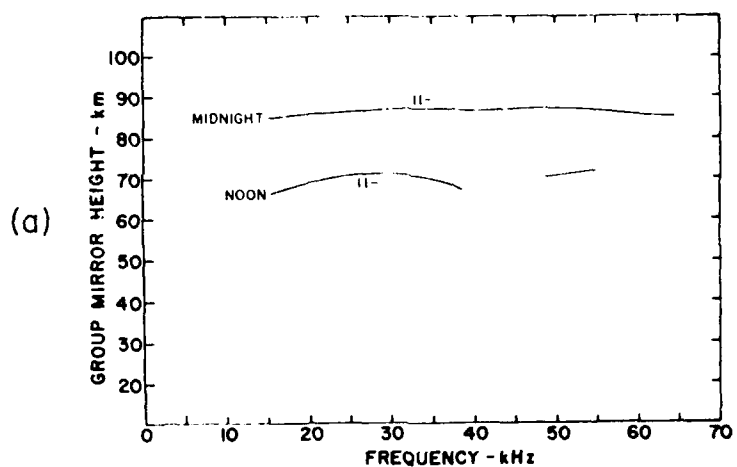


Figure 18.4. Averaged Values of Group Heights of Reflection and Reflection Coefficients vs Frequency Derived from Data Received at Pinhalzinho.

- a. Group Heights of Reflection.
- b. Reflection Coefficients.

DATA

PROPAGATION PATH: PAULA FREITAS TO IRAI (PF-IRA)
DISTANCE; 250 KM
AZIMUTH: 256°
DATA: NORMAL POLARIZATION ONLY
MEASUREMENT PERIOD: 26 MAY - 29 MAY 1980

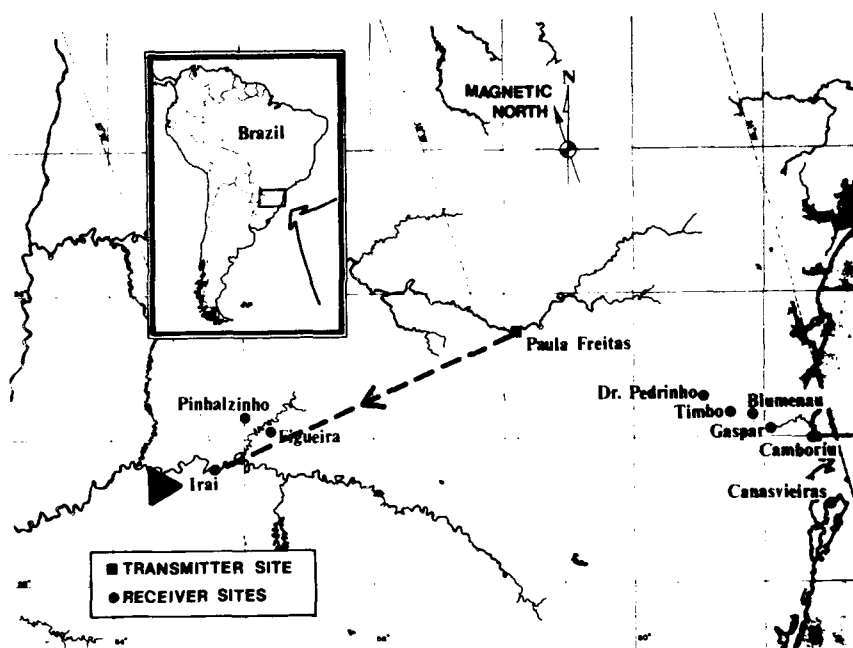


Figure 19. Path Parameters for Paula Freitas to Irai.

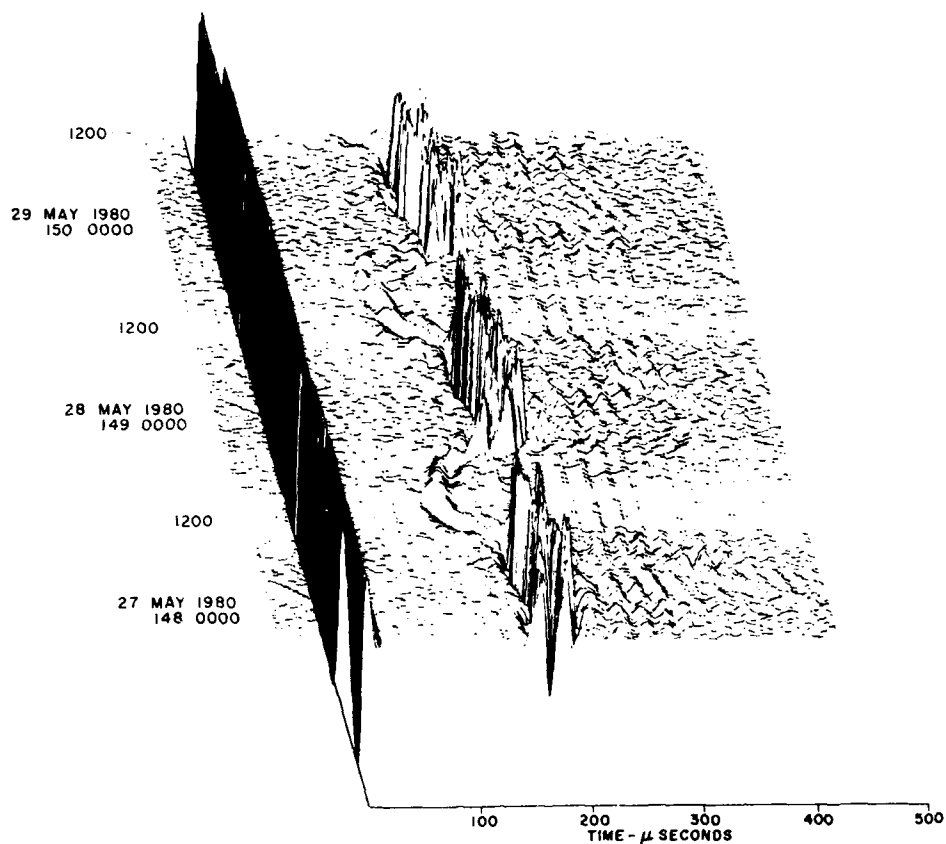


Figure 19.1. Three-Dimensional Display of Normal Skywave Data Received at Irai.

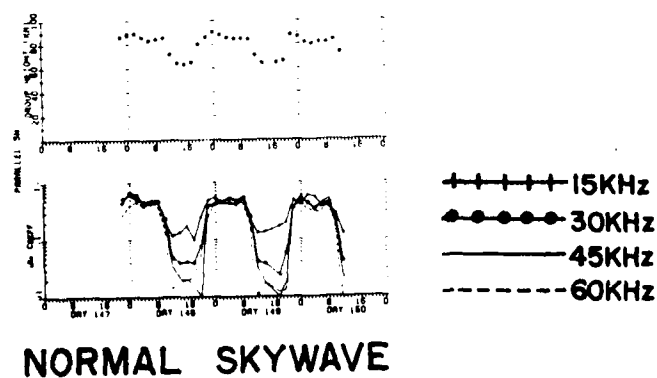
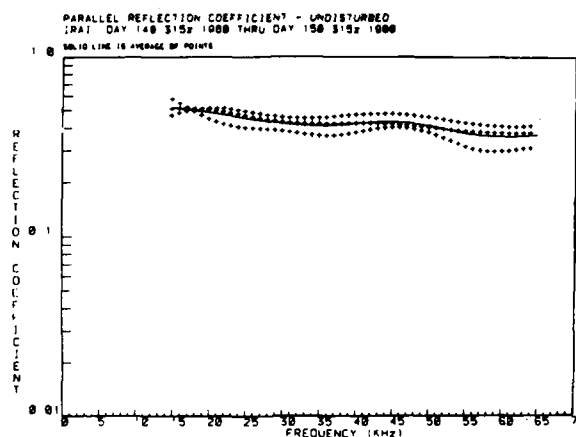
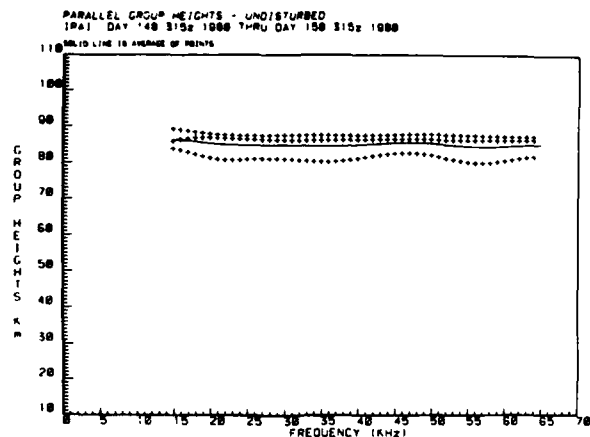


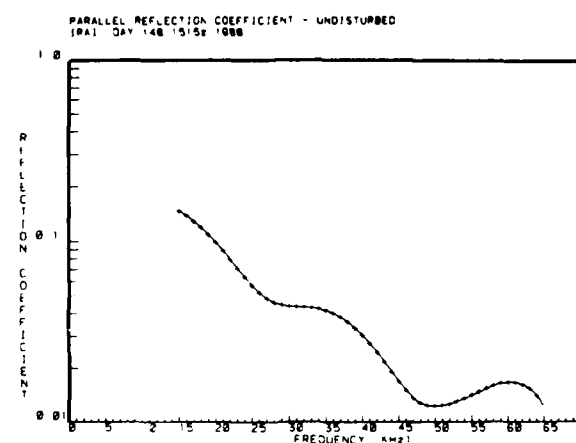
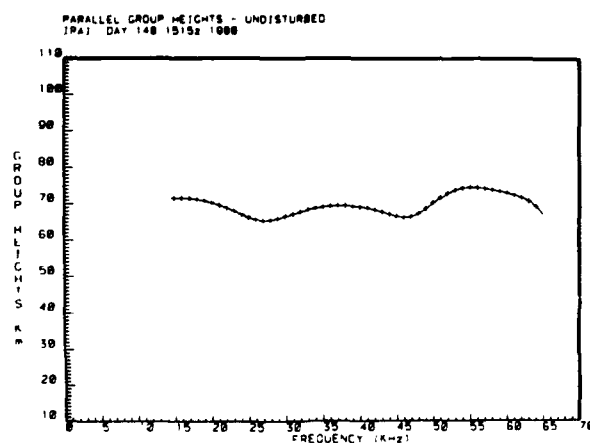
Figure 19.2. Group Heights of Reflection for 30.5 kHz and Reflection Coefficients at 15, 30, 45 and 60 kHz Derived from Normal Skywave Data Received at Irai.

(a)



NORMAL SKYWAVE

(b)



NORMAL SKYWAVE

Figure 19.3. Group Heights of Reflection and Reflection Coefficients vs Frequency Derived from Data Recieved at Iral.

- a. Local Midnight (0315 UT).
- b. Local Noon (1515 UT).

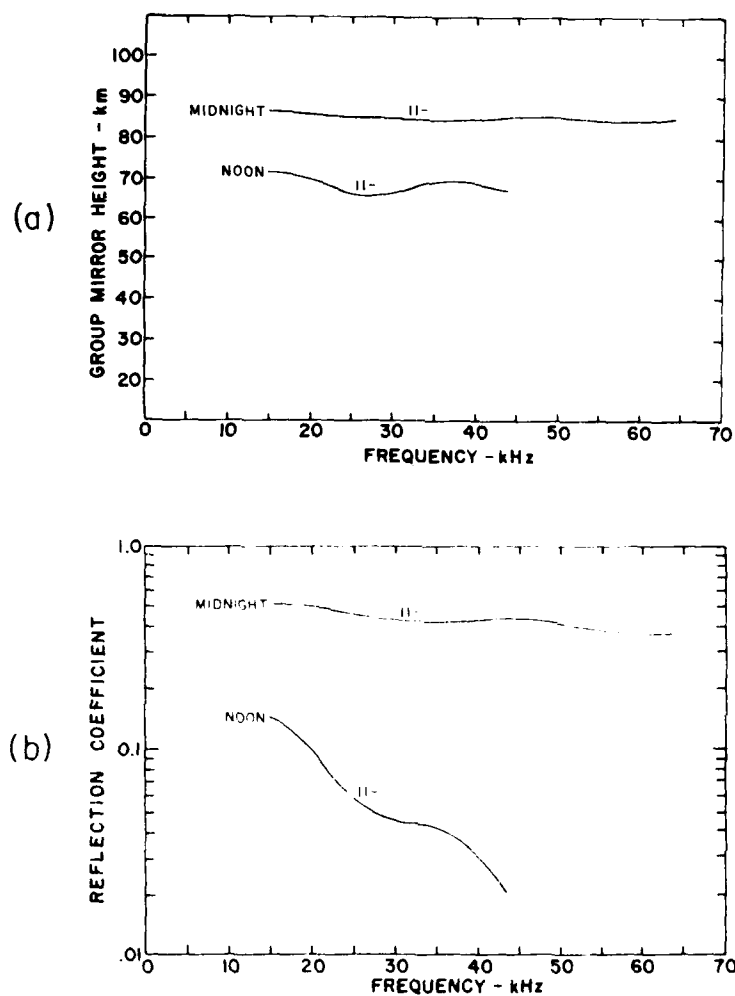


Figure 19.4. Averaged Values of Group Heights of Reflection and Reflection Coefficients vs Frequency Derived from Data Received at Irai.

- a. Group Heights of Reflection.
- b. Reflection Coefficients.

5. SELECTED FEATURES OF THE REFLECTION DATA

In this section data are shown to illustrate variations in the VLF/LF reflection properties of the ionosphere with such factors as time-of-day, direction of propagation, range and skywave polarization. In addition, a brief description is given of weak daytime pulses, seen from time-to-time, which were reflected from altitudes somewhat lower than those normally observed.

Due to the limited amount of data obtained at many of the receiving locations, the variations described below should be considered to be indicative of trends, rather than more-fully established characterizations. These trends, however, are consistent generally with those observed in earlier experimental programs, conducted at both mid- and low-geomagnetic latitudes ^{2,1}.

5.1 Day/Night Reflection Heights

A summary of noon and midnight reflection heights, derived from the data obtained at all the receiving locations, is given in Figure 20. As shown, the effective heights of reflection varied little over the frequency range from 15 kHz to 60 kHz. At noon the average height of reflection was 69 km; at midnight, it was 86 km. Throughout the 15-60 kHz range, the spreads in the heights were relatively small, usually well less than 2.5 km and 1.5 km for the noon and midnight data, respectively.

5.2 Day/Night Variations In The Reflection Coefficients

Normal ($||R_{||}$) reflection coefficients, derived from noon and midnight data obtained at a number of receiving locations to the east and west of the transmitter, are given in Figure 21. In all cases the reflection coefficients at midnight were substantially larger than those at noon, ranging from a factor of about 2 for the lowest frequencies observed (15 kHz) to an order of magnitude or more at much higher frequencies (40-60 kHz). At midnight and at noon the magnitudes of the reflection coefficients generally decreased as the frequency increased. At midnight, however, the variations were relatively small, usually being only about a factor or two over the 15-60 kHz band. In contrast, at noon the magnitudes of the reflection coefficients varied by an order of magnitude or more over the same frequency range. These results suggest that at midnight the reflections effectively came from a sharply bounded layer, while at noon there was weak ionization, below the altitudes at which the waves were reflected, that absorbed appreciable energy from the up- and down-going waves. The fact that the effective heights of reflection varied so little over the 15-60 kHz band (see Section 5.1) also supports such a characterization of the difference between the midnight and noon reflection processes.

5.3 Azimuthal Variations In The Reflection Coefficients

Comparison of the east-west (magnetic) data in Figure 21 reveals that the reflection coefficients at noon were appreciably larger for propagation to the east. This directional effect, which is due to the influence of the geomagnetic field, is in accordance with earlier experimental observations² and

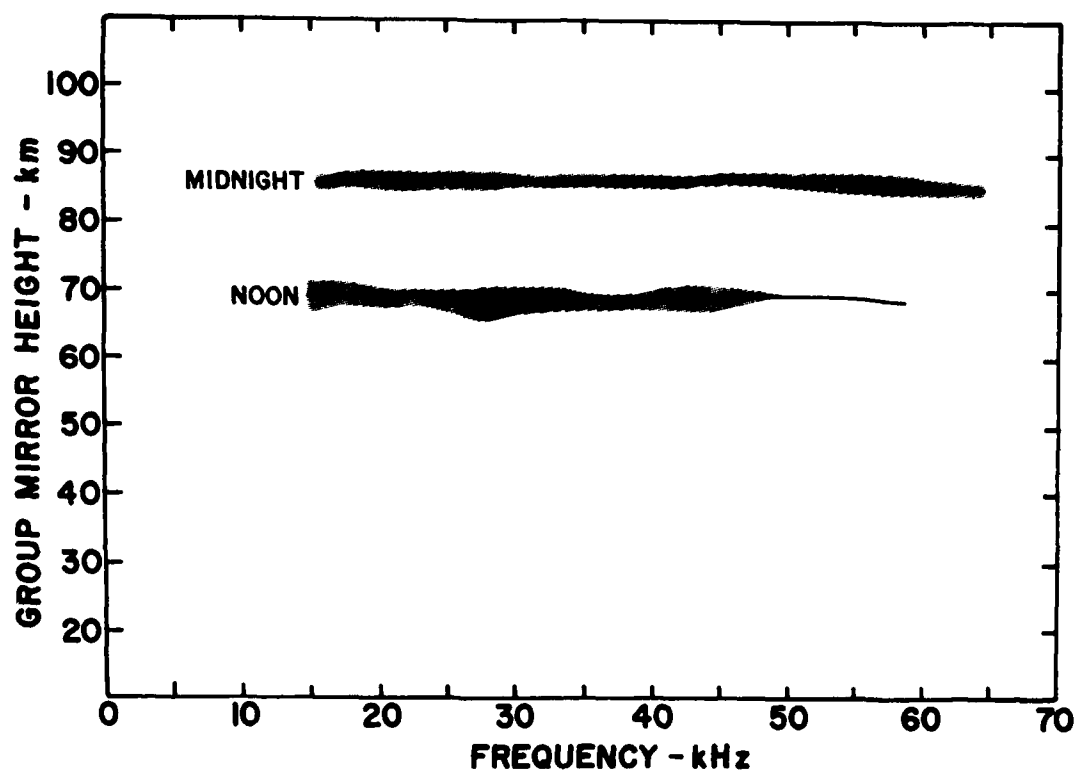


Figure 20. Summary of Noon and Midnight Group Heights of Reflection
Derived from Data Obtained at all the Receiving Locations.

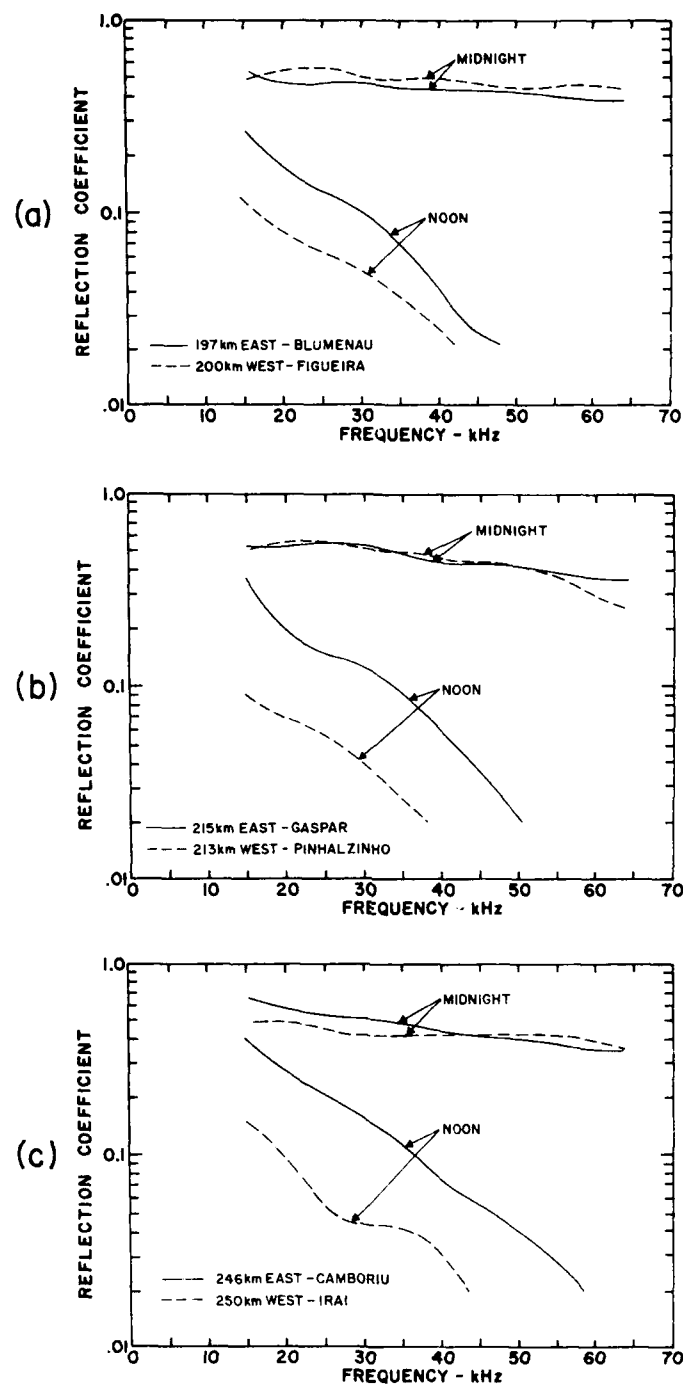


Figure 21. Normal Reflection Coefficients for Midnight and Noon Derived from Data at Selected Locations to the East and to the West of the Transmitter.

- Approximately 200 km Propagation Paths (Paula Freitas to Blumenau/Figueira).
- Approximately 215 km Propagation Paths (Paula Freitas to Gaspar/Pinhalzinho).
- Approximately 250 km Propagation Paths (Paula Freitas to Camboriu/Irai).

theoretical expectations⁵. The midnight data exhibit little east-west difference, even though the reflections came from much higher altitudes where such geomagnetic effects would normally be expected to be stronger, because of the reduced collisional forces associated with the lower neutral densities at those heights. The absence of appreciable geomagnetic effects in the midnight data suggests again, as described in Sections 5.1 and 5.2, that the nighttime reflection process can be characterized as having been more sharply bounded than the daytime process.

5.4 Variations In The Reflection Coefficients With Range

Figures 22 and 23 summarize the variations in the magnitudes of the normal reflection coefficients with range (or, in effect, incidence angle) that were derived from the pulse reflection data. In Figure 22 data are given at four frequencies over the 15-60 kHz band for six receiving locations, ranging from about 156 to about 280 km to the east of the transmitter. This corresponds, effectively, to a measure of the reflectivity of the ionosphere over a range of incidence angles from about 48-64 degrees in the day, or, about 42-48 degrees at night. The data show that the magnitudes of the reflection coefficients generally increase with increasing range, or more grazing incidence angle, with the trend being especially pronounced in the daytime.

Figure 23 shows 20 kHz reflection coefficients derived from data obtained at locations to the east and west of the transmitter. To the east, the reflection coefficient increases monotonically as the length of the propagation path increases. To the west, however, there is an apparent dip in the coefficient at a range of about 215 km (corresponding to an incidence angle of 57 degrees), which may be indicative of a quasi-Brewster's angle effect in the ionosphere. These data agree almost exactly with similar data obtained near the geomagnetic equator in Brazil in an earlier experimental program¹ (Rasmussen et al).

5.5 Comparison Of Normal And Converted Reflection Coefficients

Only a small amount of data pertaining to the polarization rotation effects produced in the ionosphere by the geomagnetic field were acquired during the experimental campaign. The results of those observations are summarized in Figure 24, which gives normal ($_{||}R_{||}$) and converted ($_{||}R_{\perp}$) reflection coefficients derived from noon and midnight data obtained at three locations to the east of the transmitter. As shown, the normal reflection coefficients were larger than the converted coefficients, with the difference being especially great during the daytime for frequencies below about 30 kHz. In general, the polarization conversion at night was substantially greater than in the daytime, as expected from consideration of the relative effects of electron-neutral collisions in the reflection process. Theoretical considerations also indicate, generally, that while the normal reflection coefficients should increase as the distances from the transmitter become greater and greater (as described in Section 5.1), the conversion coefficient's should decrease. Unfortunately, the

5. Crombie, D.D. (1958) Differences between E-W and W-E propagation of VLF signals over long distances, *J. Atmos. Terr. Phys.* **12**: 110

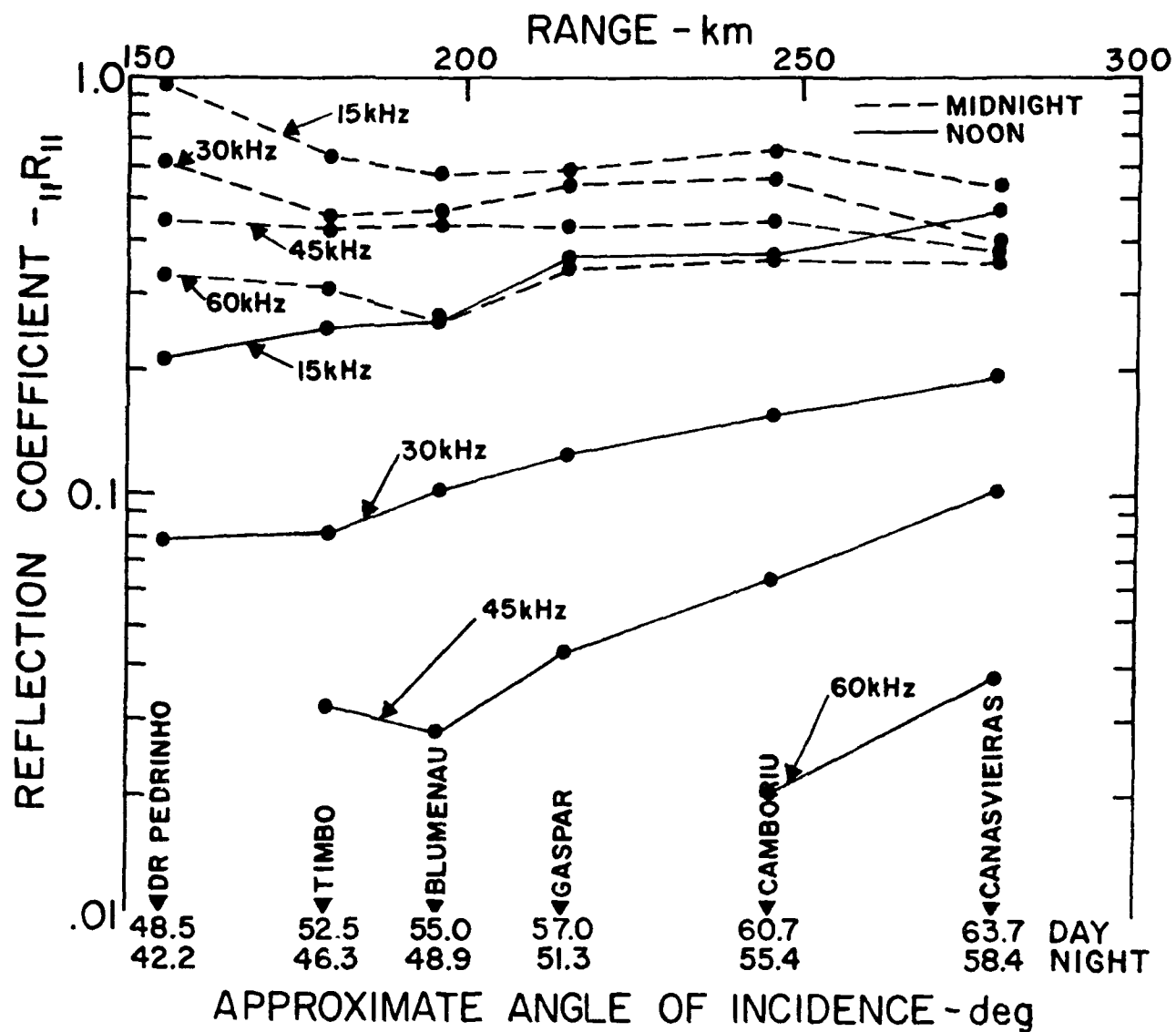


Figure 22. Variation in Normal Reflection Coefficients with Range and Angle of Incidence for Locations East of the Transmitter.

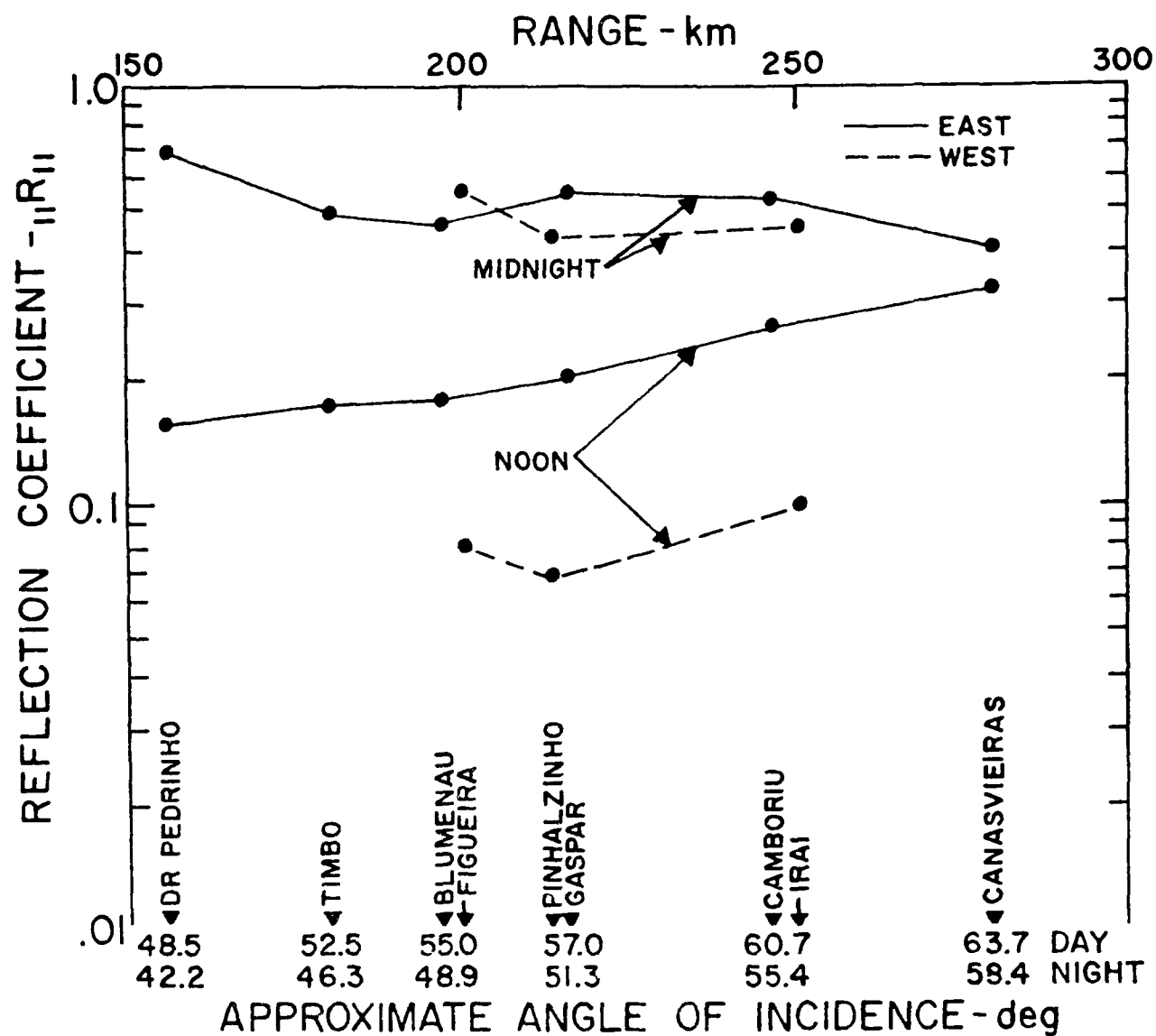


Figure 23. Normal Reflection Coefficients for 20 kHz Derived from Midnight and Noon Data Obtained at Receiving Locations to the East and West of the Transmitter.

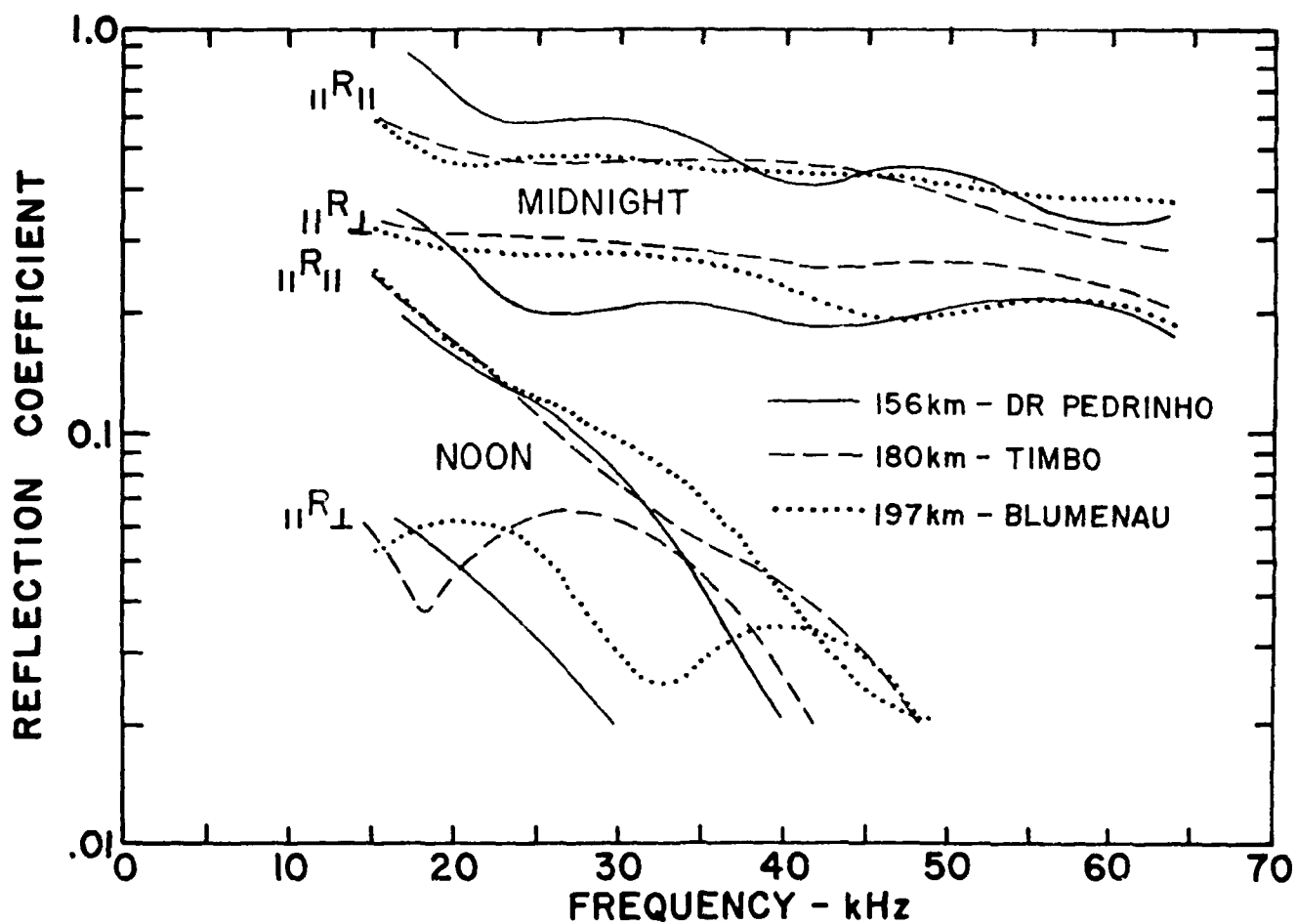


Figure 24. Normal and Converted Reflection Coefficients Derived from Midnight and Noon Data from Three Locations East of the Transmitter.

polarization rotation data that was acquired during the experimental campaign was too sparse to test this theoretical expectation adequately.

5.6 Evidence Of Weak Reflections From Below The Normal D-Region

The data acquired during sunrise periods were inspected for evidence of reflections coming from altitudes below the normal D-region, such as those observed earlier in similar mid-latitude experiments ^{6, 7} which were attributed to a 'C-layer' of ionization produced by the combined action of cosmic rays and solar illumination. A total of 57 sunrise recordings were made during the 22 days comprising the experimental campaign. Only rarely were recordings made during any given sunrise at more than two locations. Of the 57 sunrise recordings, approximately 40 percent showed evidence of reflections below the normal D-region. In most cases, however, the reflections were very weak and partially mixed with the D-region reflections; that is, only the leading edge of the received pulses could be resolved from the later arriving, D-region, reflections. In addition, there were sunrises for which the low altitude reflections were observed at one receiving location, but not another.

Figure 25 shows data acquired over a four-day period at Camboriu, 246 km to the east of the transmitter. Examples of weak reflections, believed to have come from a C-layer, are outlined by circles in the Figure. Such reflections are most easily seen in the data of May 17, where the leading edges of the daytime skywaves were nearly stationary, and distinct from later arriving (D-region) reflections that moved in accordance with the solar zenith angle. However, on other days shown in the Figure, such distinct reflections could only be seen for very short periods around sunrise and sunset.

Very clear evidence of the reflections occurred during sunrise on May 17, in observations made simultaneously at Timbo, Camboriu and Canasvieiras, at distances of 180, 246, and 280 km, respectively, to the east of the transmitter. The pulse reflection data recorded at those sites at 1015 UT, when the solar zenith angle was about 86 degrees, is given in Figure 26. In the three traces of Figure 26a, two skywave pulses are seen, which are clearly separated from an earlier arriving groundwave pulse. The first skywave (labeled C in each tract) is presumed to have been reflected from a C-layer in the lower ionosphere, whereas the second, much stronger, skywave is presumed to have been reflected from D-region ionization produced by Lyman- α radiation from the sun. Based on the arrival times of the early skywave reflections and the path lengths over which the observations were made it is estimated that the effective height of the C-layer that produced the reflections was 67 km.

Figure 26b shows effective plane-wave reflection coefficients derived from the C-layer reflections. The coefficients provide estimates of the reflection properties of the C-layer as a function of frequency and incidence angle, which can then be used to infer a conducting-slab model of the layer.

-
6. Rasmussen, J.E., Kossey, P.A., and Lewis, E.A (1980) Evidence of an ionospheric reflecting layer below the classical D region, *J. Geophys. Res.* **85**: 3037-3044.
 7. Bain, W.C. and Kossey, P.A. (1987) Characteristics of a reflecting layer below the classical D region" *J. Geophys. Res.* **92**: 12,443-12,444.

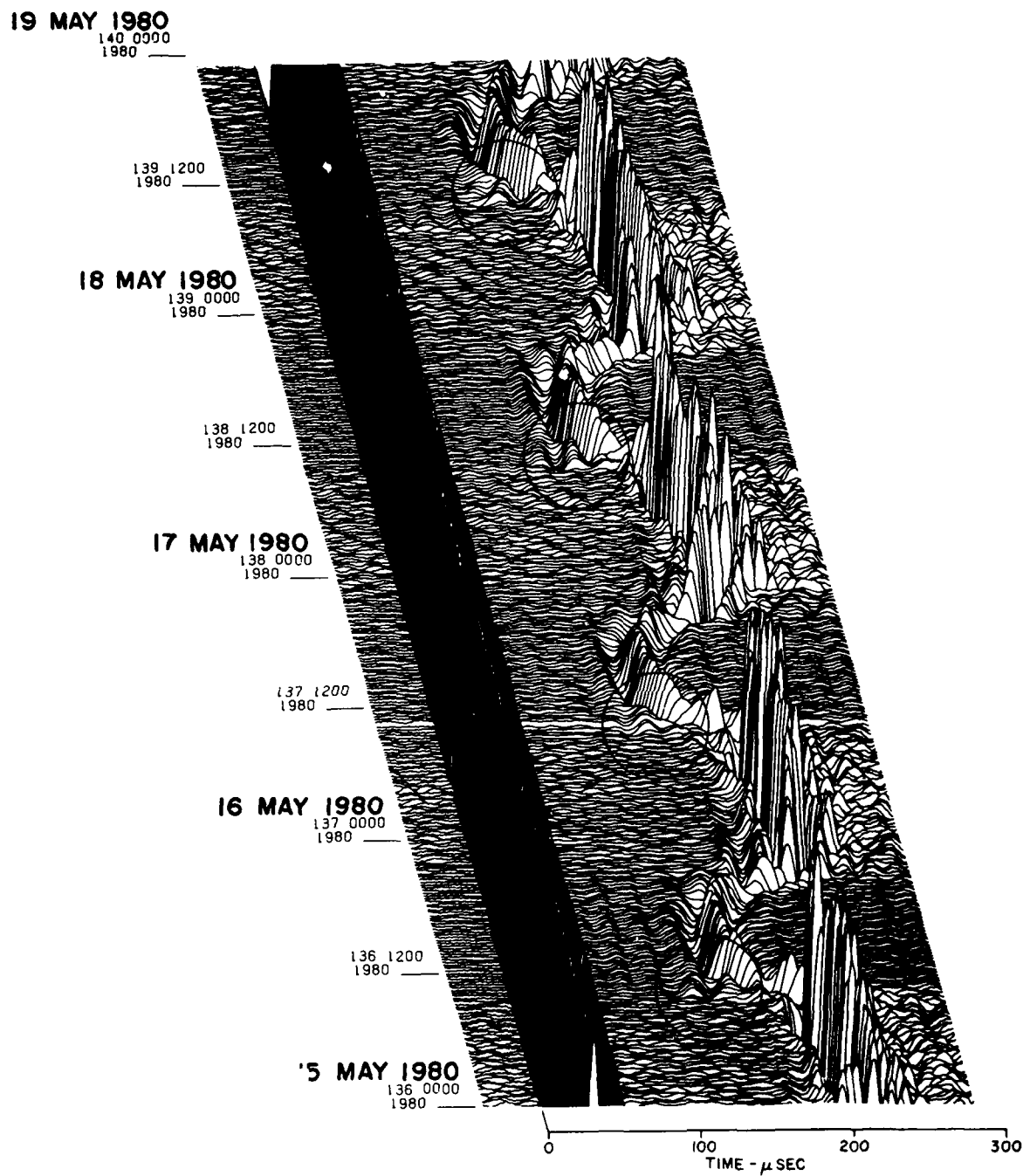


Figure 25. Data Obtained at Camboriu Showing Weak Reflections (circled areas) from Altitudes below the Normal D-Region.

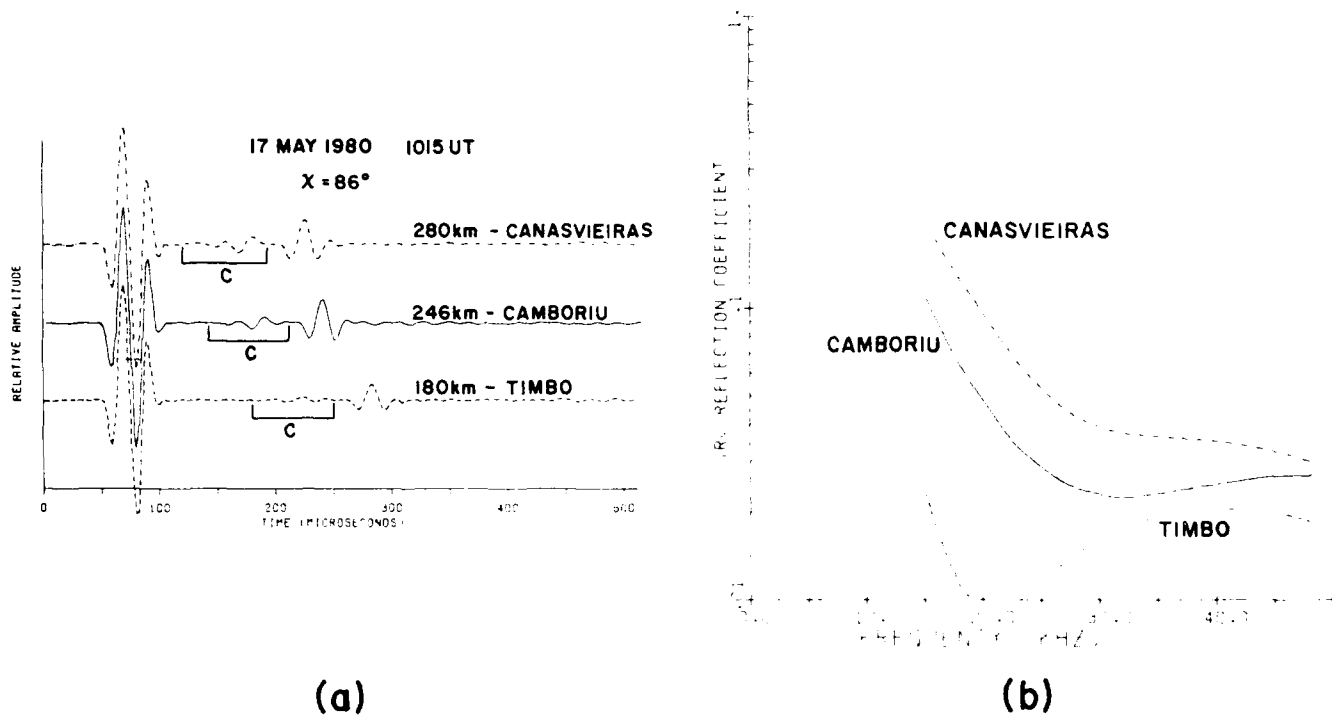


Figure 26. Data Recorded on 17 May (Day 138) 1980 at Timbo, Camboriu and Canasvieiras.

- a. Normal Skywave Data Showing Weak Reflections below the Normal D-Region (C).
- b. Normal Reflection Coefficients Derived from the "C" Portions of the Received Skywaves.

As described by Kossey and Lewis⁸, an estimate of the thickness of the slab can be obtained from the frequencies at which the relative nulls occur in the reflection coefficients. The magnitudes of the reflection coefficients are then used in determining an effective conductivity of the slab. From the data of Figure 26b, it was estimated that a 10-km thick slab, having a uniform conductivity of 10^{-7} Siemens/m, could describe the ionization (phenomenologically) that produced the C-layer reflections. This model contrasts with a more strongly ionized, 6-km thick slab, located at 60 km altitude that was inferred from earlier pulse reflection measurements at a mid-latitude location in the United States⁷.

If the low altitude reflections that were observed in Brazil did indeed come from a layer produce/d by cosmic rays, it is not too surprising that its features might differ appreciably from those observed at higher latitudes. This follows, qualitatively at least, from consideration of the geomagnetic field conditions. In Brazil, the measurements were made where the geomagnetic field had a dip-angle of only about 15 degrees; that is, the field was almost horizontal. It is surmised that 'he nearly horizontal geomagnetic field produces a shielding effect to charged particles, thus reducing the ability of the cosmic rays to penetrate deeply into the lower atmosphere. At higher latitudes, where the geomagnetic field has a much larger dip-angle, such shielding effects are expected to be very much weaker. For example, at the mid-latitude location where the pulse reflection data were used to infer a relatively strongly ionized, 6-km thick layer, at 60 km altitude, the dip-angle of the geomagnetic field was almost 70 degrees.

Too little appropriate data were acquired during the experiments in Brazil to attempt to characterize the nature of the C-layer at low latitudes. The limited data that were obtained, however, provide useful information on how future experiments might be designed to better exploit the pulse reflection technique for investigating the C-layer. For example, the data of Figure 26 illustrate that the lengths of the propagation paths in such experiments should be carefully chosen. If the path is too short, (that is, the incidence angle of the pulses on the layer is too steep) the reflections may be too weak to be clearly discerned. For example, the C-layer reflection observed in Timbo, 180 km from the transmitter, was almost too weak to be measured; while in Canasvieiras, at a distance of 280 km, it was relatively strong, and easily measured. On the other hand, at Canasvieiras, there was very little separation between the groundwave, C-layer and D-region pulse reflections, owing to the relatively long propagation path. At the intermediate distance of 246 km, at Camboriu, however, there was ample separation between the observed pulses, and the amplitude of the C-layer reflection was relatively strong.

5.7 Unusual Moving High Altitude Nighttime Reflections

Often at night unusual, moving, reflections were observed coming from regions well above the altitudes normally associated with the VLF/LF pulse reflections. The reflections tended to begin at a high altitude around 0200 UT and, in most cases, drifted downward over a period of 6-8 hr before disappearing during the sunrise transition period. Sometimes, however, the reflections began to drift upward again, about 2 hr before sunrise. These moving reflections can be easily seen in many of the

8. Kossey, P.A. and Lewis, E.A. (1981) The Reflection Properties of Conducting Slabs, RADC-TR-80-371, ADA098940.

quasi 3-dimensional displays of reflection data given in this report. A five-day sample of such data is given in Figure 27. It is hoped that future research will provide the necessary analyses to characterize these unusual nighttime reflections and the ionization processes that produce them.

6. ELECTRON DENSITY MODELS OF THE LOWER IONOSPHERE

Phenomenological models of the lower ionosphere can be derived from steep-incidence VLF/LF reflection data using mathematical inversion techniques such as those summarized by Sechrist⁹. Under normal ionospheric conditions this is not an easy task, since the polarization rotation effects of the geomagnetic field cannot usually be ignored. In addition, there is a question as to the uniqueness of models derived from reflection data. Nevertheless, since the VLF/LF reflection properties are very sensitive to electron densities below about 90 km at night, and below 75 km during the day, such data provide an important means for developing and validating models of the lower ionosphere.

Figure 28 shows electron-density models of the low latitude ionosphere in Brazil, derived from the pulse reflection data. The models were obtained using a trial-and-error approach, which employed full-wave and iterative computational techniques. In doing this, data from all nine of the receiving sites, were included so that the derived models were made to produce computational results consistent with a large number and variety of experimental data.

The technique involved the choice and refinement of trial electron density models of the lower ionosphere that served as inputs to a full-wave computational program, used to calculate theoretical values of VLF/LF reflection coefficients and effective heights of reflection, across a wide frequency band. The calculated values were then compared to those derived from the experimental data, and the differences between them were used as the basis for adjusting the trial electron density profiles. Finally, for each electron density model a root-mean-square (RMS) error was determined from the theoretical (computer) and experimental values. As such, the RMS errors provided a means for comparing the various electron density models under consideration.

Based on the strong tendency for the experimental values of the reflection coefficients to decrease monotonically with increasing frequency, trial electron-density profiles were chosen that varied exponentially with altitude. Figure 28 shows the noon and midnight electron-density models, having the smallest RMS errors, that were obtained from the numerous exponential models that were tested. In the notation of Wait and Spies¹⁰, which is often used to characterize such models, the noon model is described by a $\beta = 0.43 \text{ km}^{-1}$ and a $h = 70 \text{ km}$, and the midnight model by $\beta = 0.8 \text{ km}^{-1}$ and $h = 83 \text{ km}$. For the noon model, the average RMS error between the calculated and experimental values for the magnitudes of the normal reflection coefficients was 1.4 dB over the 15-50 kHz band and averaged over the nine receiving locations in Brazil. The corresponding RMS error in the effective heights of reflection was 1.2 km. For the midnight model, the RMS errors were 1.8 dB and 1.0 km, respectively,

9. Sechrist, C.F. (1974) Comparison of techniques for measurement of D region electron densities, *Radio Sci.* **9**: 137-149.

10. Wait, J.R. and Spies, K.P. (1964) Characteristics of the earth-ionosphere waveguide for VLF radio waves, *Nat. Bur. Stds., Tech. Note* 300.

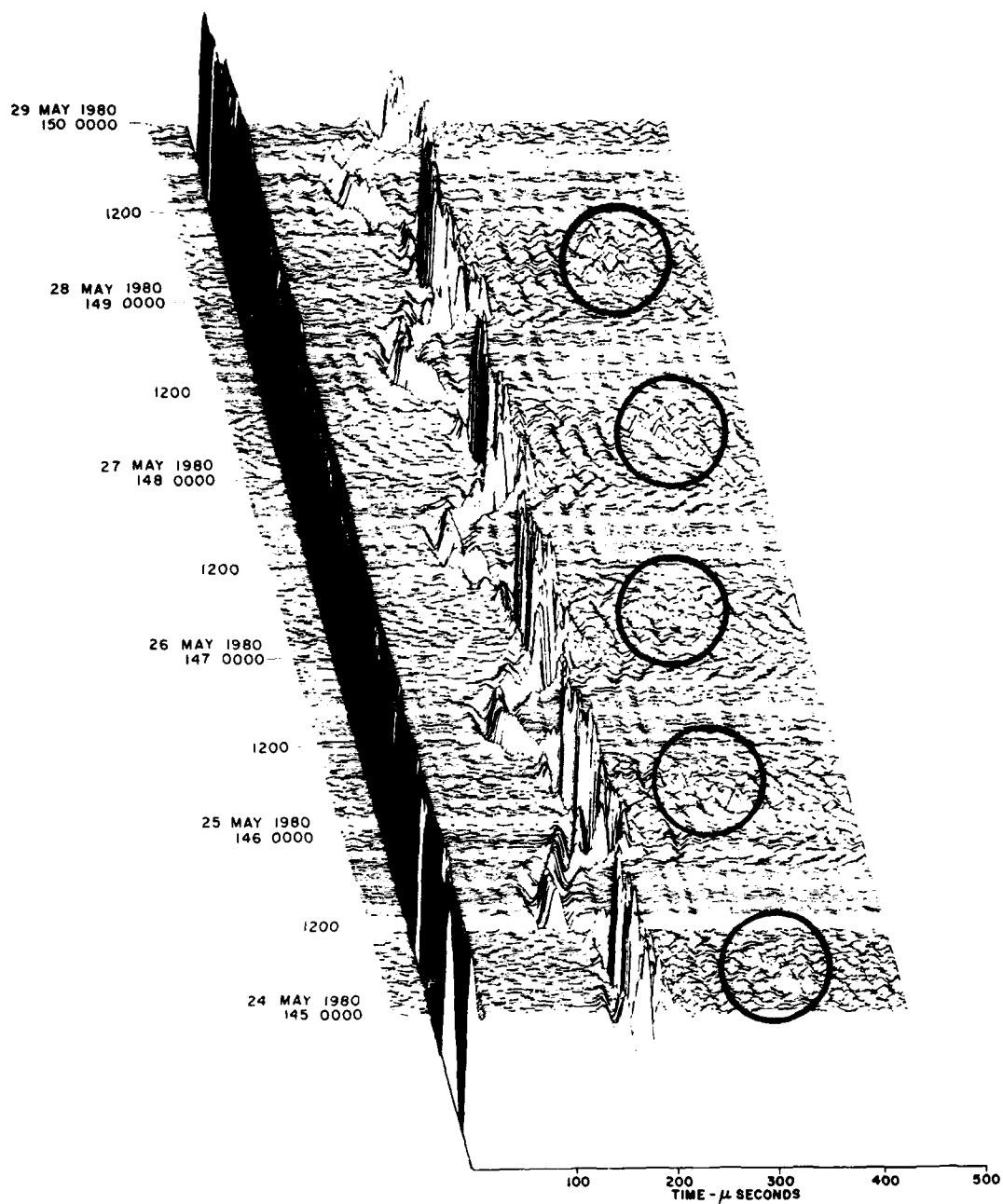


Figure 27. Data Obtained at Camboriu Showing Moving Reflections (circled areas) During the Nighttime coming from Relatively High Altitudes above the D-Region.

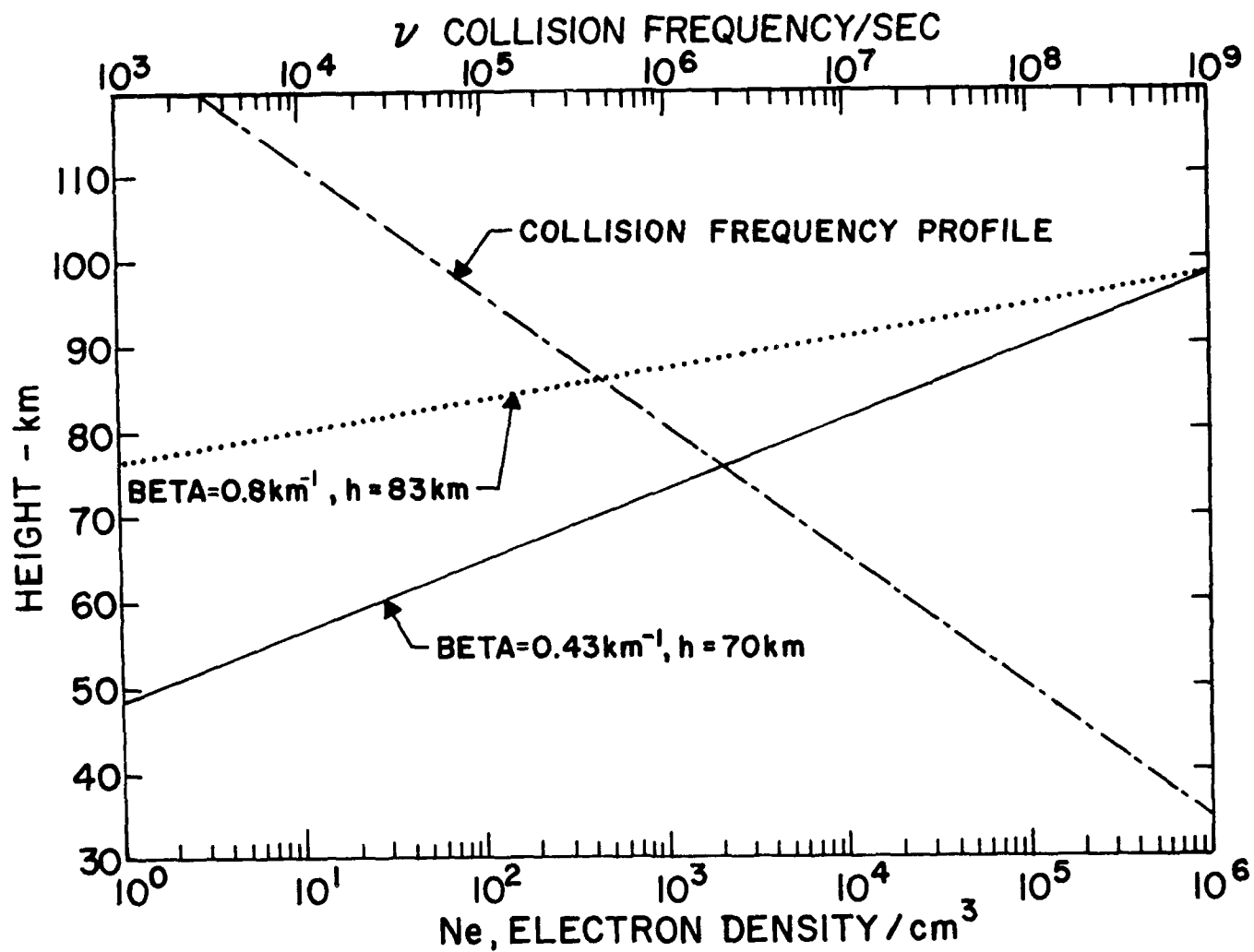


Figure 28. Electron Density Profiles of Low Latitude Ionosphere Derived from the VLF/LF Reflection Data Gathered During this Series of Measurements.

determined from data over an even wider frequency band of 15-65 kHz. The agreements between the experimental and calculated values for the two models are very good, based on earlier experiences with developing such phenomenological models of the ionosphere for example, Lewis et al².

7. SUMMARY

Observations of VLF/LF pulse reflections from the lower ionosphere, acquired at a relatively low geomagnetic latitude in Brazil, have been presented. In addition, the use of the data to determine effective heights of reflection and to provide a measure of the plane-wave reflection coefficients of the ionosphere, derived from such data, were discussed. Although the models are phenomenological, and not mathematically unique, they should be useful as inputs in longwave propagation prediction codes. More generally, the VLF/LF reflection data given in this report should be useful for validating other electron density models of the lower ionosphere, such as those derived from long path VLF/LF radiowave observations or from theoretical considerations of the chemistry of the low latitude atmosphere; that is, such models should have VLF/LF reflection properties that are consistent with experimental data such as the data described in this report.

Other reflection data acquired during the experiments require further study to characterize their properties and to identify the processes that may be responsible for them. These include weak daytime reflections from layers below the classical D-region, seen during sunrise periods and moving reflections from altitudes well above those normally expected with VLF/LF waves, observed from time to time, at night.

References

1. Rasmussen, J.E., Lewis, E.A., Kossey, P.A., Reginaldo Dos Santos, Edsel De Freitas Coutinho, Kahler, R.C., and Klemetti, W.I. (1975) *Low Frequency Wave-Reflection Properties of the Equatorial Ionosphere*, AFCRL-TR-75-0615, AD A025111.
2. Lewis, E.A., Rasmussen, J.E., and Kossey, P.A. (1973) Measurements of ionospheric reflectivity from 6 to 35 kHz, *J. Geophys. Res.* **78**: 3903-3912.
3. Kossey, P.A., Turtle, J.P., Pagliarulo, R.P., Klemetti, W.I., and Rasmussen, J.E. (1983) VLF reflection properties of the normal and disturbed polar ionosphere in northern Greenland, *Radio Sci.* **18**: 907-916.
4. Bracewell, R.N., Budden, K.G., Ratcliffe, J.A., Straker, T.W., and Weekes, K. (1951) The ionospheric propagation of low- and very-low-frequency radio waves over distances less than 1000 km, *Proc. Inst. Electr. Eng.* **98**(III), 221-236.
5. Crombie, D.D. (1958) Differences between E-W and W-E propagation of VLF signals over long distances, *J. Atmos. Terr. Phys.* **12**: 110.
6. Rasmussen, J.E., Kossey, P.A., and Lewis, E.A. (1980) Evidence of an ionospheric reflecting layer below the classical D region, *J. Geophys. Res.* **85**: 3037-3044.
7. Bain, W.C. and Kossey, P.A. (1987) Characteristics of a reflecting layer below the classical D region" *J. Geophys. Res.* **92**: 12,443-12,444.
8. Kossey, P.A. and Lewis, E.A. (1981) The Reflection Properties of Conducting Slabs, RADC-TR-80-371, ADA098940.
9. Sechrist, C.F. (1974) Comparison of techniques for measurement of D region electron densities, *Radio Sci.* **9**: 137-149.
10. Wait, J.R. and Spies, K.P. (1964) Characteristics of the earth-ionosphere waveguide for VLF radio waves, *Nat. Bur. Stds., Tech. Note* 300.